การพัฒนาฟิล์มแบคทีเรียเซลลูโลสนาโนคอมพอสิตสำหรับการประยุกต์ใช้ในทางการแพทย์

นายจีรัณ กิ่งแก้ว

วิทยานิพนธ์นี้เป็นส่วนหนึ่งของการศึกษาตามหลักสูตรปริญญาวิศวกรรมศาสตรดุษฎีบัณฑิต
สาขาวิชาวิศวกรรมเคมี ภาควิชาวิศวกรรมเคมี
คณะวิศวกรรมศาสตร์ จุฬาลงกรณ์มหาวิทยาลัย
ปีการศึกษา 2554

DEVELOPMENT OF BACTERIAL CELLULOSE NANOCOMPOSITE FILM FOR MEDICAL APPLICATIONS

Mr. Jeerun Kingkaew

A Dissertation Submitted in Partial Fulfillment of the Requirements
for the Degree of Doctoral of Engineering Program in Chemical Engineering
Department of Chemical Engineering
Faculty of Engineering
Chulalongkorn University
Academic Year 2011

Thesis Title	DEVELOPMENT OF BACTERIAL CELLULOSE NANOCOMPOSITE FILM FOR MEDICAL APPLICATIONS
By	Mr. Jeerun Kingkaew
Field of Study	Chemical Engineering
Thesis Advisor	Associate Professor Muenduen Phisalaphong, Ph.D.
Thesis Co-advisor	Associate Professor Neeracha Sanchavanakit, Ph.D.

Accepted by the Faculty of Engineering, Chulalongkorn University in Partial Fulfillment of the Requirements for the Doctoral Degree

……Dean of the Faculty of Engineering
(Associate Professor Boonsom Lerdhirunwong, Dr.Ing.)

THESIS COMMITTEE

……Chairman
(Associate Professor Tharathon Mongkhonsi, Ph.D.)

……Thesis Advisor
(Associate Professor Muenduen Phisalaphong, Ph.D.)

……Thesis Co-advisor
(Associate Professor Neeracha Sanchavanakit, Ph.D.)

……Examiner
(Associate Professor Bunjerd Jongsomjit, Ph.D.)

……Examiner
(Assistant Professor Chanchana Tangwongsan, Ph.D.)

……External Examiner
(Chada Phisalaphong, Ph.D.)

จีรัณ กิ่งแก้ว: การพัฒนาฟิล์มแบคทีเรียเซลลูโลสนาโนคอมพอสิตสำหรับการประยุกต์ใช้ในทางการแพทย์. (DEVELOPMENT OF BACTERIAL CELLULOSE NANOCOMPOSITE FILM FOR MEDICAL APPLICATIONS) อ.ที่ปรึกวิทยานิพนธ์หลัก: รศ.ดร.เหมือนเดือน พิศาลพงศ์, อ.ที่ปรึกษาวิทยานิพนธ์ร่วม: รศ.ทญ.ดร.นีรชา สารชวนะกิจ, 122 หน้า.

เพื่อดัดแปลงคุณสมบัติของฟิล์มแบคทีเรียเซลลูโลส (BC) ให้มีความเหมาะสมต่อการใช้งานในทางการแพทย์โดยมีวัตถุประสงค์ที่เจาะจงเช่นเพื่อใช้เป็นวัสดุปิดแผล ในงานวิจัยนี้จึงได้ทำการพัฒนาขึ้นแผ่นฟิล์มที่มีองค์ประกอบผสมของแบคทีเรียเซลลูโลส-ไคโตซาน (BCC) และ แบคทีเรียเซลลูโลส-ว่านหางจระเข้ (BCA) โดยวิธีการแช่แผ่นแบคทีเรียเซลลูโลสในสารละลายไคโตซาน-กรดอะซิติก และเจลว่านหางจระเข้ จากนั้นแผ่นฟิล์มทั้งสองจะถูกนำไปวิเคราะห์คุณสมบัติทางกายภาพและชีวภาพ นอกจากนี้แผ่นฟิล์มดังกล่าวจะถูกนำไปทดสอบการเข้ากันได้กับเซลล์ เคอราติโนไซท์และไฟโบรบลาสต์ของมนุษย์ ต่อไป

พบว่าแผ่นฟิล์ม BCC และ BCAให้คุณสมบัติทางกายภาพและชีวภาพมีความแตกต่างไปจากแผ่นฟิล์ม BC ดั้งเดิม สำหรับแผ่นฟิล์ม BCC จากการทดสอบด้วยอินฟราเรดทางโครงสร้างโมเลกุลพบว่า โมเลกุลของแบคทีเรียเซลลูโลสและไคโตซานมีปฏิสัมพันธ์ระหว่างกัน ส่งผลให้สมบัติทางกล ความเป็นผลึก การแพร่ผ่านของไอน้ำ และออกซิเจน ความสามารถในการดูดซึมน้ำและขนาดเส้นผ่านศูนย์กลางเฉลี่ยของรูพรุนของแผ่นฟิลม์ลดลง ในขณะที่ความสามารถในการต่อต้านการเจริญเติบโตของแบคทีเรียแกรมบวก *สแตปฟิโลคอคคัส ออเรียส* และรา *แอสเปอร์จิรัส ไนเจอร์*เพิ่มขึ้น นอกจากนี้แผ่นฟิล์ม BCC ยังสนับสนุนการเกาะ การเจริญเติบโตและการเพิ่มจำนวนของเซลล์ เคอราติโนไซท์และไฟโบรบลาสต์ สำหรับแผ่นฟิล์ม BCA จากการทดสอบด้วยอินฟราเรดทางโครงสร้างโมเลกุลพบว่า โมเลกุลของแบคทีเรียเซลลูโลสและว่านหางจระเข้มีปฏิสัมพันธ์ระหว่างกัน โดยเมื่อเปรียบเทียบกับแผ่นฟิล์ม BC ดั้งเดิม แผ่นฟิล์ม BCA มีสมบัติทางกล ความเป็นผลึก ขนาดเส้นผ่านศูนย์กลางเฉลี่ยของรูพรุนที่ลดลง แต่มีการแพร่ผ่านของออกซิเจน ความสามารถในการดูดซึมน้ำและการต่อต้านการเจริญเติบโตของรา *แอสเปอร์จิรัส ไนเจอร์*ที่เพิ่มขึ้น ผลของการทดสอบความเข้ากันได้ทางชีวภาพ แสดงให้เห็นว่า แผ่นฟิล์ม BCA ไม่เพียงแต่สนับสนุนการเกาะของเซลล์ เคอราติโนไซท์และไฟโบรบลาสต์ แต่ยังส่งเสริมการเจริญเติบโตและการเพิ่มจำนวนของเซลล์ดังกล่าวด้วย ผลการทดลองนี้แสดงให้เห็นว่าแผ่นฟิล์มแบคทีเรียเซลลูโลสที่ถูกดัดแปลงด้วยวิธีการแช่ในสารละลายไคโตซานและแช่ในเจลว่านหางจระเข้ มีคุณสมบัติที่เป็นประโยชน์สำหรับการนำไปใช้เป็นวัสดุปิดแผล

ภาควิชา.....วิศวกรรมเคมี..... ลายมือชื่อนิสิต.....

สาขาวิชา.....วิศวกรรมเคมี..... ลายมือชื่อ อ. ที่ปรึกษาวิทยานิพนธ์หลัก.....

ปีการศึกษา.....2554..... ลายมือชื่อ อ. ที่ปรึกษาวิทยานิพนธ์ร่วม.....

5071860421: MAJOR CHEMICAL ENGINEERING
KEYWORDS : BACTERIAL CELLULOSE / CHITOSAN / ALOE VERA / COMPOSITE FILM / WOUND HEALING

JEERUN KINGKAEW: DEVELOPMENT OF BACTERIAL CELLULOSE NANOCOMPOSITE FILM FOR MEDICAL APPLICATIONS. ADVISOR: ASSOC. PROF. MUENDUEN PHISALAPHONG, Ph.D., CO-ADVISOR: ASSOC. PROF. NEERACHA SANCHAVANAKIT, Ph.D., 122 pp.

To modify the properties of bacterial cellulose (BC) in order to be suitably used in a specific medical application such as wound dressing, in this research, the bacterial cellulose-chitosan (BCC) and bacterial cellulose-*Aloe vera* (BCA) composite films were developed by immersing the purified BC pellicle in chitosan acetic acid solution and *Aloe vera* clear gel. Then both of the developed composite films were characterized for physical and biological properties. In addition, the biocompatibility of BCC and BCA films on human keratinocytes and fibroblasts was evaluated.

It was found that the physical and biological properties of BCC and BCA films were changed from those of the pristine BC film. In case of the BCC film, the FTIR result indicated the intermolecular interaction between BC and chitosan. The mechanical properties, the crystallinity, the water absorption capacity, the water vapor transmission rate, the oxygen transmission rate and the average pore diameters were decreased, whereas the antimicrobial abilities against gram positive bacteria, *Staphylococcus aureus* and fungi, *Aspergillus niger* of films were enhanced. Moreover, BCC films supported adhesion, growth and proliferation of both of human keratinocytes and fibroblasts. In case of BCA film, the FTIR result indicated the intermolecular interaction between BC and *Aloe vera*. When compared with the pristine BC film, the mechanical properties, the crystallinity and the average pore diameter were decreased whereas; the oxygen transmission rate and the antifungal ability against *Aspergillus niger* were enhanced. Biocompatibility tests of BCA films revealed that not only the films supported adhesion of human keratinocytes and fibroblasts but also promoted growth and proliferation of those cells. Our results indicated that the modified BC films by immersing it into chitosan solution and *Aloe vera* gel exhibited advantageous properties to be used as wound dressing material.

Department :……Chemical Engineering.. Student's Signature ……..……

Field of Study :…Chemical Engineering.. Advisor's Signature ……..……

Academic Year : 2011…….. Co-advisor's Signature ……

ACKNOWLEDGEMENTS

I would like to express my deeply gratitude to all who gave me the possibility to complete this thesis. First, I am particularly grateful for my advisor, Associate professor Dr.Muenduen Phisalaphong for her nice guidance, valuable discussions and warm encouragement. I am also appreciated Associate professor Dr. Neeracha Sanchavankit, my co-advisor for her valuable suggestions and guidance. Moreover, I also grateful for the members of thesis examination committee, Associate Professor Dr.Tharathon Mongkhonsi, Associate Professor Dr.Bunjerd Jongsomjit, Assistant Professor Dr.Chanchana Tangwongsan, and Dr. Chada Phisalaphong, who gave helpful suggestions and information for this thesis. I would like to thank the Royal the Office of the Higher Education Commission, Thailand for supporting by grant fund under the program Strategic Scholarships for Frontier Research Network for the join Ph.D. Program Thai Doctoral degree for this research. Finally, I would like to dedicate this thesis to my parents and my families for their always support and encouragement as well as my friends in the Department of Chemical Engineering, Chulalongkorn University.

CONTENTS

PAGE

CHAPTER PAGE

CHAPTER PAGE

CHAPTER PAGE

LIST OF TABLES

LIST OF FIGURES

FIGURE PAGE

FIGURE PAGE

FIGURE PAGE

FIGURE PAGE

FIGURE PAGE

CHAPTER I
INTRODUCTION

1.1 Introduction

Cellulose as a linear polysaccharide is the most abundant polymer in nature. It forms the basic structural matrix of the cell wall of nearly all plants and algae. Moreover, some animal, fungi and bacteria genera can assemble cellulose (Brown, 1996). However, these organisms are devoid of photosynthetic capacity and usually required glucose or some organic substrates synthesized by a photosynthetic organism to assemble their cellulose. Several bacteria are in conditions to produce solid extracellular cellulose, as reported from the genera *Acetobacter* (formerly *Gluconacetobacter*), *Agrobacterium*, *Achromobacter*, *Aerobacter*, *Azotobacter*, *Rhizobium*, *Sarcina*, *Salmonella*, and *Escherichia* (Shoda and Sugano, 2005). Special attention was given to the strains from *Acetobacter xylinum*, which is the most widely used species, to synthesize cellulose as fibers or known as Bacterial cellulose (BC). Plant and bacterial cellulose are chemically similar, β-1,4 glucans, but the degree of polymerization differs from about 13,000 to 14,000 for plant and about 2,000 to 6,000 for BC (Jonas and Farah, 1998). Cellulose derived from plant is unpurified cellulose associated with other kind of natural fiber such as lignin and hemicelluloses, while bacterial cellulose is nearly-purified cellulose (Phisalaphong and Jatupaiboon, 2008). BC has unique properties including ultra-fine network structure, high water holding capacity, high crystallinity, hydrophilicity, high purity, and high tensile strength.

BC has a wide range of potential applications in many fields such as BC/BC composites used as a separation membrane (Brown, 1989; Dubey et al., 2002), a mixing agent or a viscosity modifier in food industry (Brown, 1989; Jonas and Farah, 1998), light transmitting optical fibers (Brown, 1989), membranes for fuel cells (Brown, 1989), optoelectronics devices (Nogi et al., 2005), fibers in paper industrial (Jonas and Farah, 1998; Shah and Brown, 2005), stereo diaphragms (Jonas and Farah,

1998), and immobilization matrices of proteins or chromatography substances (Jonas and Farah, 1998; Sokolnicki et al., 2006). The prevalent application of BC is in the biomedical field, as it is highly useful for wound dressing (Cienchanska, 2004, Sanchavanakit et al., 2006; Czaja et al., 2006), artificial skin (Jonas and Farah, 1998; Czaja et al., 2007; Klemm et al., 2001), dental implants, vascular grafts, catheter covering dressing, dialysis membrane, coatings for cardiovascular stents, cranial stents, tissue replacement, controlled-drug release carriers (Wan and Millon, 2005), membranes for tissue-guided regeneration (Wan and Millon, 2005; Czaja et al., 2007), vascular prosthetic devices (Charpentier et al., 2006), membrane in antibacterial applications (Barud et al., 2006), membrane/scaffold for tissue engineering (Rambo et al., 2008; Luo et al., 2008; Czaja et al., 2007; Li et al., 2009), material in bone tissue engineering fields (Wan et al., 2006; Chen and Zheng, 2009), artificial blood vessels (Klemm et al., 2001; Backdahl et al., 2006) and scaffold for tissue engineering of cartilage (Svensson et al., 2005). The innovative biomaterial for medical fields still has been continuously developed in a wide range of good candidate materials such as alginate, polyurethane, PVA and chitosan. One method to improve properties of BC is by the addition of some substances with specific properties in to BC, For example, Luo et al. (2008) prepared a composite of BC and collagen for potential tissue engineering applications by incorporating collagen into BC nutrient medium attempting to use the synergic beneficial aspects of both polymers.

Chitosan has been recognized for application in various fields including biomedical area. It has been known for its absorption of exude, anti-fungal, anti-microbial, anti-viral and wound-healing properties. Chitosan is useful as a wound management aid to reduce scar tissue. Moreover, chitosan may be used to inhibit fibroplasias in wound healing, and to promote both tissue growth and differentiation in tissue culture (Muzzarelli et al., 1999).

Aloe vera has been shown to have multiple beneficial properties during wound healing, including the abilities to penetrate tissue, anesthetize tissue, preclude microbial and viral growth, act as an anti-inflammatory agent and dilate capillary beds and enhance blood flow (Grindlay and Reynolds, 1986). In addition, *Aloe vera* may be used to inhibit fibroplasia in wound healing process and to promote both tissue growth and differentiation in tissue culture (Davis et al., 1994; Heggers et al., 1996).

Therefore, this study aims to develop the nano-composites based on BC film from microbial synthesis under static conditions by *Acetobacter xylinum* in coconut-water. Microstructure and mechanical properties of the BC-base films were then characterized. Furthermore, the growth of human cell on BC-base films was examined. The present study would provide indications for the preparation of the BC-base films for using in medical fields.

1.2 Objectives

The overall objective of this study is to improve the properties of bacterial cellulose film by impregnation of substances with specific properties into bacterial cellulose. Specifically, the study aimed:

1. To develop BC-Chitosan (BCC) and BC-*Aloe vera* (BCA) film by impregnation method.
2. To investigate the biocompatibility with human skin fibroblasts and keratinocytes of biosynthesized BC-chitosan film.
3. To investigate the characteristics and biocompatibility with human skin fibroblasts and keratinocytes of BCC and BCA films.

1.3 Research scopes

1. *In vitro* study of human keratinocytes and fibroblasts on the biosynthesized BC-chitosan films in culture plate.
2. Prepare BCC by immersing bacterial cellulose pellicles in chitosan-acetic acid solution.
    2.1 Examine effects of molecular weight of chitosan between 30,000, 80,000 and 200,000.
    2.2 Characterizing the developed BCC films by:
        a. Scanning Electron Micrographs (SEM) for preliminarily investigating morphology.

b. Universal testing machine for determining tensile strength, Young's modulus and elongation at break.

c. Fourier Transform Infrared (FTIR) spectrometer for identifying the chemical structure.

d. X-Ray Diffraction (XRD) for finding crystallinity index.

e. Brunauer-Emmett-Teller (BET) for identifying the pore size, surface area, and pore size distribution.

f. Water absorption capacity (WAC).

g. Water vapor permeation tester for measuring water vapor transmission rate (WVTR).

h. Oxygen permeation tester for measuring oxygen transmission rate (OTR).

i. Antimicrobial activity.

2.3 *In vitro* study of human keratinocytes and fibroblasts on the BCC films in culture plate.

2.4 *In vitro* study of released of chitosan from BCC films.

3. Prepare BCA film by immersing bacterial cellulose pellicles in *Aloe vera* gel.

3.1 Characterizing the developed BCA following (2.2)

3.2 *In vitro* study of human keratinocytes and fibroblasts on the BCA film in culture plate.

3.3 *In vitro* study of released of active ingredients of *Aloe vera* as reducing sugar from BCA film.

1.4 Dissertation overview

This dissertation is organized as the list below.

Chapter II shows all background, theory and literature reviews about relating to this study. First, cellulose, bacterial cellulose (BC), chitosan and *Aloe vera* are described in terms of properties, sources, and applications. Then wound dressing, interm definition, and characteristics are discussed. Finally, the modification of BC is explained and compared its properties with the pristine BC.

Chapter III presents the experimental design in term of materials and method. First, Chemical and Equipment list are showed in this chapter. Then the preparation of BC and BC composite films is explained, Finally, The characterization methods of all films are revealed.

Chapter IV presents the characteristics of bacterial cellulose chitosan composite films (BCC) which are prepared by impregnation method. Moreover, the Cytotoxicity and biocompatibility of bacterial cellulose chitosan composite (BCC-MW *n*) films prepared by biosynthesis method are presented.

Chapter V presents the characteristics of bacterial cellulose-*Aloe vera* (BCA) films which are prepared by impregnation method. Also, this chapter will show the differential property of the BCA film when compared to unmodified BC film.

Chapter VI presents the conclusion of this dissertation. Moreover, recommendations are also discussed.

CHAPTER II
BACKGROUND AND LITERATURE REVIEW

2.1 Background

2.1.1 Cellulose

Cellulose is one of the most importance structure elements in plants as the main component of cell walls. It is also formed by some type of algae, fungi, bacteria, and marine animals. Physically, cellulose is a linear polymer of D-glucose residues joined by β-1, 4-glycosidic linkages as polysaccharides. Cellulose molecules form long chains in polycrystalline fibrous bundles that contain crystalline as well as amorphous regions.

Cellulose is insoluble in water, in dilute acids, and most organic solvents; but slightly soluble in sodium hydroxide. Cellulose molecule form straight, almost fully extended chain as shown in Figure 2.1. The cellulose chains are organized in a crystalline or semi-crystalline lattice, thus giving rise to micro fibrils with high tensile strength. Chemical formula of cellulose is $(C_6H_{10}O_5)_n$. In general, the advantages of cellulose include high specific strength and good thermal stability.

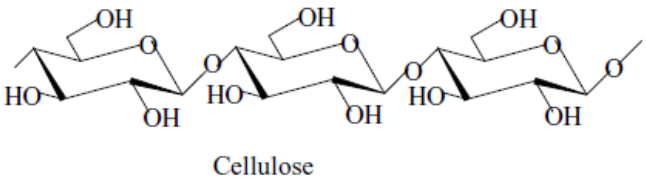

Figure 2.1 Structure of Cellulose (Krajewska, 2004).

The structure of cellulose can be defined traditionally as four major types: cellulose I, cellulose II, cellulose III and cellulose IV. All of them have a difference in polarity of the cellulose chains. The backbone conformations of the chains themselves are essentially identical. Cellulose I is native cellulose, found in wood, cotton, and other plants. Cellulose II is made either by soaking cellulose I in strong alkali solutions or by dissolving it in the viscose process. The regenerated cellulose II products are known as rayon for the fiber form and cellophane for the film form. Cellulose III can be made by treating cellulose with ethylamine. Cellulose IV may be obtained by treatment with glycerol or alkali at high temperatures. Going from the polymorphic forms of cellulose back to cellulose I is difficult but can be accomplished by partial hydrolysis (Gardner and Blackwell, 1974).

2.1.2 Bacterial Cellulose

Bacterial cellulose (BC) is a product of primary metabolism processes of some microbes. It is produced by some species of microbial such as *Zoogloea*, *Salmonella*, *Rhizobium*, *Escherichia*, *Pseudomonas*, *Aerobacter*, *Azotobacter*, *Alcaligenes*, and *Acetobacter* (Brown, 2007; Jonas and Farah, 1998). The overview of bacterial cellulose producers was shown in Table 2.1 (Jonas and Farah, 1998). The most studied and most used BC-producing bacterium specie is *Acetobacter xylinum* (Klemm et al., 2001). *Acetobacter xylinum* was found to be superior to many accounts as compared with the plant one. It is an obligate aerobe bacterium usually found in vinegar, alcoholic beverages, fruit juices, fruits, vegetables, and most likely in rotting ones as well (Klemm et al., 2001). *Acetobacter xylinum* is a simple Gram-negative, rod shaped, and aerobic bacterium, which has an ability to synthesize a large quantity of high-quality cellulose organized as twisting ribbons of microfibrillar bundles (Czaja et al., 2006; Sanchavanakit et al., 2006). It can be produced from many different substrates such as HS liquid medium (noted by Hestrin and Schramm, 1954, consisting of D-glucose, peptone, yeast extract, disodium phosphate, citric acid), Nata de pina and Nata de coco medium, the medium consist of pineapple water and coconut water as carbon source in medium, respectively. Morphologically, the

reproducible pellicle is obtained by controlling parameters of bacterial growth, for instance, the composition of the culture media, pH, temperature, and oxygen tension.

Table 2.1 Bacterial cellulose producers (Jonas and Farah, 1998).

Organisms(genus)	**Cellulose produced**	**Biological role**
Acetobacter	Extracellular pellicle Cellulose ribbons	To keep in aerobic environment
Aerobacter	Cellulose fibrils	Flocculation in wastewater
Agrobacterium	Short cellulose	Attach to plant tissue
Alcaligenes	Cellulose fibrils	Flocculation in wastewater
Pseudomonas	No distinct fibrils	Flocculation in wastewater
Rhizobium	Short fibrils	Attached to most plant
Zoogloea	Not well defined	Flocculation in wastewater

The synthesis of cellulose in *Acetobacter xylinum* occurs between the outer membrane and cytoplasma membrane by a cellulose-synthesizing complex, which is in association with pores at the surface of the bacterium (Figure 2.2).

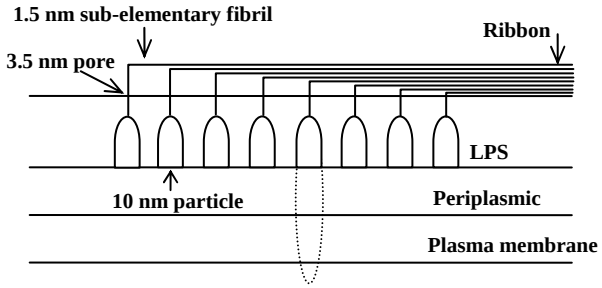

Figure 2.2 Scheme for the formation of bacterial cellulose (Jonas and Farah, 1998).

The most importance enzyme in this process is cellulose synthase. It was partially purified and cloned. A principal biochemical pathway from a basic monosaccharide, glucose to cellulose was proposed (Figure 2.3), which should be

linked to cell growth as well as to cellulose formation. The synthesized cellulose leaves the pores as nano-fibrils and from together with many synthesized fibrils a ribbon of crystalline cellulose. A self-assembly process should be responsible for the crystallization after the polymerization of the fibrils was completed (Jonas and Farah, 1998).

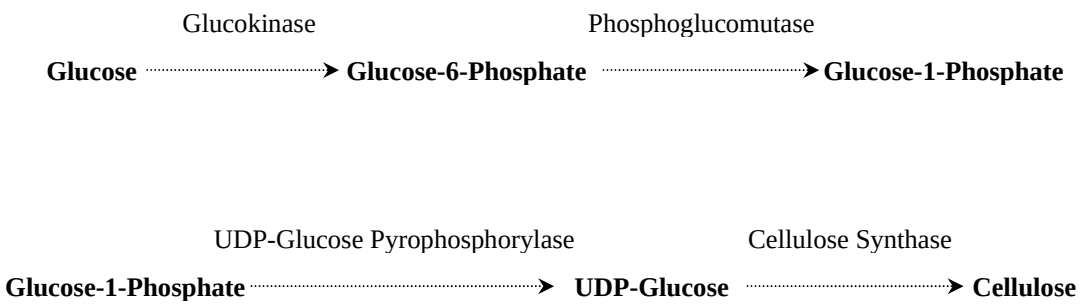

Figure 2.3 Proposed biochemical pathway for cellulose synthesis in *Acetobacter xylinum* (Jonas and Farah, 1998).

The bacterium extrudes linear glucan chains from its terminal complexes that are composed of few catalytic sites of extrusion. Approximately 10-100 linear glucan chains aggregate to form into twisting nanofibers. The nano-fiber from a single bacterial cell with a rectangular cross section of 2 x 3 nm aggregate further to from ribbon with a diameter of about 70-80 nm and they are about 20 μm long. The ribbons are spun into the liquid medium and intertwine with ribbons from other cells to form into a gelatinous suspension or pellicle (Brown, 1996). The lateral dimension of BC increases as bacteria grow and as the population increases. During bacterial growth, new production sites for BC become available. Hence, the BC fibril or ribbon widens. BC fibrils aggregate due to hydrogen bonding and Van der Waals forces. These forces cause the fibrils to interact, and they are held apart by adsorbed water layers. When the water layers evaporate, the hydroxyl groups of fibril chains associate irreversibly, and highly crystalline cellulose sheet is formed (Brown, 2007).

The morphology of BC depends on the growing culture environment. For a static culture, a leather-like pellicle of overlapping and intertwined ribbons formed (Jonas and Farah, 1998). On the other hand, an agitated medium forms

irregular BC granules and fibrous strands. The bacterium increases its population by consuming the glucose and oxygen initially dissolved in the liquid medium. When the oxygen has decreased, only the bacteria with access to air can continue their BC-producing activity. The bacteria below the surface are considered dormant, but can be reactivated by using the liquid as inoculums for a new culture medium (Klemm *et al.*, 2001). Given that BC is extruded as a very fine fibril, it is logical to start fine-tuning its morphology during biogenesis (Brown, 2007).

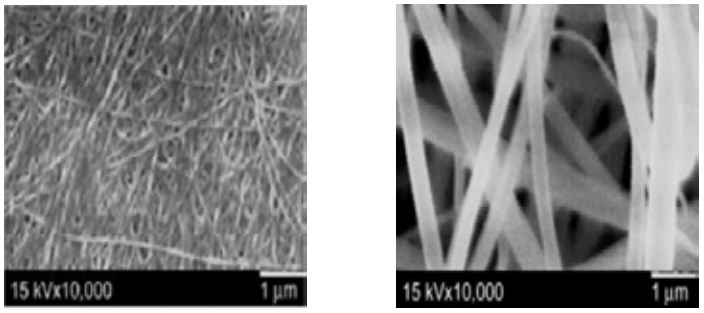

(a) (b)

Figure 2.4 A comparison of microfibrillar organization between (a) BC and (b) commercial grade regenerated cellulose membrane from plants (Phisalaphong et al., 2007).

BC traditionally originates as a white gelatinous pellicle on the surface of the liquid medium in a static culture. These bacteria produce ultrafine fiber network structure of fibrils with an average diameter of 70-80 nm. Together, the mesh of these fibrils forms a gelatinous membrane. The size of BC fibrils is about 10-20 times smaller than that of regenerated plant cellulose, whereas a sample of regenerated plant cellulose had a microfiber network structure of fibrils with an average diameter of 500-800 nm, as demonstrated in Figure 2.4 (Phisalaphong et al., 2007). This unique structure in nano-scale results in a larger surface area. It is extremely hydrophilic, absorbing 60 to 700 times its weight in water (Suwanmajo, 2006). BC retains its long fibrils and exceptional strength because it is formed in a hydrophilic matrix and needs no treatment.

2.1.3 Modification of bacterial cellulose

Alteration of BC morphology during its biogenesis is a concept that uses various polymers to investigate the facet of cellulose formation in BC was review by Brown (2007). The modification of bacterial cells is another way to alter BC morphology was showed in Table 2.2. As miscible polymers such as hemicelluloses, cellulose derivatives and dyes are added into the BC-producing bacterium growth medium, the aggregation of nanofibers is altered due to the competitive adsorption of polymers in the medium. Polymerization and crystallization are separable mechanisms in BC biogenesis. Subsequent to BC polymerization, the polymer added in the medium can associate and co-crystallize with BC, producing an intimately blended composite material.

Table 2.2 Modification of BC Biogenesis (Brown, 2007).

Modification	**Resulting**
Xyloglucan	-Crystallity of fibrils was changed. -Lower stiffness or breaking stress.
Xylan	-Ribbons were coherent, heavy bundles instead of flat and twisting. - Ribbon width decreased as aggregation of fibril subunits was controlled.
Phosphomannan	-Fibrils are oriented in parallel. -Aggregation time of fibrils is delayed.
Pectin	-Increased extensibility and decreased breaking stress compared to pure BC.
Glucomannan, Galactomannan	-Induced coalescence of fibrils and dramatic reduction of crystallinity.
Glucuronoxylan,	-Crystallinity of BC was modified.
Dextransucrase, Alternansucrase	-Produce soluble BC with new structure.

2.1.4 Chitin and Chitosan

Chitin is recognized as the second most myriad of polysaccharide after cellulose. Chitin is a natural component in crustaceans which was obtained from shell fish, crabs, prawn, shrimp and some insects. It can be produced from some microbial. Chitin and chitosan have nearly similar feature as shown in Figure 2.5. Chitin is consisted of a linear chain of acetyl glucosamine groups whereas chitosan is obtained by extracting enough acetyl groups ($CO\text{-}CH_3$), this process is called deacetylation. The term “degree of deacetylation” is used to represent the amount of N-glucosamine units in molecules. If the degree of deacetylation is higher than 50%, it will be classified as chitosan. In contrast, when the deacetylation is lower than 50%, the term chitin is used (Krajewska, 2004).

Chitosan can be dissolved in agent such as 1-10% (v/v) aqueous acetic acid (pH below 6). Free amine groups in chitosan renders polyelectrolytic effect to the polymer backbone. These groups are also active sites for many chemical modification and conjugations. Organic acid such as acetic, formic, and lactic acids are used for dissolving chitosan and most commonly used is 1% acetic acid solution (pH~4.0). Chitosan is soluble in 1% hydrochloric acid but insoluble in sulfuric and phosphoric acids. The solubility of chitosan solution is poor above pH 7. At higher pH, precipitation or gelation will occur. Chitosan form polycation complex with anionic hydrocolloid and provides gel. Like cellulose, chitosan functions normally as a structural polysaccharide, but differs from cellulose in its properties. Chitosan have unique properties, including polyoxy salt formation, ability to form films, cheated metal ions and optical structural characteristics (Majeti and Kumar, 2000). Hence, chitosan has well chemical and biological qualities that can be used in many medical applications.

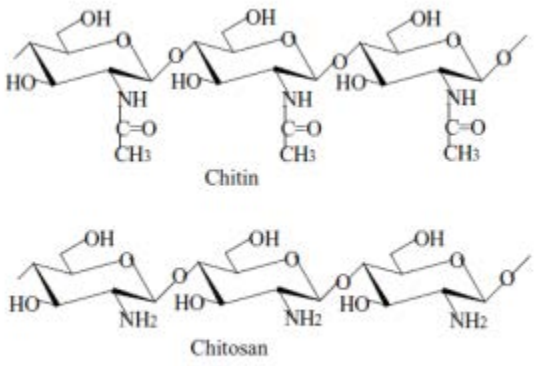

Figure 2.5 Structure of chitin and chitosan (Krajewska, 2004).

The applications of chitosan have been found in many fields, for instance, wastewater treatments, photography, cosmetics, opthalmology, agricultures, paper finishing, drug-delivery systems, food industries, and etc (Majeti and Kumar, 2000). In an artificial skin, chitosan has many distinctive biomedical properties. Chitosan, with the structural characteristics similar to glycosamino glycans, chitosan could be considered for developing substratum for skin replacement. Moreover, chitosan may be used to inhibit fibroplasia in wound healing, and to promote both tissue growth and differentiation in tissue culture (Muzzarelli et al., 1999). Chitosan is useful as a wound management aid to reduce scar tissue. Other applications have also been discovered in controlled release of lactic acid bacteria during butter and cottage cheese production by encapsulating the bacteria in chitosan beads (Majeti and Kumar, 2000). Chitosan has been used in the regenerative medicine. Its characteristic properties have been reviewed by Muzzarelli (2009) as shown in Table 2.3.

Table 2.3 Characteristic of chitosan in regenerative medicine

Application	Characteristic properties
Wound healing	- Chemoattraction and activation of macrophages and neutrophils to initiate the healing process. - Promotion of granulation tissue and re-epithelization. - Entrapment of growth factors to accelerate the healing. - Limitation of scar formation and retraction. - Stimulation of integrin-mediated cell motility and increase in vitro angiogenesis. - Release of glucosamine and N-acetylglucosamine monomers and oligomers, and stimulation of cellular activities. - Intrinsic antimicrobial activity and controlled release of exogenous antimicrobial agents to prevent infection.

2.1.5 *Aloe vera*

Aloe vera (*Aloe barbadensis* Miller) is a member of the *Liliaceal* family. It is a cactus-like plant that grows in hot and arid areas widely scattered in the Mediterranean Sea, Middle East, Africa, China, Japan, and the Southern U.S.A. *Aloe vera* is a perennial plant with turgid green leaves joined at the stem in a rosette pattern. The leaves of a mature plant have a saw-like spike along their margins, which grow from a short stalk near ground.

Aloe vera leave contains two major liquid sources, yellow latex from the outer layer (exudate) and the clear gel from the inner layer (mucilage). The yellow latex contains glycosidic derivative of anthraquinones such as aloin (barbaloin), aloesin, p-coumaric acid, aloe-emodin, etc., which are very bitter in taste. The fresh clear gel is about 98.5 to 99.2 % water. The total solid that remains after the water have been removed ranges from 0.8 to 1.5 % of the total weight (Femenia et al., 1999, McAnally, 1999; Surjushe et al., 2008). The major constituents of that solid are mucilage, fiber, monosaccharides, polysaccharides, proteins, glycoproteins, vitamins, ash, fats, aloin, resin, and low–molecular-weight substances such as ß-sitosterol,

diethylhexylphthalate, vitamins, and beta-carotene (McAnally, 1999). More than 60% of the remaining solid being made up of polysaccharides (Femenia et al., 1999). Aloe polysaccharides consist of linear chains of β 1-4 linked glucose and mannose molecules: owing to the presence of these two simple hexose sugars, they are also called glucomannans. The linear chains range in size from a few molecules to several thousand molecules. Different molecular-sized fractions may possess different physical characteristics and widely differing potential biological activities. Compositions that include enzymes, organic acids, inorganic salts, amino acids and alkaloids have been noted (McAnally, 1999). Different investigators have reported different polysaccharide structures, which may be due to different geographical origins or to the use of different varieties or subspecies. Acetylated mannan has a range of interesting biologic activities as described below. Recently the effect glycoproteins on cell proliferation- promoting activity have been reported (Yagi et.al., 1997).

The ingredients and they properties, which found in an *Aloe vera* leaf they have been many reported (Surjushe et al., 2008). They are divided into the following categories and shown in Table 2.4

Table 2.4 Ingredients contained in the *Aloe vera* leaf (Surjushe et al., 2008).

Ingredients	**Advantages**
Ligin	-It posses the property of penetrating the human skin.
Saponins	-They have been used in detergents, foaming agents and contain antiseptic properties.
Sugars	-Monosaccharides, such as glucose and fructose, and polysaccharides. Polysaccharides are the most important types of sugars. They aid in proper digestion, maintain cholesterol levels, improve liver functions and promote the strengthening of bones.
Amino Acids	-Amino Acids are the building blocks of proteins, which manufacture and repair muscle tissue.

Table 2.4 (continue) Ingredients contained in the *Aloe vera* leaf.

Ingredients	Advantages
Minerals	-Calcium: essential for proper bone and teeth density. -Manganese: a component of enzymes necessary for the activation of other enzymes. -Sodium: controls the body fluids not become high acidic/alkaline. -Copper: enable iron to work as oxygen carriers in the red blood cells. -Magnesium: used by nerves and muscle membranes to help conduct electrical impulses. -Potassium: regulate the acidic or alkaline levels of body fluid. -Zinc: contribute to the metabolism of proteins, carbohydrates and fat. -Iron: controls the transportation of oxygen around the body via the red blood cells.
Vitamins	-Vitamins A, C, and E: crucial antioxidants that combat dangerous free radicals in the body. -Vitamin B & Choline: concerned with the production of energy, amino acid metabolism and developing muscle mass. -Vitamin B12: responsible for the production of red blood cells -Folic acid: help develop new blood cells.
Enzymes	-Peroxidase, Aliiase, Catalase, Carboxypeptidase, Lipase, Cellulase, Amylase, and Alkaline Phosphatase. They help to break down food and assist in digestion. Some enzymes help break down fats while others break down starches and sugars.
Sterols	-Sterols are important anti-inflammatory agents. -Cholesterol, Sitosterol, Campesterol and Lupeol. These sterols contain antiseptic and analgesic properties. They also have pain killing properties similar to aspirin.

2.1.6 Wound healing and wound dressing

The healing process begins after the patient was injured or surgical immediately. Normal wound healing is a dynamic process proceeds via progression through three overlapping phases: inflammation, granulation or proliferation (tissue formation) and re-epithelialization or maturation (tissue remodeling). The healing mechanism involves various factors, such as wound types, cell types, biochemical factors and extracellular matrix molecules (Schonfelder, 2005). Hanna (1997) explained the three phases of wound healing; the inflammatory stage or substrate stage occurs immediately after wounding and lasts approximately four days. In these stage are consist of many processes for examples, hemostasis, debridement, and decontamination. The proliferative or fibroblastic stage begins after the end of inflammatory stage and lasts approximately 21 days. Collagen synthesis, neovasculature formation, and re-epithelialization processes had occur in this state. Maturation or remolding is the final state of wound healing. This stage starts at approximately 21 days post- injury and continues until 1-2 years after injury. The phases of wound healing are summarized in Figure 2.6.

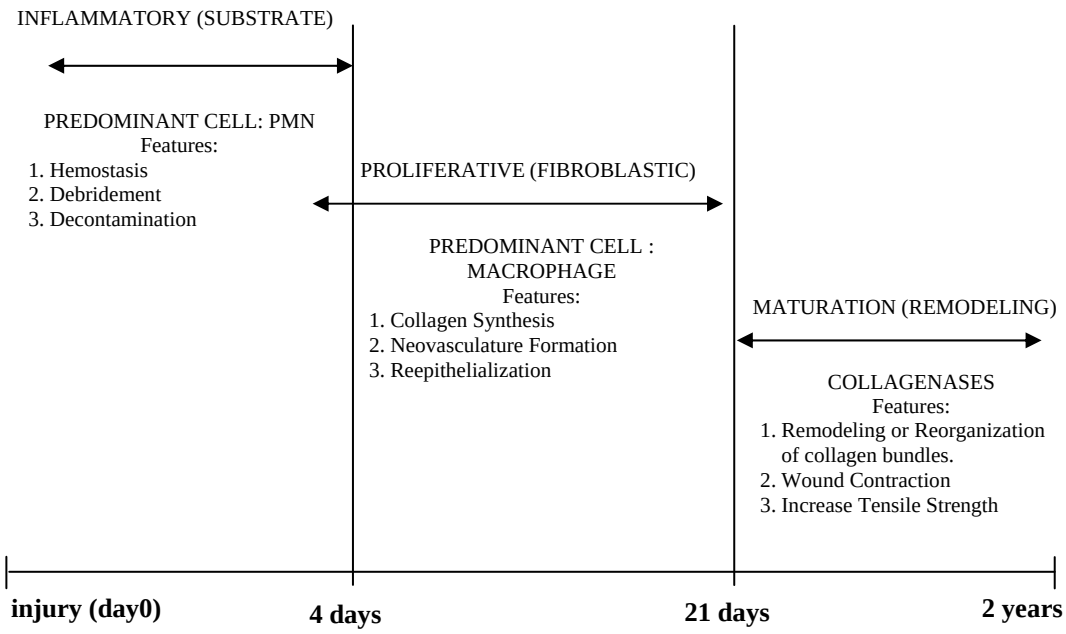

Figure 2.6 Timeline of normal wound healing phases (Hanna, 1997).

Stashak et al. (2004), summarized the suitable properties of material used for wound dressing should had an ability to absorb exudates and toxic components from the wounds surface, maintain a high humidity at the wound/dressing interface, allow gaseous exchange, provide thermal insulation, protect the wound from bacterial penetration, be nontoxic, be removed easily without trauma to the wound. Moreover, It should be acceptable handling qualities (resistance to tear and disintegration when wet or dry), and be sterilizable.

In past, wound healing was covered and maintained by natural dressing for example own patient tissue and other foreign matter. Wound closure require a material to restore the epidermal barrier function and became incorporated into wound healing, whereas materials used for wound cover rely on the ingrowths of granulation tissue for adhesion (Hanna, 1997). For a modern wound healing, the new alternative materials which used as wound dressing were developed by several researchers.

2.2 Literature review

2.2.1 Bacterial cellulose of medical applications

Bacterial Cellulose (BC), produced by *Acetobacter* species, has gained attention in the research realm for its favorable properties; such as its remarkable mechanical properties in both dry and wet states, ultra-fine network structure, porosity, water holding capacity, high degree of crystallinity, moldability, biodegradability and excellent biological affinity (Shoda and Sugano, 2005; Sanchavanakit et at., 2006). Because of these properties, BC has a wide range of potential applications as a food matrix, a dietary fiber, an acoustic or filter membrane and ultra-strength paper, including use in the biomedical field such as a temporary dressing to heal skin burns and as scaffold in tissue engineering fields. It is expected to be a new biochemical commodity with diverse applications, if its mass production process could be improved.

Fontana et al. (1990), study the application of BC as temporary skin substitutes. The product, called Biofills, can provide non-woven, shaped objects in medicine such as artificial skin for burn and skin injury treatment. It displays dramatic

clinical results such as immediate pain relief, diminished post-surgery discomfort, faster healing, reduced infection rate, and reduced treatment time and cost. Moreover, Mayall et al., (1990) used a Biofill skin substitute in the treatment of trophic ulcerations of the limbs and showed that this material was very effective by shortening the cicatrisation time, reducing the contamination, and saving the cost of treatment.

Klemm et al. (2001) Synthesized BC in tubular shape by grown it in a static culture molded in BASYC® tubes (a hollow – shaped tube mimicking blood vessel shape).They found that BC microvessels have high mechanical strength in wet state, enormous water retention value, low surface roughness of inner surface, high moldable in situ and it can sustain a mean tensile force of 800 mN. The author reported that the white rats that the BASYC® tube was covered with the connective tissue and small vessel. Neither an inflammation reaction nor an encapsulation of the implant was observed. These results demonstrate the high potential of BASYC® as an artificial blood vessel in microsurgery.

Yang et al. (2002) reported the composite chitosan–cellulose membranes prepared by coating chitosan on filter paper. They found that the tensile strength of the composite membranes coated with different chitosan concentrations increases with increasing chitosan concentration. The obtained composite membrane provided tensile strength larger than the plain cellulose support, in both wet and dry states.

Cienchanska (2004) reported that the composite material which made form Bacterial cellulose and chitosan have good mechanical properties in wet state, high moisture-keeping properties, release of mono- and oligosaccharides under lysozyme action, bacteriostatic activity against Gram negative and Gram positive bacteria and bactericidal activity against Gram positive bacteria. These features make modified bacterial cellulose an excellent dressing material for treating different kinds of wounds, burns and ulcers.

Svensson et al. (2005) demonstrated that BC supports chondrocyte proliferation. When compared to tissue culture plastic and alginate, BC showed significantly higher levels of chondrocyte growth at similar levels of in vitro immune response. The Young’s modulus of BC was in the same range as articular cartilage.

These result indicated that BC appeared to have potential as a scaffold for tissue engineering of cartilage.

Backdahl et al. (2006) evaluated the potential of bacterial cellulose to function as a scaffold for tissue engineered blood vessels in vitro. The nanofibrils' network of BC was much denser close to the medium/air transition zone than on the opposite side (porous side). The Young's modulus matched carotid arteries, about 3 MPa. BC allowed room for human smooth muscle cells (SMCs) ingrowth and proliferation. SMCs attracted to both side of the BC. Thus, BC exhibited properties that were promising for use in future tissue engineered blood vessels.

Czaja et al. (2006) studied on Biofills that provided non-woven, shaped objects in medicine such as artificial arteries, vessels, skin, and etc. It still has been utilized for several skin injury treatments such as basal cell carcinoma/skin graft, severe body burns, facial peeling, sutures, dermabrasions, skin lesions, chronic ulcers, and both donor and receptor sites in skin grafts. In addition, the wound healing effects of never-dried BC were fully biocompatible and also successfully protected burn wounds from excessive external fluid loss, thus accelerating the entire process of healing.

Sanchavanakit et al. (2006) studied the growth of human keratinocytes and fibroblasts on bacterial cellulose film. Their results were the first direct demonstration that BC film supported the growth, spreading, and migration of human keratinocytes but not those of human fibroblasts.

Wan et al. (2006) studied on synthesis and characterization of hydroxyapatite (HAp)-bacterial cellulose (BC) nanocomposites. They found that HAp crystals were observed on the surfaces of BC fibers previously phosphorylated, modified in a $CaCl_2$ solution, and finally soaked in 1.5 SBF. The thickness of the HAp depositions could be controlled by soaking duration. It was concluded that porous HAp-BC nanocomposites could be prepared via a biomimetic process. The XRD and FTIR analysis demonstrated that the HAp crystals formed on the BC had low crystallinity and the crystallite size were in nano scale and the formed HAp crystals contained certain carbonate, resembling the natural bone apatites. Therefore, the result indicated that the HAp-BC with porous 3-D network structure and expected high

mechanical performance were good prospect to be explored as alternative materials in bone tissue engineering filed.

Luo et al. (2008) demonstrated the composite collagen–bacterial cellulose (COL/BC) membranes were prepared by adding collagen to the culture medium of *Acetobacter xylinum*. They found that the structure of BC network changes when collagen was present in the nutrient medium. The micro-morphology of COL/BC was more rugged and porous than that of BC.

Cai and Kim, (2009) developed a new bio-composite material by immersing wet BC pellicle in poly ethylene glycol (PEG) aqueous solution followed by freeze-drying process. The result showed that BC/PEG has a very well interconnected porous network structure and large aspect surface. SEM images showed that PEG molecules was coated on the BC fibril surface and penetrated into BC fiber networks. The TGA result showed that the thermal stability was improved but the Young's modulus and tensile strength tended to decrease. Biocompatibility of composite was preliminarily evaluated by cell adhesion studies using 3T3 fibroblast cells. The cells incubated with BC/PEG scaffolds for 48 h were capable of forming cell adhesion and proliferation, which showed much better biocompatibility than the pure BC.

2.2.2 Chitosan for medical applications

Chitosan has been studied widely as a wound dressing material, and known in many medical applications, for instance, implantation, topical ocular, transparent membrane, and wound-healing. It was employed for tissue reconstruction and wound healing. Biochemistry and histology of chitosan in wound healing has been reviewed by Muzzarelli (1989). Application of chitosan wound dressing made the chronic ulcers heal faster. The graft take was excellent and the re-epithelialization process was faster. It was extremely satisfactory particularly at donor site with painless healing. Chitosan could use to inhibit fibroplasia in wound healing, to promote tissue growth, and to differentiate in tissue culture (Muzzarelli et al., 1999). Moreover, it has an aptitude to stimulate cell proliferation and histoarchitectural tissue organization (Muzzarelli, 1989).

The biological properties like bacteriostatic and fungistatic properties are particularly useful for wound treatment. The antimicrobial properties are particularly useful for wound treatment. Chitosan possess the antimicrobial activity, coming from various factors, such as molecular weight, degree of deacetylation, pH-value, and temperature. However, the main factors affecting the antibacterial activity of chitosan are molecular weight and concentration (Liu et al., 2006).

Kendra and Hadwiger (1984) examined the antifungal effect of chitosan oligomers on *Fusarium solani* f. sp. *pisi* and *Fusarium solani* f. sp. *phaseoli*. The antifungal activity of chitosan oligomers on tested fungi was found to increase as the polymer size increased.

Chitosan is effective in inhibiting growth of bacteria. Wang (1992) examined the antibacterial effects of chitosan in vitro against a variety of bacteria typical in food. Chitosan was most effective against *Staphylococcus aureus* and *Escherichia coli.*

Fang et al. (1994) reported that the growth of *Aspergillus niger* was inhibited by chitosan. Chitosan at the concentration of 5.0 mg/mL induced considerable leakage of UV-absorbing and proteinaceous materials from *Aspergillus niger* at pH 4.8.

Jeon et al. (2001) studied the antibacterial effects of three different molecular weight chitosan. Bactericidal activity against all bacteria decreased with decreasing molecular weight.

The blending of polymers, for new materials with improving chemical and physical properties, has been received considerable attention of many researchers in the past several decades. The final properties of the blends are determined by the miscibility of the polymers, which is greatly favored by formation of intermolecular hydrogen bonds between the component polymers (Yin et al., 2006). Because of the similar structure between cellulose and chitosan, there may be sufficiently similar to facilitate the formation of homogeneous composite films. Suto and Ui (1996) displays the chemical cross-linking of chitosan/hydroxypropyl-cellulose blends with glyoxal and glutaraldehyde. Based on the similarity of the backbones of chitosan (CHI) and hydroxypropylcellulose (HPC) they assumed that these polymers were miscible in the blend. The cross-linked films were shown to be amorphous, although the uncross-

linked films retained cholesteric liquid crystalline order. It has been reported that the hydrophilic property of chitosan could be modified via blending with PEG and PVA (Kweon and Kang; 1999; Zhang et al., 2002).

Wu et al. (2004) prepared new composite material, chitosan and cellulose blends using trifluoroacetic acid as a co-solvent. The cellulose-chitosan membranes used as a wound dressing might prevent wound from excessive dehydration. The chitosan-cellulose blend membranes demonstrated effective antimicrobial capability against *Escherichia coli* and *Staphylococcus aureus*. These results indicated that the chitosan-cellulose blend membranes might be suitable to be used as a wound dressing with antibacterial properties. Also blending cellulose with chitosan was expected to be a useful method to improve the mechanical

2.2.3 *Aloe vera* for medical applications

The whole gel extract of *Aloe vera* has been reported to have various pharmacologic properties, specifically to promote wound, burn, and frost-bite healing, in addition to having anti-inflammatory, antifungal, and hypoglycemic properties (Reynolds et al., 1999).Wound healing is considered to be composed of three overlapping events: inflammation, new tissue formation, and matrix remodeling (Dunphy et al., 1974; Krishnan, 2006). Protein factors related to wound healing have been investigated, such as growth factors, cell migration related factors, matrix-forming factors, and matrix-degradation factors.

Winters et al. (1981) Studied about lectin-like substance in *Aloe vera* gel from fresh leaf and commercial *Aloe vera* gel extracts. From the results revealed that the fresh leaf substance have been promoted the attachment and growth of normal human cells, but not tumor cells; while, the commercial *Aloe vera* gel substance were found equally cytotoxic to normal human and tumor cells.

Agarwal (1985) studied the effect of oral consumption of *Aloe vera* gel on risk factors of heart disease. Five thousand patients were presented symptoms of heart disease. The patients consumed breads prepared with wheat flour and *Aloe vera* gel at two meals a day for a period of three months. There was a marked reduction in

total lipids, serum cholesterol, and serum triglycerides. In addition, patients who also had diabetes showed reductions in fasting and post-meal blood glucose levels.

Davis et al. (1989) evaluated the effects of food grade and colorized *Aloe vera* on full thickness wounds induced in ICR mice. In an oral study, mice received the food grade *Aloe vera* (100 mg/kg/day) in the drinking water for two months. For a topical study, mice received 25% colorized *Aloe vera* in a vehicle cream or vehicle cream alone on each wound for 6 days. Wound diameter was used as a measure of healing in control and treated animals. In both studies, wounds healed more rapidly in *Aloe vera* treated mice compared to untreated or vehicle controls, suggesting that food grade and colorized *Aloe vera* were effective treatments in the healing of wounds. In 1992, Davis et al. reported that *Aloe vera* gel extract stimulated fibroblast growth in a synovial model and also enhanced wound tensile strength and collagen turnover in wound tissue

Visuthikosol et al. (1995) studied effect of *Aloe vera* gel to healing of burn wound compared with vaseline gauze. Twenty-seven patients with partial thickness burn wound were treated with *Aloe vera* gel and vaseline gauze. They found that *Aloe vera* gel treated lesion healed faster than the vaseline gauze area. The average time of healing in the aloe gel area and vaseline gauze for treated burn wound were 11.89 and 18.19 days, respectively.

Ferro et al. (2003) suggested that *Aloe vera* gel could inhibit the growth of gram-positive bacteria, *Shigella flexneri* and *Streptococcus pyrogenes* . Effective growth inhibition for up to 24 hours was achieved with concentrations of 100 mg of *Aloe vera* gel per ml. The activities of *Aloe vera* gel were low in comparison with the activities ampicillin and nalidixic. However, it was suggested that the use of *Aloe vera* as an ingredient in anti-microbial products might be beneficial given the direct effect of the gel on accessible areas of the body.

Yoa et al. (2009) studied effect of API, a polysaccharide fraction was isolated from fresh *Aloe vera* leaves on human fibroblasts proliferation. They reported that the API has an excellent protect activity to fibroblasts; no cytotoxicity and it can promote proliferation of human fibroblast *in vitro*. The authors have discussed that, for the therapeutic action of API to burns, the promotion proliferation activity to

fibroblasts could result from the positive effect of API on the production of glucogen, DNA synthesis, and the formation of collagen in human fibroblast.

Jettanacheawchankit et al. (2009) investigated the effects of Acemannan on Gingival fibroblasts (GFs) proliferation keratinocyte growth factor-1 (KGF-1), vascular endothelial growth factor (VEGF), and type I collagen production. Acemannan, β-(1,4)-acetylated polymannos, was extracted from fresh *Aloe vera* pulp gel by homogenization, centrifugation, and alcohol precipitation. The researchers treated GF cells with different concentrations of acemannan. They found that acemannan had no cellular toxicity towards GFs and significantly induced newly DNA synthesis. Acemannan concentrations between 2–16 mg/ml significantly stimulated KGF-1, VEGF, and type I collagen expressions. These findings suggest that acemannan have a significant in the oral wound healing.

CHAPTER III
EXPERIMENTAL

3.1 Material and chemicals

3.1.1 Microbial strains

The *Acetobacter xylinum* strain AGR 60 kindly supplied by Mr. Pramote Tammarat, the Institute of Food Research and Product Development, Kasetsart University, Bangkok, Thailand was used in this study.

3.1.2 Chemicals

The details of chemicals used in this experiment are shown in Table 3.1.

Table 3.1 The chemicals used in this experiment.

Chemical	Supplier (country)
Sucrose	Ajax Finechem (Australia)
Ammonium sulfate	Ajax Finechem (Australia)
Sodium hydroxide	Rankem (India)
Acetic acid	QRec (New Zealand)
Chitosan	Seafresh Chitosan (Lab) company limited (Thailand)
Aloe vera	Local market, Ban Phaeo, Samut sakhon, (Thailand)
Ethanol	Mallinckrodt (Malaysia)
Sodium chloride	Ajax Finechem (Australia)
Sodium acetate	Loba Chemie (India)

Table 3.1(continue) The chemicals used in this experiment.

Chemical	Supplier (country)
Hydrochloric acid	Ajax Finechem (Australia)
Glucose	Carlo Erba Reagenti, Italy
Mannose	Fluka Chemical, switzerland
3,5 dinitrosalicylic acid (DNS)	Fluka Chemical, switzerland
Sodium potassium tartrate tetrahydrate	Carlo Erba Reagenti, Italy
Dimethylsulfoxide (DMSO)	Merk Schuchardt, Germany
Thiazolyl Blue Tetrazolium Bromide (3-(4,5-Dimethyl-2-thaizolyl)-2,5-diphenyl-2H-tetrazolium bromide)	USB Corpoation, USA

3.1.3 Equipments

- Scanning electron microscopy, SEM (JOEL JSM-5410LV, Tokyo, Japan)
- Fourier Transform Infrared (FTIR) spectrometer (Perkin Elmer Spectrum One Massachusetts, USA)
- Universal Testing Machine (Hounsfield H 10 KM, Redhill, England)
- X-ray diffraction (Bruker AXS Model D8 Discover,USA)
- Brunauer-Emmett-Teller (BET) surface area analyzer (Model ASAP 2020, USA)
- UV-vis spectrophotometer (Shimadzu UV-2550, Tokyo, Japan)
- Autoclave (Model Tomy Autoclave SS-325, Nerima-ku, Tokyo, Japan)
- Moulinex blender (Model DAE1, Thailand)
- Microplate reader (Bio-Rad Benchmark 550, California, USA)

3.2 Culture media and methods

3.2.1 Culture medium and bacterial cellulose preparation

The medium for the inoculums was coconut-water supplemented with 5.0% (w/v) sucrose, 0.5% (w/v) ammonium sulfate $(NH_4)_2SO_4$, and 1.0% (v/v) acetic acid. The culture medium was sterilized at 110 ^{0}C for 5 min. Preculture was prepared by transferring cells from a stock culture to 500 ml medium, and incubated statically at 30 ^{o}C for 7 days. The preculture broth was added to the main culture medium and 75 ml activated medium was placed in a glass Petri dish (φ 14.5 cm) and incubated at 30 ^{0}C for 7 days. All samples were first purified by washing with distilled water and then they were treated with 1% (w/v) NaOH at room temperature to remove bacterial cells followed by a rinse with distilled water until pH came to neutral. Afterward, the wet purified BC pellicle was air-dried at room temperature (30 ^{0}C) and stored in plastic film at room temperature.

3.2.2 Impregnated bacterial cellulose-chitosan film preparation

The wet purified BC pellicle was immersed in chitosan (Mw of 30,000, 80,000, and 200,000) - acetic acid solution for 36 h. Then all samples were air-dried by placing them on Teflon sheet at room temperature. In order to remove remaining acetic acid from the BC-chitosan (BC-C) composite film, the film was rinsed in distilled water at room temperature for several times until the pH became neutral. Afterward, the film of BC-C - free acetic acid was air-dried at room temperature (30 ^{0}C) and stored in plastic film at room temperature.

3.2.3 Impregnated bacterial cellulose-*Aloe vera* film preparation

Aloe vera gel was prepared by aseptic technique. After harvesting, the *Aloe vera* leaves were washed with tap water. In order to obtain the *Aloe vera* gel, the epidermis or green rind of *Aloe vera* leaf was removed and washed with distilled water several times to remove the exudates from it gel surface. The washed gels were

immersed in 70% ethanol for 15 minute and then they were rinsed with sterilized distilled water to remove the residual ethanol. Afterward the sterilized gels were homogenized in a sterilized household blender. The sterilized homogenize gels were freshly prepared before used. The wet purified BC pellicle was immersed in *Aloe vera* gel for 36 h afterward, the BC-*Aloe vera* (BC-A) film was air-dried at room temperature ($30\ ^0$C) and stored in plastic film at room temperature.

3.3 Characterization

The developed films were characterized by Scanning electron micrographs (SEM) for investigating morphology, by Brunauer-Emmett-Teller (BET) for determining the pore size, porosity, and pore size distribution, by universal testing machine for determining tensile strength, Young's modulus, and elongation at break, by Fourier transform infrared (FT-IR) spectrometer for identifying the chemical structure, and by X-ray diffraction(XRD) for estimating crystallinity index. Moreover, biological characteristic of the films were investigated by *in vitro* study of human cells on the developed films in individual wells of falcon twenty-four-well plates.

3.3.1 Morphology

The examination of the film morphology was performed by scanning electron microscopy (SEM) (JSM- 5410LV, JOEL, Tokyo, Japan) at Scientific and Technological Research Equipment Centre, Chulalongkorn University. The BC, BCC and BCA films were frozen in liquid nitrogen, immediately snapped, and vacuum-dried. Then, the samples were sputtered with gold in a Balzers-SCD 040 sputter coater (Balzers, Liechtenstein) and photographed. The coated specimens were kept in dry place before experiment. SEM was obtained at 15 kV which is considered to be a suitable condition since too high energy can be burn the samples.

3.3.2 Fourier transform infrared spectroscopy

Fourier transform infrared (FTIR) spectroscopy (Spectrum One, Perkin Elmer, Massachusetts, USA).is used primarily to identify the chemical structure of the samples (BC, BCC, BCA films and chitosan powder). All samples were ground into small pieces, mixed with Potassium bromide (KBr) in the ratio 1:100 by weight (sample 1 mg/KBr 100 mg) and then compressed into pellet. FTIR spectra of the developed film were recorded with Perkin Elmer (Spectrum One, Massachusetts, USA) in the region of 4000–400 cm^{-1} and the resolution equal to 4.0 cm^{-1} at Scientific and Technological Research Equipment Centre, Chulalongkorn University.

3.3.3 X-Ray diffraction

X-ray diffraction (XRD) patterns of the polymers and BC/BC-composite were determined with a diffactometer (Bruker AXS Model D8 Discover, USA). The operation conditions were as follows: power 40 kV and 30 mA. The crystallinity index (C.I.) was calculated from the reflected intensity data using the Segal et al. method, and calculated using the following formula:

$$C..I.(\%) = \frac{\left(I_{020} - I_{am}\right)}{I_{020}} \times 100$$

Where I_{020} is the maximum intensity of the lattice diffraction, and I_{am} was the intensity at $2\theta = 18^{o}$.

3.3.4 Brunauer-Emmett-Teller

Pore size and surface area of the samples were measured by a Brunauer-Emmett-Teller (BET) surface area analyzer (Sorptomatic 1990, Quantachrome Instruments, Florida, USA). The samples were placed in the sample cell, which was then heated up to 75 °C and held at this temperature for 5 h. The samples were cooled down to room temperature and ready to measure the surface

area. There were three steps to measure the surface area: adsorption step, desorption step and calibration step.

3.3.5 Mechanical property

In this study, the tensile strength, Young's modulus and elongation at break of BC, BCC and BCA dried films were measured by Universal Testing Machine (Hounsfield H 10 KM, Redhill, England) at Scientific and Technological Research Equipment Centre, Chulalongkorn University. The load cell capacity was 1 kN. The film samples were cut into strip-shaped specimens 10 mm width and 10 cm length. The test conditions followed ASTM D882 as a standard test method for tensile elastic properties. Two ends of the specimens were placed between the upper and lower jaws of the instrument, leaving a length of 6 mm of film in between the two jaws. Extension speed of the instrument was 10 mm/min. The tensile strength and break strain were the average value determined from at least five specimens.

3.3.6 Water absorption capacity

The water absorption capacity (WAC) was determined by immersing the pre-weighted of dried samples in distilled water at room temperature until equilibration. The sample was then removed from the water. After excess water at the surface of the sample was blotted out with Kimwipes paper, the weight of the swollen sample was measured and the procedure was repeated until there was no further weight change. Water content was determined by gravimetric method (Kim *et al*., 1996) and calculated using the following formula:

$$WAC(\%) = \frac{W_h - W_d}{W_d} x100$$

Where W_h and W_d denoted the weight of hydrate and dry sample, respectively.

3.3.7 Water vapor permeability measurement

The water vapor transmission rate (WVTR) of the BC, BCC and BCA films with area of 50.00 cm^2, was measured at Thai packaging centre, Thailand Institute of Scientific and Technological Research. The test conditions followed ASTM E-96 with desiccant method. The determination of WVTR was done at 38 ^oC and 98% relative humidity. The test specimen was sealed to the open mount of test dish containing a desiccant, and the assembly placed in a controlled atmosphere. Periodic weighting was performed to determine the rate of water vapor movement through the specimen into the desiccant.

3.3.8 Oxygen permeability measurement

The oxygen transmission rate (OTR) of the dried BC, BCC and BCA films was determined with an oxygen permeation analyzer: Illinois Instruments (Johnsburg, IL) Model 8000 at Thai packaging centre, Thailand Institute of Scientific and Technological Research. The test condition followed ASTM D3985. The determination of OTR was done at 23 ^oC and 0 % relative humidity. The film was held in such a manner that it separated two side of test chamber. One side was exposed to a nitrogen atmosphere, while the other side was exposed to an oxygen atmosphere. A. Testing was completed when the concentration of oxygen in the nitrogen side was constant.

3.3.9 Antimicrobial ability testing

The antimicrobial properties of BC, BCC, and BCA films were examined against 3 types of bacterial and fungal strains: *Escherichia coli*, *Staphylococcus aureus*, and *Aspergillus niger*. The films were cut into round-shaped sample of 38 mm diameter according to the method described by AATCC TM 39-1989. The incubation was 24 h at 37 °C under aerobic conditions for *Escherichia coli* and *Staphylococcus aureus* while the test of *Aspergillus niger* was performed in the AGAR plate for a week of inoculation at 30°C. Before the antibacterial and antifungal

assay, all BC, BCC, and BCA films were sterilized by UV irradiation for 20 min in each side.

3.4 *In vitro* cells study

In this study, the cytotoxicity of BC and BC-composite films against L929 mouse fibroblasts was evaluated. In addition, the tissue compatibility of BC and BC-composite films was evaluated by growth and spreading of keratinocytes and fibroblasts on each material. The test samples were punched into round-shaped samples of 14 mm diameter. The samples were sterilized by UV irradiation for 20 min in each side and transferred aseptically to 24-well culture plates. Proliferations of cells on the films were determined by MTT assay. The experiments were conducted in triplicate. The number of living cells was determined using MTT assay.

3.4.1 Cytotoxicity test

The cytotoxicity was evaluated based on a procedure modified from the ISO10993- 5 standard test method using the mouse fibroblast cell line L929 purchased from the American Type Culture Collection. The experiments were conducted in triplicate. The cell culture was cultured in Dulbecco's modified Eagle's medium supplemented with 10% fetal bovine serum, 100 units/ml penicillin, 100 μg/ml streptomycin, 1% L-glutamine and 2 mg/l lactalbumin. The cultures were maintained at 37°C in a humidified atmosphere of 5% CO_2 and 95% air. A single-cell suspension of L929 cells was obtained after trypsinization, and the cells were counted in a hemocytometer. The films were sterilized by UV irradiation for 20 min in each side, transferred aseptically to 24-well culture plates and incubated at 37◦C in serum-free culture medium (SFM) for 24 h. The weight of film per volume of medium ratio was 10 mg/ml. The extraction medium from the film incubation was used to culture L929 mouse fibroblast cells. SFM was used as control. The cells were cultured in 24-well plates at concentrations of 5×10^4 cells in 500 μl culture medium per well, and the cells were allowed to attach to the plates for 16 h in a humidified atmosphere of 5% CO_2 and 95% air at 37°C. Then, the cell-culture medium was replaced with 500 μl of

the 100% (v/v) extraction medium, the 50% (v/v) extraction medium or the control medium. The number of living cells was finally quantified using the 3-(4, 5-dimethyl-2-thiazolyl)-2,5-diphynyl-tetrazoluim bromide (MTT) assay.

3.4.2 Attachment and proliferation

Two types of cells were used in this study: human-transformed skin keratinocytes (HaCat) and human gingival fibroblasts (GFs). Keratinocytes and fibroblasts were grown in DMEM supplemented with 100 units/ml penicillin, 100 μg/ml streptomycin and 10% FBS. When the cells reached 80% confluence, they were serially sub-cultured. For fibroblast, cells from the 3^{rd} to the 7^{th} subculture passages were used in the described experiments. Both cultures were incubated at 37°C in a humidified atmosphere containing 5% CO_2. Air-dried BC and BC composite films were punched into round samples of 14 mm in diameter. The samples were sterilized by UV irradiation for 20 min in each side and transferred aseptically to 24-well culture plates. The experiments were conducted in triplicate. Culture medium (500 μl) was added to each well to equilibrate the samples for 30 min before cell seeding. Attachment and proliferation of skin keratinocytes and fibroblasts on BC and BC composite films were determined by MTT assay (Sanchavanakit *et al*., 2006) Briefly, cells were seeded into 24-well culture plates at an initial density of 3×10^4 and 5×10^4 cells per well for attachment and proliferation, respectively on BC film, BC composite film and polystyrene culture plate control. Cells were incubated at 37°C in a humidified atmosphere containing 5% CO_2 for 16 h and collected for attachment assay while replaced for another 48 h with SFM for proliferation assay of both keratinocytes and fibroblasts, respectively. The number of living cells was determined using the MTT assay. Cell morphological imaging was performed using a SEM.

3.4.3 MTT Assay

The 3 - (4,5 -dimethylthiazol-2-yl) -2, 5- diphenyl-tetrazolium bromide (MTT) assay was based on the reduction of the yellow tetrazolium salt to purple formazan crystals by dehydrogenase enzymes secreted from the mitochondria of

metabolically active cells. The amount of purple formazan crystals formed was proportional to the number of viable cells. First, the culture medium was aspirated and replaced with 0.5 μg/ml MTT solution. After that, the plate was incubated for 1 h at 37 °C. The solution was then aspirated, and 900 μL of DMSO containing 125 μL of glycine buffer (0.1 M glycine, 0.1 M NaCl, pH 10) was added to dissolve the formazan crystals. Finally, after 10 min of rotary agitation, the absorbance of the DMSO solution at 540 nm was measured using a UV-vis spectrophotometer (Sanchavanakit et al., 2006).

3.5 *In vitro* released studies

3.5.1 Released of chitosan

The release characteristics of chitosan content from the BCC films were investigated by total immersion method (Suwantong et al., 2007). The relevant buffer-simulated gastric fluid USP pH 1.2, acetate buffer pH 5.5, and phosphate buffer pH 7.4 were used as releasing medium. Each specimen (square plate; 2.5 x 2.5 cm^2) was immersed in 30 ml of the releasing medium at the temperature of 37 ^oC. At a specified immersion period ranging from 0 to 268 h, either 1ml of a sample solution was withdrawn and an equal amount of the fresh medium was refilled. The amounts of chitosan content in the sample solutions were determined using the ninhydrin method (Leane et al., 2004). Actual amount of chitosan in the BCC composite film was determined. Each 2.5 x 2.5 cm^2 of sample was hydrolyzed by 37% HCl at the temperature 100 ^oC for 30 min. After that, 20% NaOH was added in order to neutralize the solution and then the sample solution was centrifuged at 2500 rpm for 30 min. The amount of chitosan content in the supernatant was determined using the ninhydrin method.

3.5.2 Released of active ingredients of *Aloe vera* gel as saccharide

The released characteristic of active ingredients of *Aloe vera* as saccharide from BCA film was investigated by total immersion method (Suwantong

et al., 2007). The relevant buffer-simulated gastric fluid USP pH 1.2, acetate buffer pH 5.5 and phosphate buffer pH 7.4 were used as releasing medium. Each specimen (square plate; 2.5 x 2.5 cm^2) was immersed in 30 ml of the releasing medium at the temperature of 37^oC. At a specified immersion period ranging from 0 to 168 h, either 1 ml of a sample solution was withdrawn and an equal amount of the fresh medium was refilled. The amounts of polysaccharide content in the sample solutions were determined by using acid hydrolysis and analyzed by DNS method. Actual amount of saccharide content in the BCA composite film was determined. Each 2.5 x 2.5 cm^2 of sample was immersed in 30 ml of the distilled water at the temperature of 37 ^oC for 12 h and the samples was removed to the fresh distilled water again. The sample was collected to determine the amount of saccharide. The process was repeated until cannot detect the amount of saccharide in sample. Then, the sample was centrifuged at 2500 rpm for 30 min. The supernatant was collected in order to determine amount of polysaccharide by DNS method.

3.5.3 Ninhydrin analysis

Lithium acetate buffer (10 ml) was prepared by dissolving 4.08 g of lithium acetate dihydrate in approximately 6ml of deionized water. The pH of the resulting solution was adjusted to 5.2 using glacial acetic acid and the volume adjusted to 10 ml with deionized water. The ninhydrin reagent was freshly prepared on the day of the assay by adding 4M lithium acetate buffer (10 ml) to 0.8 g ninhydrin and 0.12 g hydrindantin in 30 ml DMSO. For the assay, 0.5 ml of reagent was added to 0.5 ml of the sample in a glass scintillation vial. The vials were immediately capped, briefly shaken by hand and heated in boiling water for 30 min to allow the reaction to proceed. After cooling, 15 ml of a 50:50 ethanol:water mixture was added to each vial. The vials were then vortexed for 15 s in order to oxidise the excess of hydrindantin. The absorbance of each solution was measured on a UV spectrophotometer at 570 nm and the concentration of chitosan in the sample calculated from a standard calibration curve (Leane, *et al*., 2004).

3.6 Statistical analysis

Results are expressed as the average value with mean standard deviation for triplicate samples. The results were statistically analyzed for significantly differences among the sample groups, calculated using a two-tailed *t*-test for a 95% confidence limit ($P>0.05$). Data of percentage points of the *t* –Distribution were shown in Table A1.

CHAPTER IV
BACTERIAL CELLULOSE-CHITOSAN FILM

To extent the applications of BC, some of it properties must be modified. The various method to modify BC which have been several reported such as bacterial cellulose-alginate films were developed by supplementing alginate into the culture medium (Kanjanamosit et al., 2009), BC/hydroxyapatite composite was prepared by using BC absorbed carboxymethyl cellulose (CMC) to initiate nucleation of calcium deficient hydroxyapatite for used in bone healing application (Zimmermann et al., 2009), the nanoporous membrane from regenerated bacterial cellulose was developed by dissolved the BC in NaOH/ urea solution and followed by freeze-thaw process (Phisalaphong et al., 2007).

In this research, in order to enhance some properties of BC for suitable used as wound dressing, chitosan were added into BC film with two different methods. The 1st method was by the supplementation of chitosan into the culture medium during biosynthesis and the 2nd method was by soaking of BC in the chitosan- acetic acid solution. The BC-chitosan composite films prepared by the supplementation of chitosan into culture medium were referred to as BCC-MW *n*, where *n* is the molecular weight of chitosan added into medium culture whereas the BC-chitosan composite films prepared by mean of soaking of BC pellicles in chitosan-acetic acid solution were referred to as BCC*n*, where *n* is the molecular weight of chitosan used for the BC pellicles immersion.

The BC-chitosan composite films that obtained from both techniques were characterized for the physical and biological properties. In addition, the cytotoxicity of BC-chitosan composite films against L929 mouse fibroblast cells was evaluated. Finally, the biocompatibility of BC-chitosan composite film with human keratinocytes and fibroblasts were investigated.

4.1 Biosynthesized bacterial cellulose-chitosan (BCC-MW *n*) film

Our previous study, bacterial cellulose-chitosan composite (BCC-MW *n*) film was prepared by mean of biosynthesis (Phisalaphong and Jatupaiboon, 2008). The biosynthesized BC-chitosan films made *via* bio-co-polymerization by *Acetobacter xylinum*. The culture medium was coconut water containing 5.0 % sucrose, 0.5 % ammonium sulfate, 1% acetic acid and supplemented with 0.75 % chitosan which different molecular weight. In this section, BCC-MW 30,000 and BCC-MW 80,000 refer to the samples of biosynthesized BC-chitosan films supplemented with chitosan of molecular weight 30,000 and 80,000 respectively.

4.1.1 Characterization of BCC-MW *n* film

The physical and biological properties of BC and biosynthesized BC-chitosan films were characterized. The result showed that both of BC and BCC-MW *n* films displayed an ultrafine fiber network. The structure of biosynthesized BC-chitosan film was found to be thicker and denser than the BC film. The FT-IR spectra showed intermolecular interaction between the hydroxyl groups of cellulose fiber and the amino groups of chitosan. The pore size distribution of the BC, BCC-MW 30,000 and BCC-MW 80,000 films are shown in Figure 4.1. The average pore sizes of the re-swollen of BC, BCC-MW 30,000 and BCC-MW 80,000 films were 60.80±0.40 nm, 48.95±0.35 nm, and 39.70±0.40 nm, respectively. More information of those characteristics of the BC and biosynthesized BC-chitosan films has been reported elsewhere (Phisalaphong and Jatupaiboon, 2008). Table 4.1 gives a summary of overall characteristics of the BC and biosynthesized BC-chitosan films.

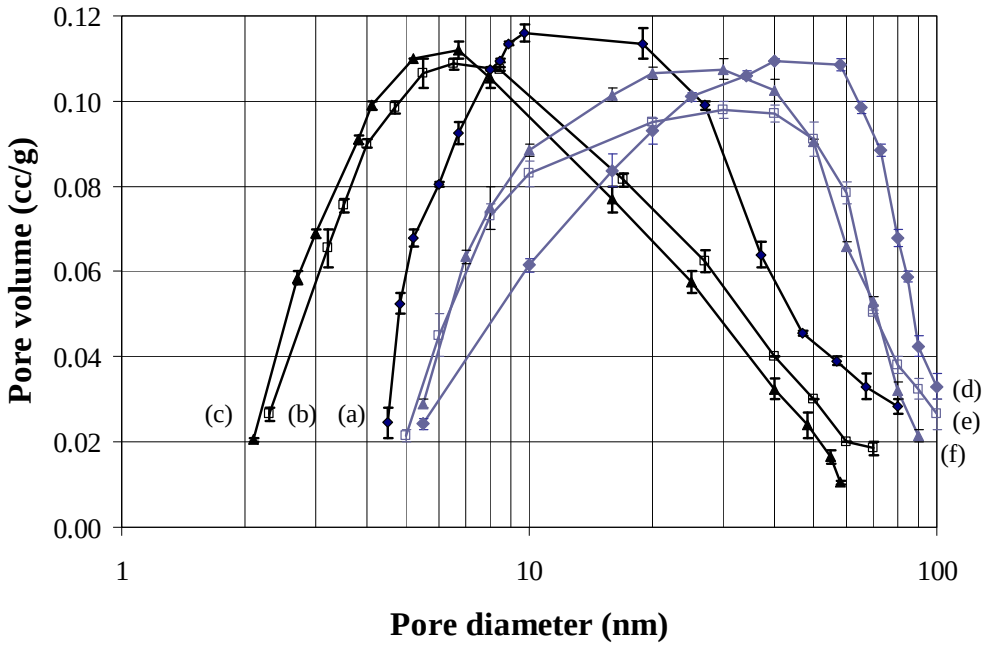

Figure 4.1 The pore size distribution of BC and biosynthesized BC-chitosan films: in dried form of (a) BC, (b) BCC-MW 30,000, and (c) BCC-MW 80,000; in re-swollen form of (d) BC, (e) BCC-MW 30,000, and (f) BCC-MW 80,000 (Kingkaew J. et al., 2010)

The antibacterial ability of the biosynthesized BC-chitosan films was evaluated. It found that the addition of chitosan with different molecular weight at 0.75% in the culture medium had no significant impact on the growth of *Escherichia coli* and *Staphylococcus aureus.* The anti-fungal ability of the biosynthesized BC-chitosan films was examined with *Aspergillus niger*. It was found that the biosynthesized BC-chitosan films had slightly improved the anti-fungal ability when compared with the BC film.

Table 4.1 Characteristics of the BC and biosynthesized BC-chitosan films ([a] $P<0.05$, significant difference in mean value relative to the control BC film) (Kingkaew, J. et al., 2010).

Property	BC		BCC-MW 30,000		BCC-MW 80,000	
	Dry	Re-swollen	Dry	Re-swollen	Dry	Re-swollen
Tensile strength (MPa)	5.32±0.26	1.45 ± 0.17	7.66±0.15[a]	2.07±0.17[a]	8.26±0.33[a]	2.72±0.21[a]
Young's modulus (MPa)	161.8±11.1	21.79±2.36	195.0±7.9[a]	33.6±1.7[a]	221.8±15.6[a]	36.1±1.2[a]
Break strain (%)	3.75±0.16	8.17±0.32	1.91±0.14[a]	5.76±0.26[a]	1.44±0.009[a]	4.36±0.21[a]
Average pore diameter (nm)	22.2±0.25	60.08±0.40	15.3±0.15[a]	49.0±0.35[a]	13.05±0.15[a]	39.70±0.40 [a]
Surface area (m^2/g)	12.8±0.1	56.0±0.8	14.1±0.1[a]	80.5±1.9[a]	15.0±0.2[a]	99.2±1.1[a]
Water absorption capacity (%)	482±24	-	606±15[a]	-	625±18[a]	-
Water vapour transmission rate ($g/m^2/day$)	1539±18	-	1578±23	-	1564±15	-

4.1.2 Cytotoxicity

Before used any material in medical applications, this materials should be evaluated for the cytotoxicity and the biocompatibility. The cytotoxicity was evaluated based on the procedure modified from the ISO 10993-5 standard test method using the L929 mouse fibroblast cell line. The number of viable cells culture was examined using the MTT assay. As seen in Figure 4.2, The percentages of viable cells culture with the extraction medium of BC, BCC-MW 30,000, and BCC-MW 80,000 for 24 h, in comparison with those cultured with fresh medium were found to be 97±2.2 %, 103±2.5 %, and 93±3.4 % with the extraction medium concentration of 5 mg/ml and 96±2.6 %, 104±2.4 %, and 94±4.8 % with the extraction medium concentration of 10 mg/ml, respectively. The results indicated that BC and biosynthesized BC-chitosan films had no toxicity against L929 cells with no statistically significant difference (P>0.05).

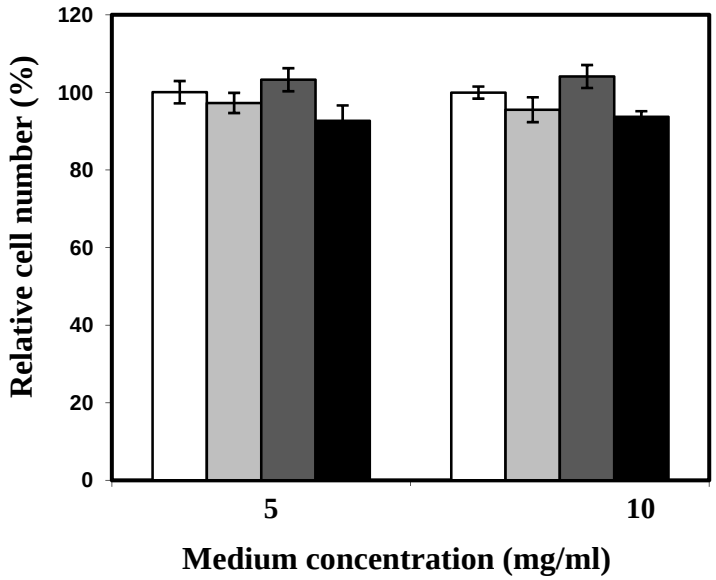

Figure 4.2 Toxicity test against L929 mouse fibroblast cell at the extraction medium concentrations of 5 mg /ml and 10 mg /ml on the (□) polystyrene control plate, (▭) BC, (▩) BCC-MW 30,000, and (■) BCC-MW 80,000 ([a] significant difference in mean value relative to the control BC film (P < 0.05), [b] significant difference in mean value relative to the control polystyrene plate (P < 0.05)).

4.1.3 *In vitro* cell study

The effects of BC and biosynthesized BC-chitosan films on the proliferation and morphology of human skin cells were investigated. The major human skin cells, human-transformed keratinocytes (HaCat), and human leg skin fibroblasts (CRL-2211) were used. The percentage of the viable cells after seeding on BC and biosynthesized BC-chitosan films from 0 to 24 and 48 h was gradually increased, as shown in Figure 4.3 and 4.4, respectively. The proliferation on BC and biosynthesized BC-chitosan films, cultures of both cell types exhibited no statistically significant difference for a 95% confidence limit (P>0.05).

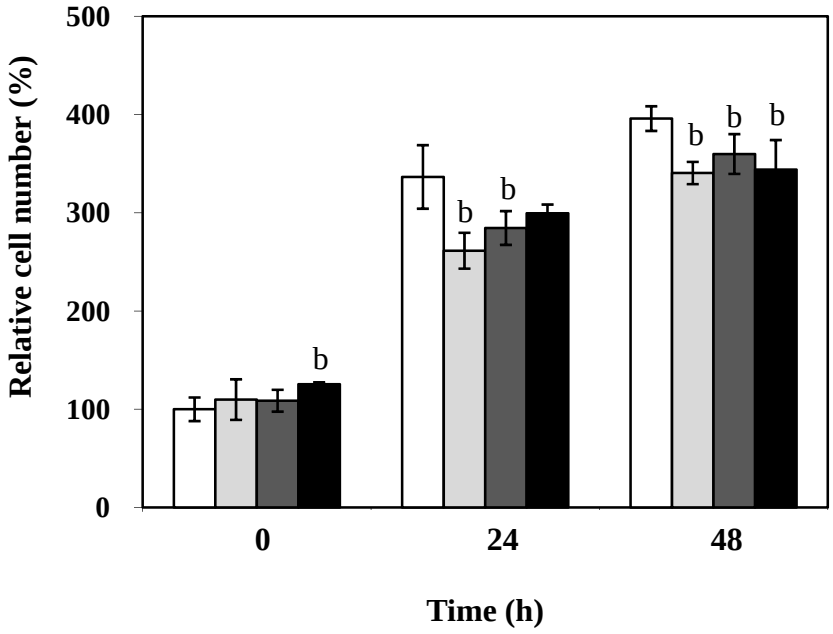

Figure 4.3 Proliferations of human skin keratinocytes on the (□) polystyrene control plate, (▭) BC, (▬) BCC-MW 30,000 and (■) BCC-MW 80,000. Percentage of living cells was assessed at 0, 24 and 48 h of culture by MTT assay ([a] significant difference in mean value relative to the control BC film (P < 0.05), [b] significant difference in mean value relative to the control polystyrene plate (P < 0.05)).

In the culture of keratinocytes, the percentage of the viable cells number increased from 100±15 % to 238±14 % and 310±8 % on the BC, 100±8 % to

262±13 % and 331±15 % on the BCC-MW 30,000 and 100±1 % to 239±6 % and 274±20 % on the BCC-MW 80,000 at 24 and 48 h, respectively, while the percentage of the number of fibroblasts increased from 100±6 % to 151±4 % and 198±8 % on the BC, 100±6 % to 124±3 % and 190±2 % on the BCC-MW 30,000 and 100±8 % to 135±7 % and 197±9 % on the BCC-MW 80,000 at 24 and 48 h, respectively.

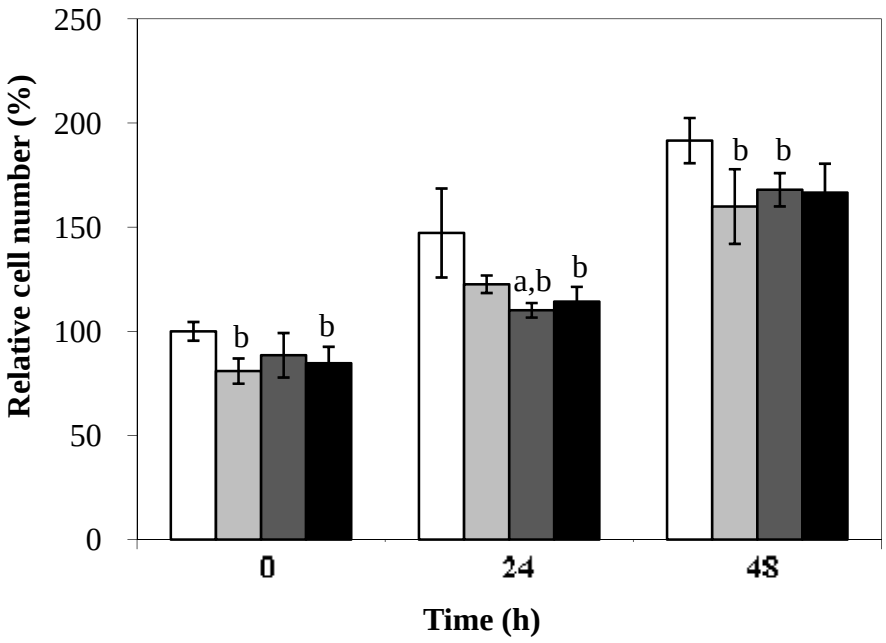

Figure 4.4 Proliferations of human fibroblasts on the (□) polystyrene control plate, (▭) BC, (▬) BCC-MW 30,000, and (■) BCC-MW 80,000. Percentage of living cells was assessed at 0, 24, and 48 h of culture by MTT assay ([a] significant difference in mean value relative to the control BC film ($P < 0.05$), [b] significant difference in mean value relative to the control polystyrene plate ($P < 0.05$)).

As seen in Figures 4.3 and 4.4, the viable cell number of both cell types on the BC and biosynthesized BC-chitosan composite films was relatively lower than that on the polystyrene control plate however, the proliferation rate of both cell was similar. This proliferation result did not only support the biocompatibility of these kinds of materials, but also showed the effectiveness to increase the cell number which would improve the wound-healing process. SEM images of keratinocytes at a 1,000X magnification of on the control plate at 24 h demonstrated well-spread keratinocytes over the surface of the plate, which was seen as a flattened epithelial-

like shape with slight trace of filopodia at 10,000X magnification of (Figure 4.6 a), whereas a lower degree of spreading and looser cell adhesion was observed in keratinocytes cultured on the BC surface, which were seen as more rounded cells, indicating fewer cell-material interactions (Figure 4.5b).

Regarding the BC surface, the patterns of cell distribution and attachment of keratinocytes on the biosynthesized BC-chitosan composite films were different. The extent of cell spreading and adhesion on the BCC-MW 30,000 and BCC-MW 80,000 surfaces was higher, as shown in Figure 4.5(c)–4.5(d), respectively. A possible explanation for this phenomenon was that the adhesion of keratinocytes. BC film was less than that of the cells to the biosynthesized BC-chitosan composite films. The influence of cell attachment from the interaction of positively charged amino groups of chitosan chains and negatively charged cell membranes has been widely reported (He et al., 2007). Therefore, the improved keratinocytes attachment on the biosynthesized BC-chitosan films could be due to the presence of chitosan on the film surface.

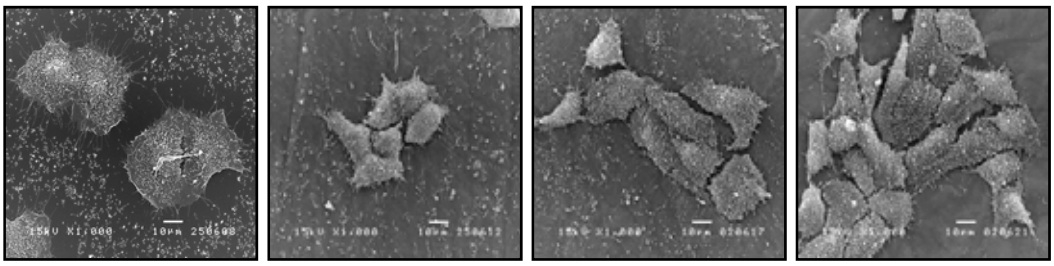

(a) (b) (c) (d)

Figure 4.5 SEM images of human skin keratinocytes at 1,000X magnification on (a) the polystyrene control plate, (b) BC film, (c) BCC-MW 30,000, and (d) BCC-MW 80,000 demonstrated at 24 h.

The SEM images of fibroblasts showed the typical elongated fibroblast pattern with good spreading on the control culture plate and all types of tested materials with no significant difference in morphology (Figure 4.7).

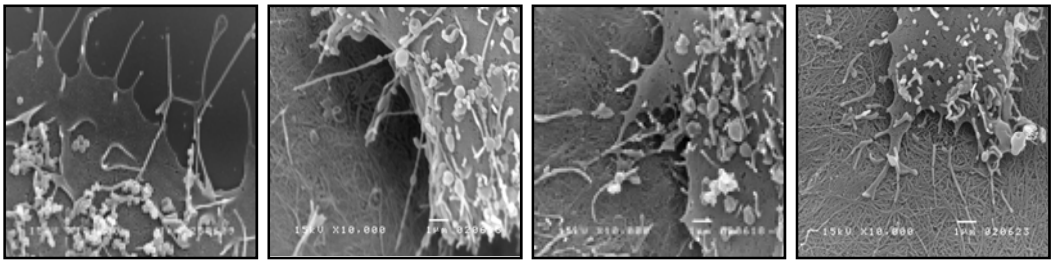

(a) (b) (c) (d)

Figure 4.6 SEM images of human skin keratinocytes at 10,000X magnification on (a) the polystyrene control plate, (b) BC, (c) BCC-MW 30,000, and (d) BCC- MW 80,000 demonstrated at 24 h.

At a high magnification of 10,000X, several of their thread-like filopodia were seen showing good interaction with the material underneath (Figure 4.8). This normal phenotypic shape suggested that the cells function biologically on these materials. According to previous works (Howling et al., 2007), chitosan does not directly enhance the rate of fibroblast cell proliferation. Chitin and its derivatives showed no direct acceleratory effect on the proliferation of fibroblasts *in vitro*. In addition, chitosan at high concentration could reduce the proliferation rate. However, the indirect stimulatory effect on fibroblast proliferation was suggested to be a result from the interaction of chitosan with the growth factors present in the serum, thus potentiating their effect. Proliferation of fibroblasts *in vivo* was suggested to be accelerated indirectly by chitin derivatives, possibly due to the formation of a polyelectrolyte complex between chitosan and heparin (Mori et al., 1997, Howling et al., 2007). In this study, the supplementation of chitosan of MW 30,000 and 80,000 in the bacterial culture medium showed no significant influence on the cell proliferation profile of the modified films compared to that of the BC film.

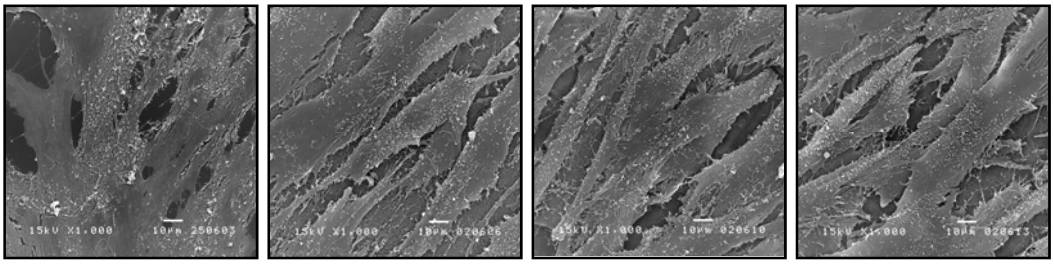

(a) (b) (c) (d)

Figure 4.7 SEM images of human skin fibroblasts at 1,000X magnification on (a) the polystyrene control plate, (b) BC, (c) BCC-MW 30,000, and (d) BCC-MW 80,000 films demonstrated at 24 h.

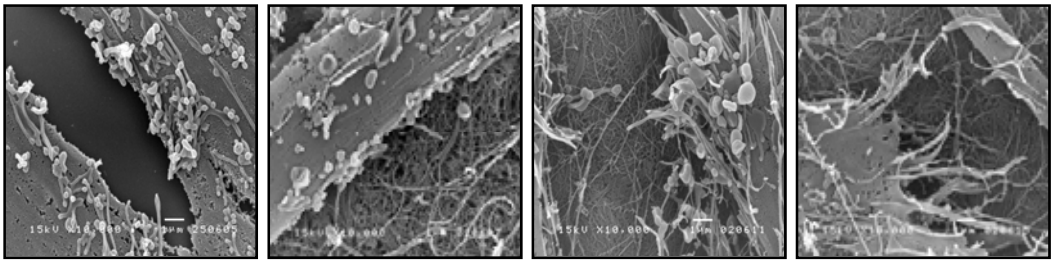

(a) (b) (c) (d)

Figure 4.8 SEM images of human skin fibroblasts at 10,000X magnification on (a) the polystyrene control plate, (b) BC, (c) BCC-MW 30,000, and (d) BCC-MW 80,000 films demonstrated at 24 h.

4.2 Impregnated BC-Chitosan (BCC) film

To extent the properties of bacterial cellulose for use as suitable material in biomedical applications, chitosan was added into BC structure. In this research, BCC films were prepared by mean of immersing wet purified BC pellicle in chitosan-acetic acid solution. In this section, BCC3, BCC8 and BCC20 refer to the samples of impregnated BC-chitosan films with chitosan molecular weight of 30,000, 80,000, and 200,000, respectively. The absorption profile is shown in Figure 4.9.

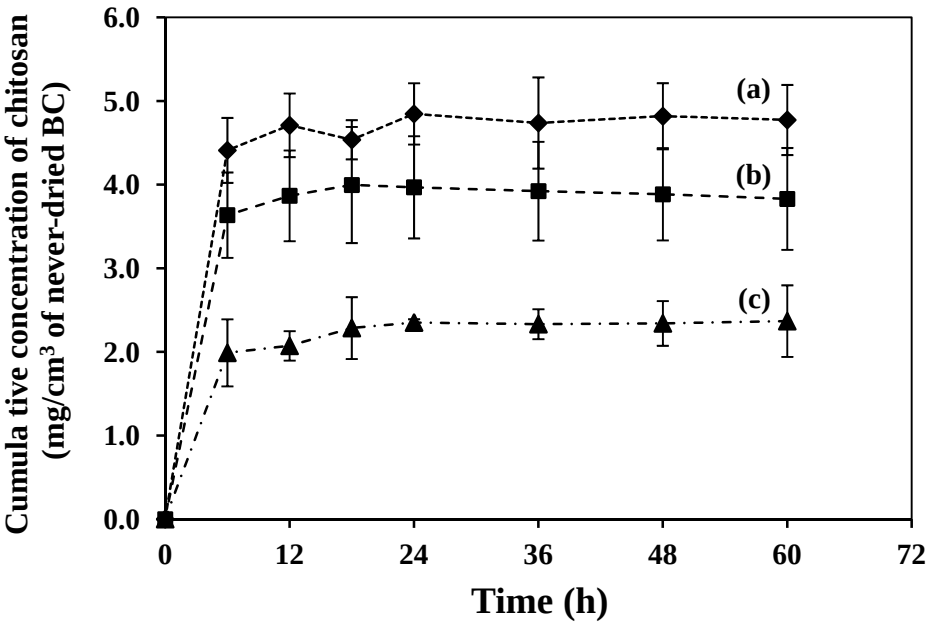

Figure 4.9 Cumulative absorption profile of chitosan solution penetrated into BC pellicles: (a) chitosan MW 30,000, (b) chitosan MW 80,000, and (c) chitosan MW 200,000.

As seen in Figure 4.9, it was indicated that chitosan could diffuse into BC pellicle. The penetration into BC pellicle of each molecular weight chitosan was in similar trends. The absorption rate suddenly increased in the first 6 h, afterward it was gradually decreased. After 24 h of absorption, the cumulative concentration of chitosan was nearly constant. Chitosan MW 30,000 could be penetrated into BC network better than chitosan MW 80,000 and chitosan MW 200,000, respectively. These results show that the molecular weight size of chitosan is an important factor that affects the absorption capacity of chitosan into BC pellicle.

4.2.1 Morphology

After treated by chitosan, the morphology of BCC film was different from the pristine BC film. The apparent of all of the BCC composite films were thicker and denser than the BC film. The thickness of BC and BCC3, BCC8 and BCC20 films are 71±2 μm, 81±2 μm, 103±9 μm, and 94±2 μm, respectively.

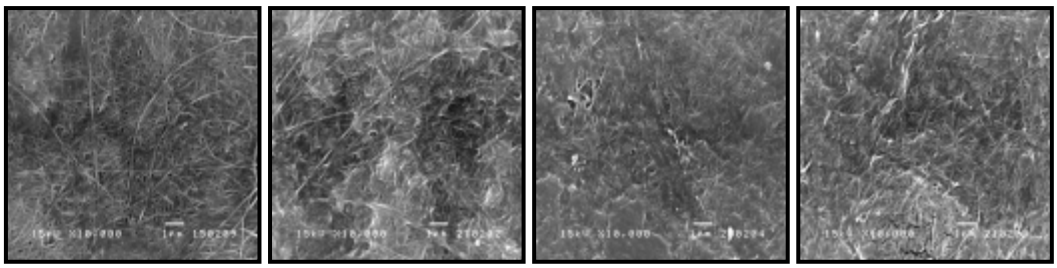

(a) (b) (c) (d)

Figure 4.10 SEM images of surface morphology of the dried films at 10,000X magnification: (a) BC, (b) BCC3, (c) BCC8, and (d) BCC20.

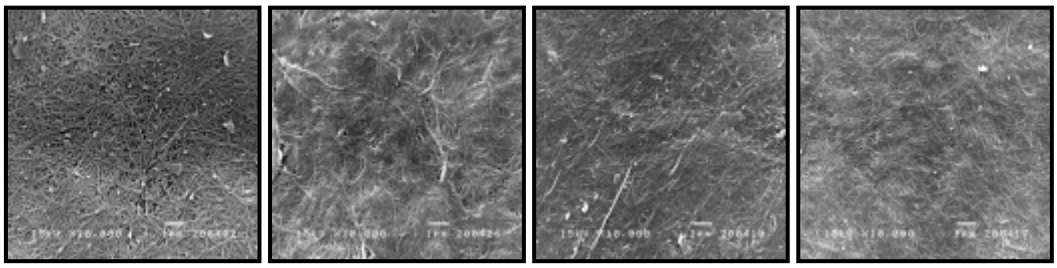

(a) (b) (c) (d)

Figure 4.11 SEM images of surface morphology of the re-swollen films at 10,000X magnification: (a) BC, (b) BCC3, (c) BCC8, and (d) BCC20.

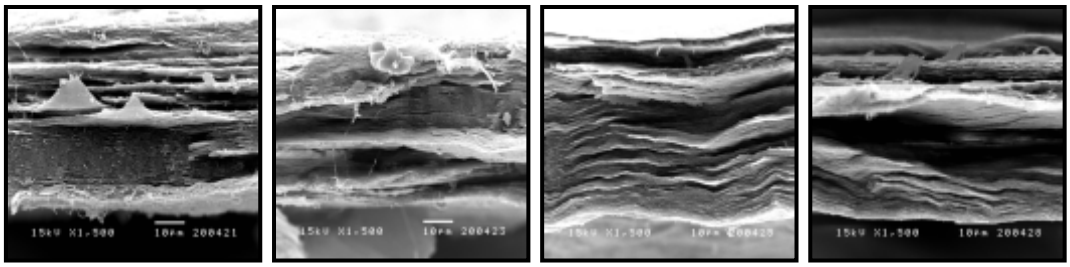

(a) (b) (c) (d)

Figure 4.12 SEM images of cross sectional morphology of the re-swollen films at 1,500X magnification: (a) BC film, (b) BCC3 film, (c) BCC8 film, and (d) BCC20 film.

SEM images in Figures 4.10-4.12 show the morphologies of surface and cross section of BC and BCC3, BCC8 and BCC20 films, respectively. Figures 4.11(a) illustrates smooth well-organized fibril networks of BC and the clear nanofibrils on

the surface. Considering Figures 4.11(b)-(d), the clear cellulose nanofibrils cannot be observed on the surface of BCC films and the hollow space of cellulose fibrils network was decreased. The average pore size diameter of the BCC film was smaller than that of the BC film. The result indicated that chitosan could penetrate into the empty spaces of BC fibrils network and formed interaction with the BC molecule (Kim et al., 2010). The previously work by UI-Islam et al. (2011) on preparation and characterization of the three dimensional BC-chitosan composite reported that chitosan not only formed layer on BC surface but also penetrated into BC fibrils networks.

4.2.2 Fourier transform infrared spectroscopy

FTIR spectroscopy is a technique to determine the specific functional groups or chemical bonds that exist in the material. The FTIR spectra of the BC and BCC films were measured from 4000–400 cm^{-1}, as shown in Figures 4.13. The BC spectra showed a broad band at wave number about 3,418 cm^{-1}, which represented N-H stretching vibration combined with O-H stretching vibration, a band at 2,895 cm^{-1} represented the aliphatic C-H stretching vibration (Kim et al., 2010), a band at around 1641 cm^{-1} was represented for the glucose carbonyl of cellulose (Phisalaphong and Jatupaiboon, 2008) and the band between 1,155-1032 cm^{-1}, which was represented for the polysaccharide structure (Balau et al., 2004). In case of chitosan powder, the band at 1598 cm^{-1} was observed which was attributed to amide group. The spectra of BCC films exhibited all of the characteristic bands of BC with the appearance of a new band between wave number 1,561-1,563 cm^{-1}, which was represented for amide group of chitosan molecule. The characteristic bands of chitosan shifted from 1598 cm^{-1} to 1,562, 1,561, and 1,563 cm^{-1} for BCC3, BCC8, and BCC20 films, respectively. The results indicated the intermolecular interaction between the hydroxyl groups of cellulose and the amino groups of chitosan.

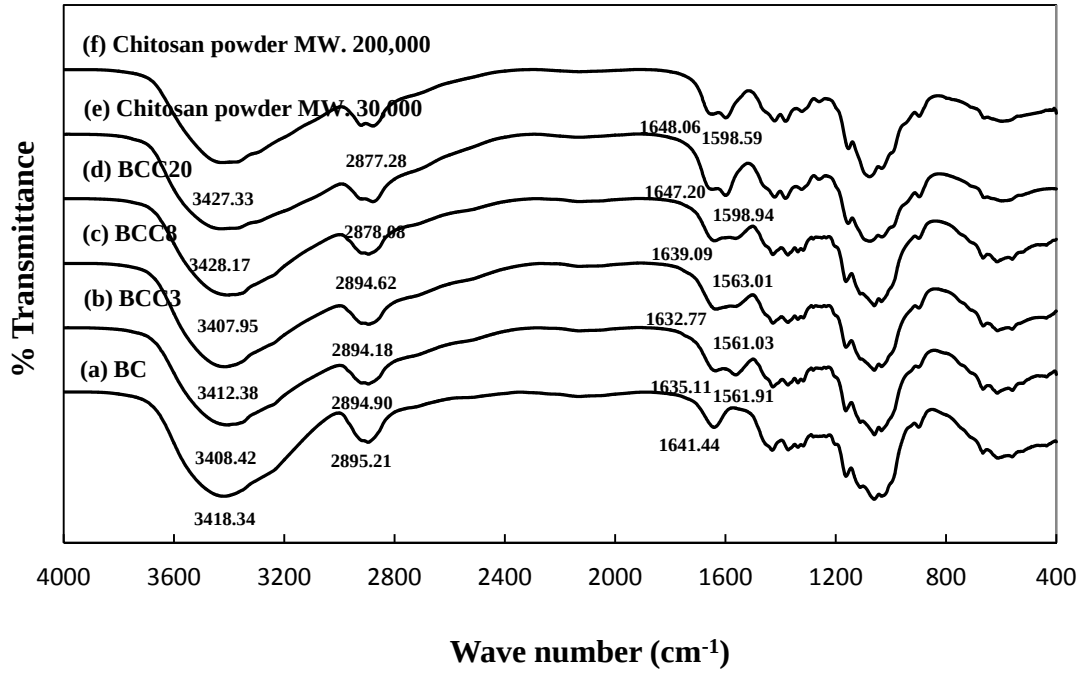

Figure 4.13 The FTIR spectra in wave number ranging from 4000 to 400 $cm^{-1}$of (a) BC film, (b-d) BCC film, and (e-f) chitosan powder.

4.2.3 X-ray diffraction

The average crystallinity index (C.I.) value was calculated from X-ray diffraction pattern. Figures 4.14 shows the diffraction patterns of BC and BCC films. The pattern of BC exhibits three main peaks at $2\theta = 14.50^{o}$, 16.72^{o}, and 22.74^{o} attributed to the$(1\ \bar{1}\ 0)$, (1 1 0), and (2 0 0) reflexions planes of cellulose I structure, respectively (Cai and Kim, 2010; Retegi, 2010). The broad diffraction peaks ($2\theta = 16.72^{o}$) were observed for BC because BC is not a completely crystalline material. The diffraction patterns of BCC3, BCC8, and BCC20 films demonstrated the three main peaks similar to the pattern of BC but the peak in $(1\ \bar{1}\ 0)$ refection plane slightly shift to wider angle.

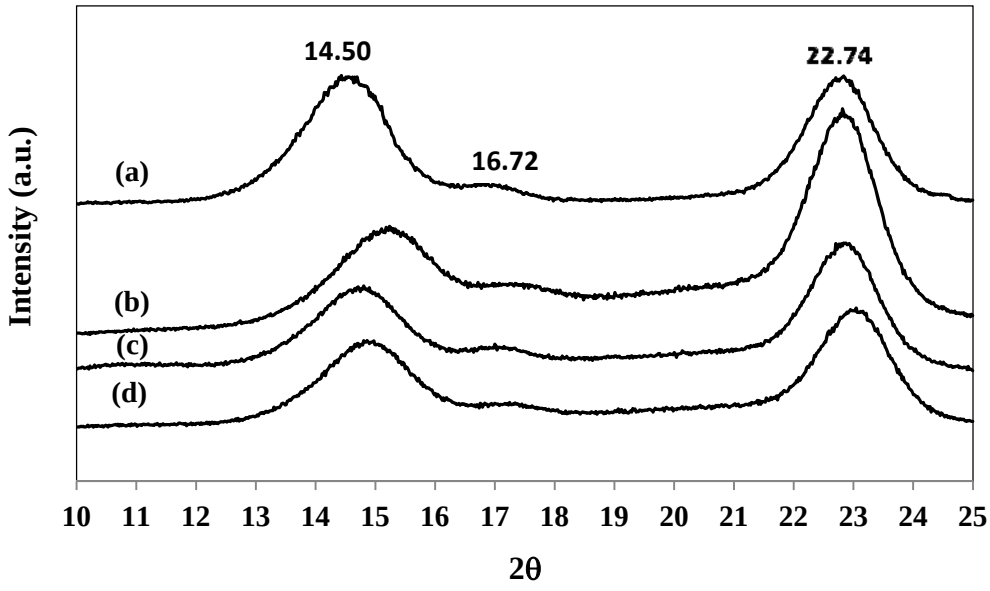

Figure 4.14 The XRD pattern of (a) BC film, (b) BCC3 film, (c) BCC8 film, and (b) BCC20 film.

The average C.I. values of BC, BCC3, BCC8, and BCC20 was 86.47, 78.07, 79.21 and 77.52, respectively. The decrease in crystallinity of BCC is due to intermolecular interaction between chitosan molecule and cellulose fibrils. In addition, the crystals of cellulose become preferentially oriented in the $(1\,\bar{1}\,0)$ reflexion plane when drying process is occurred. The modification of BC with another polymer that is the incorporation of polymer could affect the preferential orientation of the $(1\,\bar{1}\,0)$ reflexion plane resulting in this incomplete orientation of the $(1\,\bar{1}\,0)$ reflexion plane of BC which in turn leaded to a decrease in crystallinity (Cai and Kim, 2010).

4.2.4 Brunauer-Emmett-Teller

The porosity of BC and BCC films from BET analysis are shown in Table 4.2 and Figures 4.15.

Table 4.2 Average pore size and surface area of BC and BCC films analyzed with BET analysis.

Sample	**Surface area (m^2/g)**	**Average pore diameter (Å)**
BC	4.20 ± 0.09	100.0 ± 10.9
BCC3	4.40 ± 0.16	51.8 ± 7.9[a]
BCC8	3.39 ± 0.11[a]	49.8 ± 9.3[a]
BCC20	2.64 ± 0.06 [a]	56.7 ± 9.0 [a]

[a] Significant difference in mean value relative to the control BC film ($P < 0.05$).

Corresponding to results from SEM images that shown morphology of the films, the average pore diameters of BCC films were smaller than that of the BC film. The average pore diameter of the BCC3 film had no significant different from those of the BCC8 and BCC20 films, whereas the surface area of BCC films relatively decreased with increasing the MW size of chitosan. The pore size distributions as shown in Figure 4.15 revealed that chitosan could penetrate into the pore structure and filled the pores. It was shown that the pore volume of BC > BCC3 > BCC8 > BCC20, respectively.

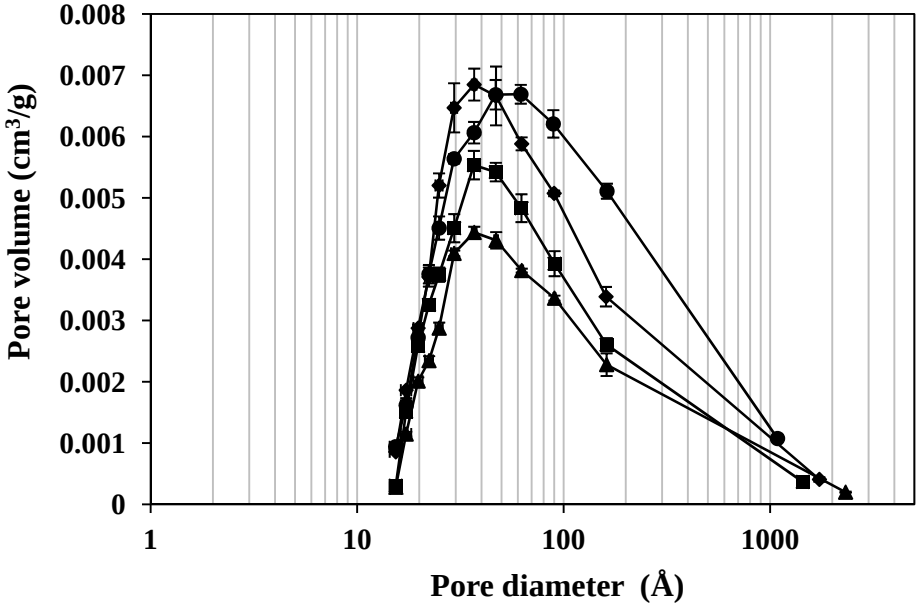

Figure 4.15 Pore size distributions of dries BC and BCC films: (●) BC, (◆) BCC3, (■) BCC8, and (▲) BCC20 films.

4.2.5 Mechanical property

In this present work, the mechanical properties of BCC films as tensile strength, Young's modulus and elongation at break were analyzed for investigating the effects of chitosan content on mechanical properties of the films. The Mechanical properties of BC and BCC films are shown in Figures 4.16-4.18. The results shown the tensile strength (Figure 4.16), Young's modulus (Figure 4.17) and elongation at break (Figure 4.18) of BCC films were slightly lower than those of the BC film. The tensile strengths of BC, BCC3, BCC8, and BCC20 films were 94.1±8.1 MPa, 71.0±5.1 MPa, 81.5±7.3 MPa, and 87.8±6.5 MPa, respectively. In the same way, Young's modulus of BCC films was slightly lower than that of the BC film; the Young's modulus of BC, BCC3, BCC8 and BCC20 films were 746±62 MPa, 640±55 MPa, 628±30 MPa, and 690±42 MPa, respectively. Since the incorporation of chitosan into the BC pellicle increases the amorphous phase fraction. This could weaken affinity of binding of the films. As discussed in XRD results, the

incorporation of chitosan could affect the preferential orientation of the $(1\,\bar{1}\,0)$ plane, which resulted in incomplete orientation of the $(1\,\bar{1}\,0)$ plane leads to the decrease of mechanical strengths of the films. Compared to BC, slight reduction of elongation at break of BCC films was observed. The elongations at break of BC, BCC3, BCC8, and BCC20 films were 26.8±2.2 %, 23.4±3.6 %, 24.6±3.7 %, and 21.6±1.3%, respectively. The flexibility and endurance of the BCC films were relatively less than those of the BC film, which could be related to the less organized fiber-network structure of the BCC films. The results suggested that the penetration of chitosan molecule into the BC network structure might have some impact on the film mechanical properties.

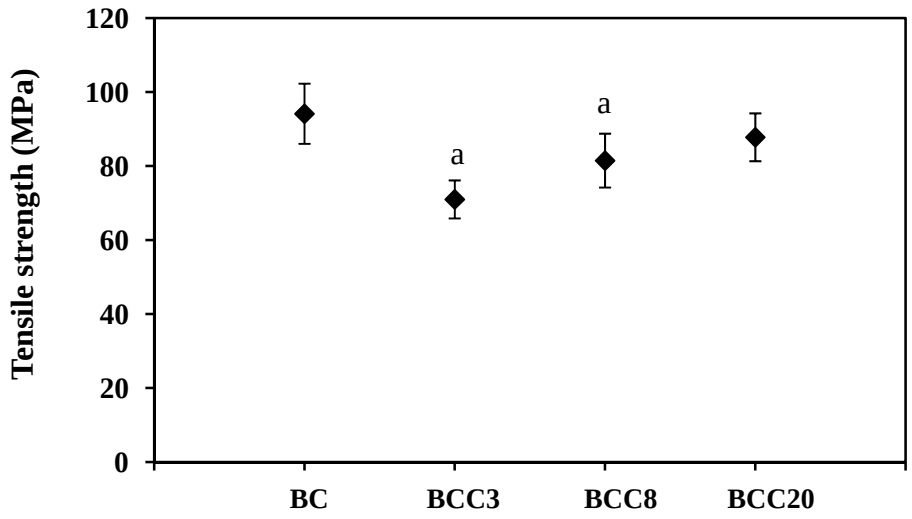

Figure 4.16 Tensile strength of BC and BCC films,[a] significant difference in mean value relative to the control BC film ($P < 0.05$).

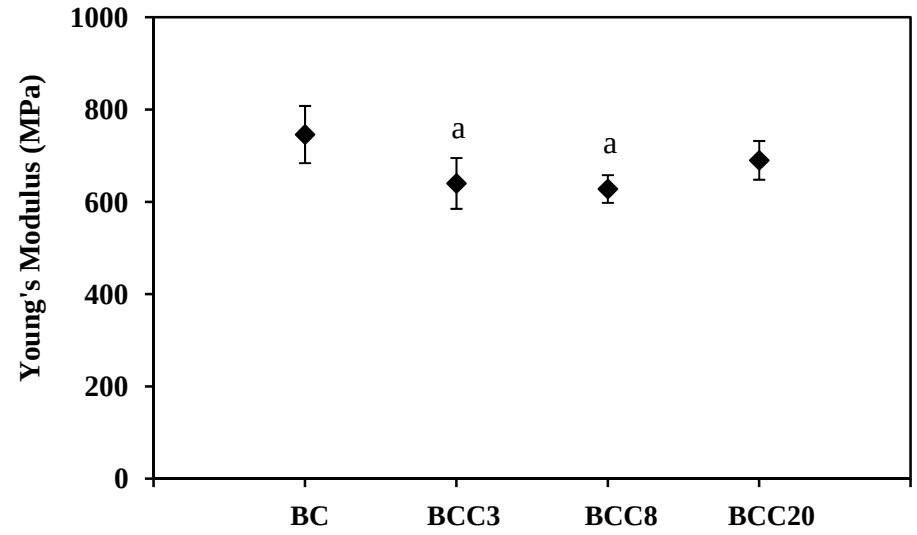

Figure 4.17 Young's modulus of BC and BCC films, [a] significant difference in mean value relative to the control BC film ($P < 0.05$).

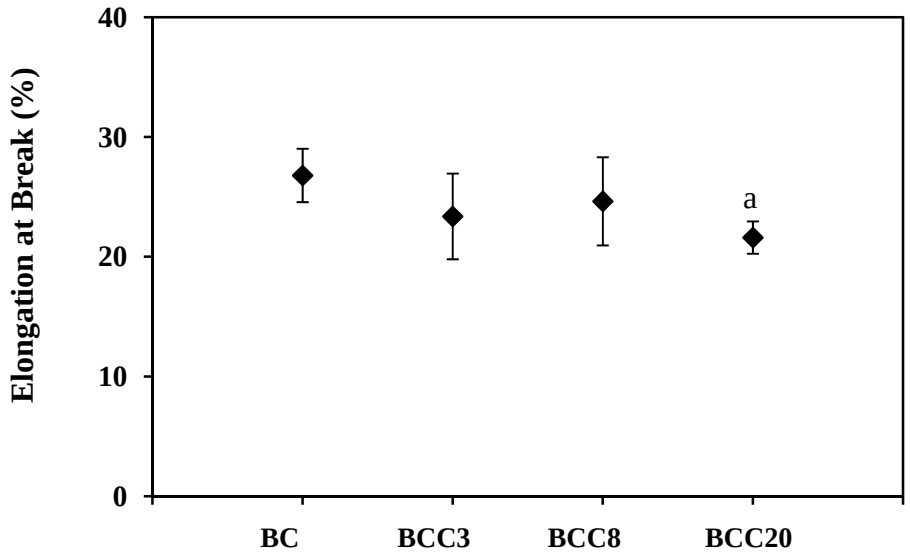

Figure 4.18 Elongation at break of BC and BCC films, [a] significant difference in mean value relative to the control BC film ($P < 0.05$).

4.2.6 Water absorption capacity

The water absorption capacity (WAC) is the important property of biomaterials that used in medical field, especially in the wound dressing application. The abilities to absorb the exudates and provide moist environment to a wound are necessary. The effect of the incorporation of chitosan on WAC is shown in Figures 4.19. The WACs of BC, BCC3, BCC8, and BCC20 were 313±29 %, 186±24 %, 174±15 %, and 216±27 %, respectively. Significant reduction (P<0.05) of WAC of the BCC films to about 56 - 65 % of that of the BC film was observed. Incorporation of chitosan into BC could form a more tightly packed network structure from the interaction between cellulose fiber-chitosan molecules (Phisalaphong et al., 2007). Therefore, the water penetration and water holding capacity of the film were less, leading to a decrease in WAC.

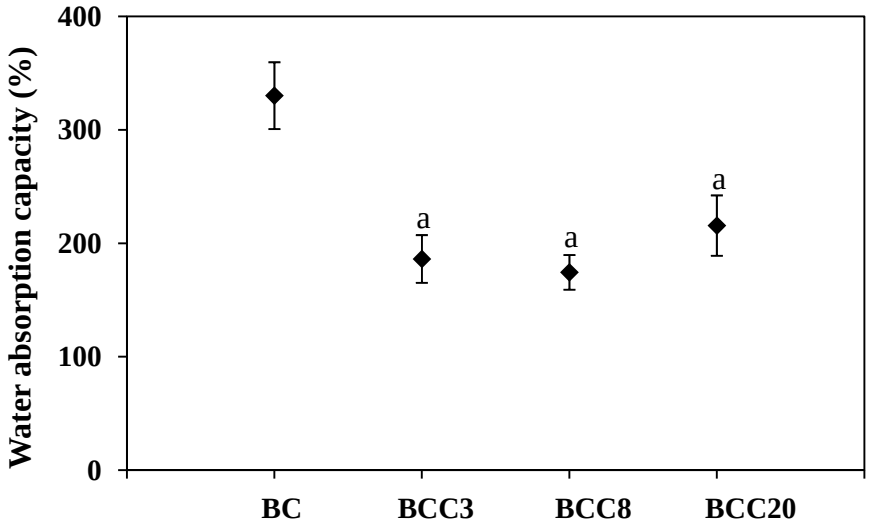

Figure 4.19 The water absorption capacity of BC and BCC films, [a] significant difference in mean value relative to the control BC film (P < 0.05).

4.2.7 Water vapor transmission rate

The water vapor transmission rate (WVTR) is an important characteristic of wound dressing. Good wound dressing should had ability to absorb

wound exudates and toxic components from the wound surface, control evaporative fluid loss from wounded skin and maintain a high humidity at the wound/dressing interface, which was a necessary property to accelerate the wound healing process (Stashak et al., 2004). Generally, the water loss for normal skin is 204.0±115.2 g/m^2/day, while that for the injured skin can range from 207±26 g/m^2/day for the first degree of burn to 5138±202 g/m^2/day for a granulating wound (Cardona et al., 1996). The WVTR of BC and BCC films were analyzed following the ASTM E 96-00 and the results are shown in Table 4.3.

Table 4.3 Water vapor transmission rate of BC film, BCC film, and commercial wound dressing (*Cardona et al., 1996; **Lowe, 2008).

Sample	**Water vapor transmission rate (g/m^2/day)**
BC	1049 ± 16
BCC3	529 ± 24[a]
BCC8	778 ± 16 [a]
BCC20	830 ± 36 [a]
Bioprocess®,*	2046 ± 249
Biobrane II®,*	1565 ± 281
Op-Site®,*	426 ± 9
Gauze**	800

[a] Significant difference in mean value relative to the control BC film ($P < 0.05$).

As can be seen in Table 4.3, the WVTR of BC film was higher than that of all types of BCC films with statistically significant difference ($P<0.05$). In case of the BCC films, the WVTR was increased with increasing MW size of chitosan. It can be explained that the incorporation of chitosan inside cellulose network resulting in the denser structure and the decrease in pore diameters, which lead to a decrease of the WVTR. On the other hand, incorporation of chitosan, especially at high MW could enhance hydrophilic property of the film. When compared with the commercial wound dressing such as Bioprocess®, Biobrane II®, Op-site® and Gauze (Cardona et

al, 1996; Lowe, 2008), the WVTRs of BC and BCC film are comparable to those of the commercial wound dressings.

4.2.8 Oxygen transmission rate

In wound healing, oxygen plays important role in supporting tissue regeneration and repair, inhibiting anaerobic bacteria and supporting the body's natural defense mechanisms. In this study, the oxygen transmission rate (OTR) of all types of test films was analyzed following the ASTM E D3985-05. Table 4.4 shows the results of the OTR of the BC and BCC films.

Table 4.4 Oxygen transmission rate of the BC film, BCC film, and commercial wound dressings ([*]Cardona et al., 1996; [**] Lowe, 2008).

Sample	**OTR ($cm^3/m^2/day$)**
BC	2.650 ± 0.028
BCC3	1.675 ± 0.092 [a]
BCC8	1.570 ± 0.028 [a]
BCC20	1.445 ± 0.035 [a]
Bioprocess®,*	247 ± 54
Gauze**	14275

[a] Significant difference in mean value relative to the control BC film ($P < 0.05$).

The average pore diameters of the BC and BCC films were bigger than the approximate diameter of oxygen molecule is 0.36 nm (Kanjanamosit et al., 2009), so that oxygen could flow through the films. The OTR of the BCC films were less than that of the BC film with statistically significant difference ($P<0.05$) because of the lower pore diameter and pore volume of these films. When compared to the commercial wound dressing such as Bioprocess® and Gauze (Cardona et al, 1996; Lowe, 2008), the OTR of BC and BCC films exhibited significant lower oxygen

transmission. Due to the small pore diameter of BC and BCC films in dry state, the corresponding values of OTR were considerably low.

4.2.9 Release of chitosan from BCC films

The cumulative releases of chitosan from BCC films in buffer pH 1.2, pH 5.5 and pH 7.4 are reported in Figure 4.20. These results showed that the maximum amount of chitosan which released from BCC3, BCC8, and BCC20 are 27.17±1.85 mg/cm^3, 22.07±0.45 mg/cm^3, and 17.98±1.32 mg/cm^3 of dried films in the buffer solution whose pH was 1.2; 27.03±2.27 mg/cm^3, 20.61±1.33 mg/cm^3, and 11.34±1.31 mg/cm^3 in the buffer solution whose pH was 5.5; 0.60±0.07 mg/cm^3, 0.46±0.12 mg/cm^3, and 0.27±0.14 mg/cm^3 in the buffer solution whose pH was 7.4, respectively.

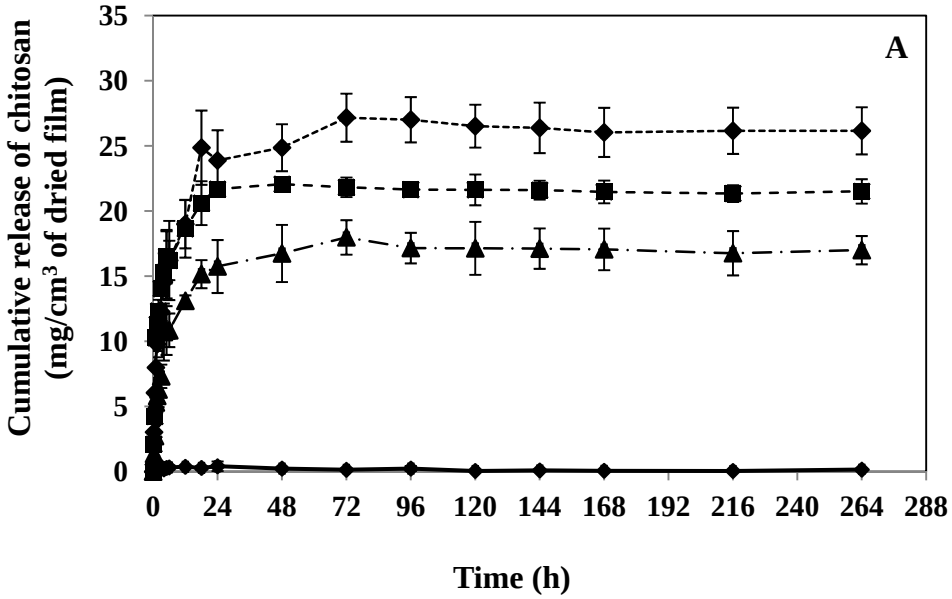

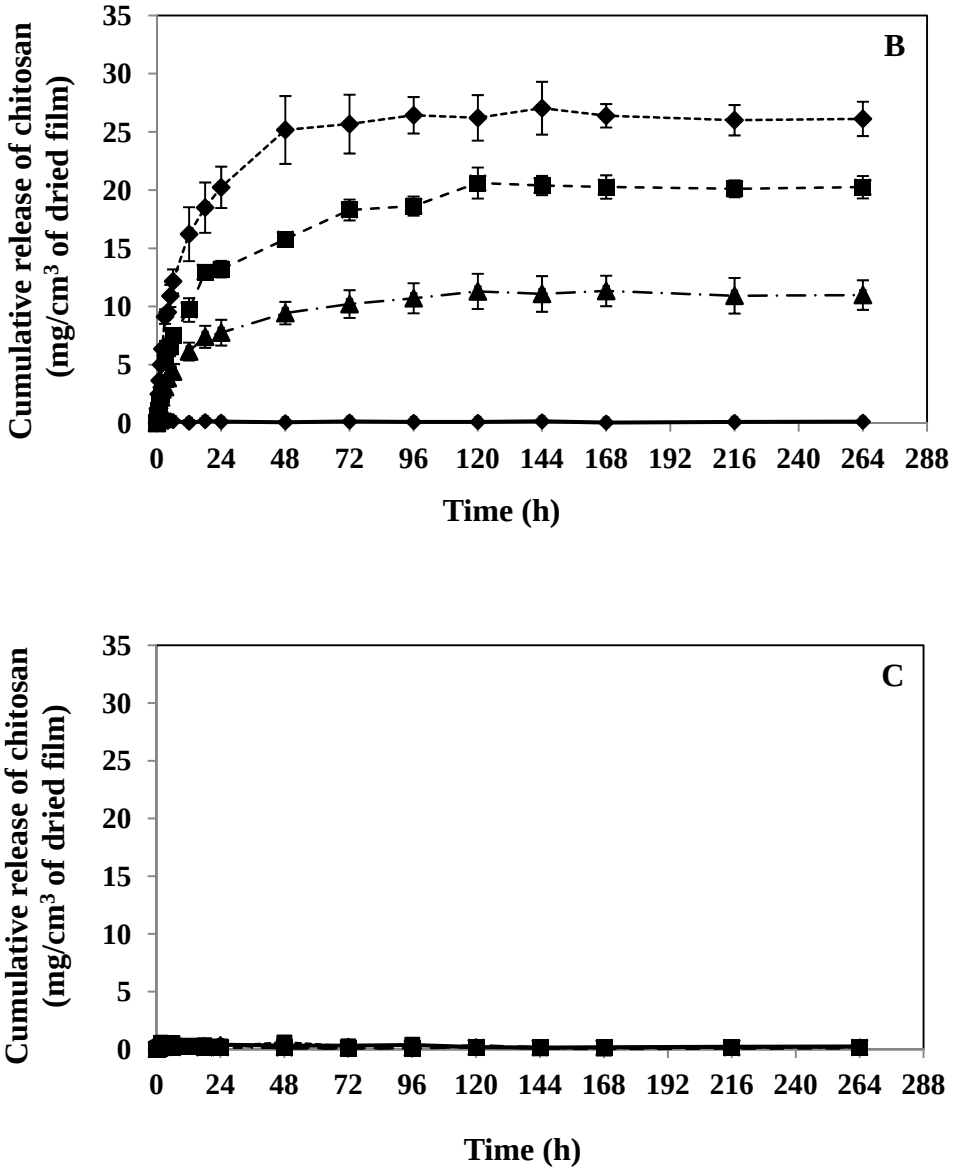

Figure 4.20 Cumulative release profile of chitosan from BCC films in (A) buffer pH1.2, (B) buffer pH5.5 and (C) buffer pH7.4; (●) BC, (◆) BCC3, (■) BCC8, and (▲) BCC20.

In buffer solution whose pH was 1.2 or 5.5, all types of BCC films showed a rapid increase in releasing chitosan during the initial 24 h of the total immersion. Afterwards, the release rate of chitosan from the BCC films into the buffer solution pH 1.2 and pH 5.5 was relatively slow and became constant at around 72 and 96 h of the immersion time, respectively. The releasing rate of chitosan in the

buffer solution pH 1.2 was higher than that of pH 5.5. At pH 7.4, no significant amount of chitosan was found in the buffer solution at all time points for all sample films. It could be explained that chitosan can be dissolved in agents which have pH below 6. The solubility of chitosan is very poor above pH 7 because the precipitation or gelation of chitosan will be occurred (Majeti and Kumar, 2000). In addition, the actual content of chitosan in BCC3, BCC8, and BCC20 films are 38.43±5.02 mg/cm^3, 24.65±0.48 mg/cm^3, and 23.89±2.54 mg/cm^3 of dried film, respectively.

4.2.10 Cytotoxicity

The cytotoxicity of BCC films against L929 mouse fibroblast cells was evaluated. As seen in Figure 4.21, The percentages of living cells with the extraction medium of BC, BCC3, BCC8, and BCC20 films for 24 h, in comparison with those cultured with the fresh medium were found to be 95.5±3.03 %, 91.6±6.26 %, 97.0±3.08 %, and 92.9±2.89 % with the extraction medium concentration of 5 mg/ml and 95.2±8.74 %, 97.8±3.27 %, 95.1±3.78 %, and 92.6±5.16 % with the extraction medium concentration of 10 mg/ml, respectively. The results indicated that the BC and BCC films had no toxicity against L929 mouse fibroblast cells. There is no statistically significant difference in mean values from the BC and the BCC films (P>0.05).

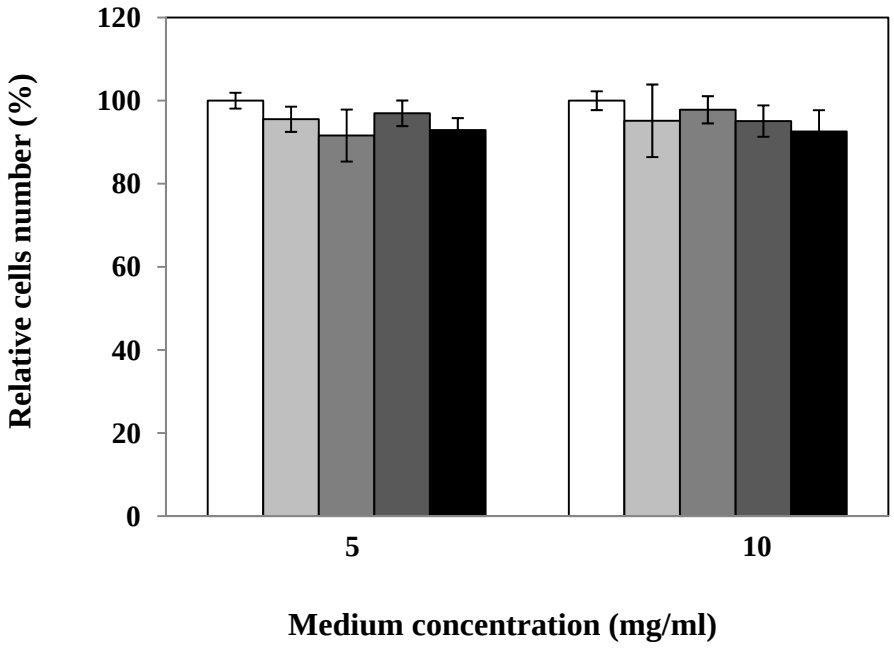

Figure 4.21 Cytotoxicity test against L929 mouse fibroblasts at the extraction medium concentrations of 5 mg /ml and 10 mg /ml on the (□) polystyrene control plate, (□) BC film, (□) BCC3 film, (□) BCC8 film, and (□) BCC20 film. The percentage of viable cells was assessed at 24 h of culture by MTT assay ([a] significant difference in mean value relative to the control BC film ($P < 0.05$), [b] significant difference in mean value relative to the control polystyrene plate ($P < 0.05$)).

4.2.11 *In vitro* cell study

For the application in the therapy of skin wounds, the biocompatibility was evaluated. The ability to support the attachment and proliferations are the foremost characteristics of potential dressing material. The proliferations of HaCat and GF cells on the BCC film are shown in Figures 4.22. The percentages of living cells after seeding on the BC and BCC films from 0 to 24 and 48 h were gradually increased for both GF and HaCat cells. In the culture of fibroblasts (GF), the percentages of cell numbers increased from 100±6 %, 145±15 %, and 230±10 % on BC; 100±4 %, 160±16 %, and 227±13 % on BCC3; 100±5 %, 200±5 %, and 292±11 % on BCC8; 100±12 %, 183±11 %, and 246±14 % on BCC20 at 0, 24 and 48 h,

respectively. The percentage of the number of keratinocytes (HaCat) increased from 100±8 %, 145±9 %, and 195±13 % on BC; 100±13 %, 141±16%, and 206±12% on BCC3; 100±11 %, 124±13 %, and 180±8 % on BCC8; 100±5 %, 141±5 %, and 215±16 % on BCC20 at 0, 24, and 48 h, respectively. At 48 h after seeding, the numbers of viability of both cell types on the BCC films were relatively higher than that of the BC film and the polystyrene control plate. The BCC3 film was the highest with no statistically significant difference (P>0.05) when relative to those of BC film. The result of the higher proliferation rate of HaCat and GF cells on BCC films might be due to the interaction of positively charged amino groups of chitosan and negatively charged cell membranes (He et al., 2007). In the similar way, GF cells could be proliferated on the BCC films in higher level than polystyrene control plate and the BC film. Morphologies of HaCat and GF cells on polystyrene plate, BC, BCC3, BCC8, and BCC20 films at 24 h after seeding are revealed in Figure 4.24-4.27.

HaCat could attach on BC and BCC films with different morphologies. The well-spread keratinocytes was seen on BCC films, whereas HaCat attached on the BC with lower degree of spreading and looser cell adhesion. The result showed that HaCat cells could attach and spread on the BCC films better than on the BC film. The growth of GF cells on the polystyrene control plate demonstrated normal cell morphology as flattened epithelial-like shape. GF cells could also attach and grown on the BCC films better than on the BC film.

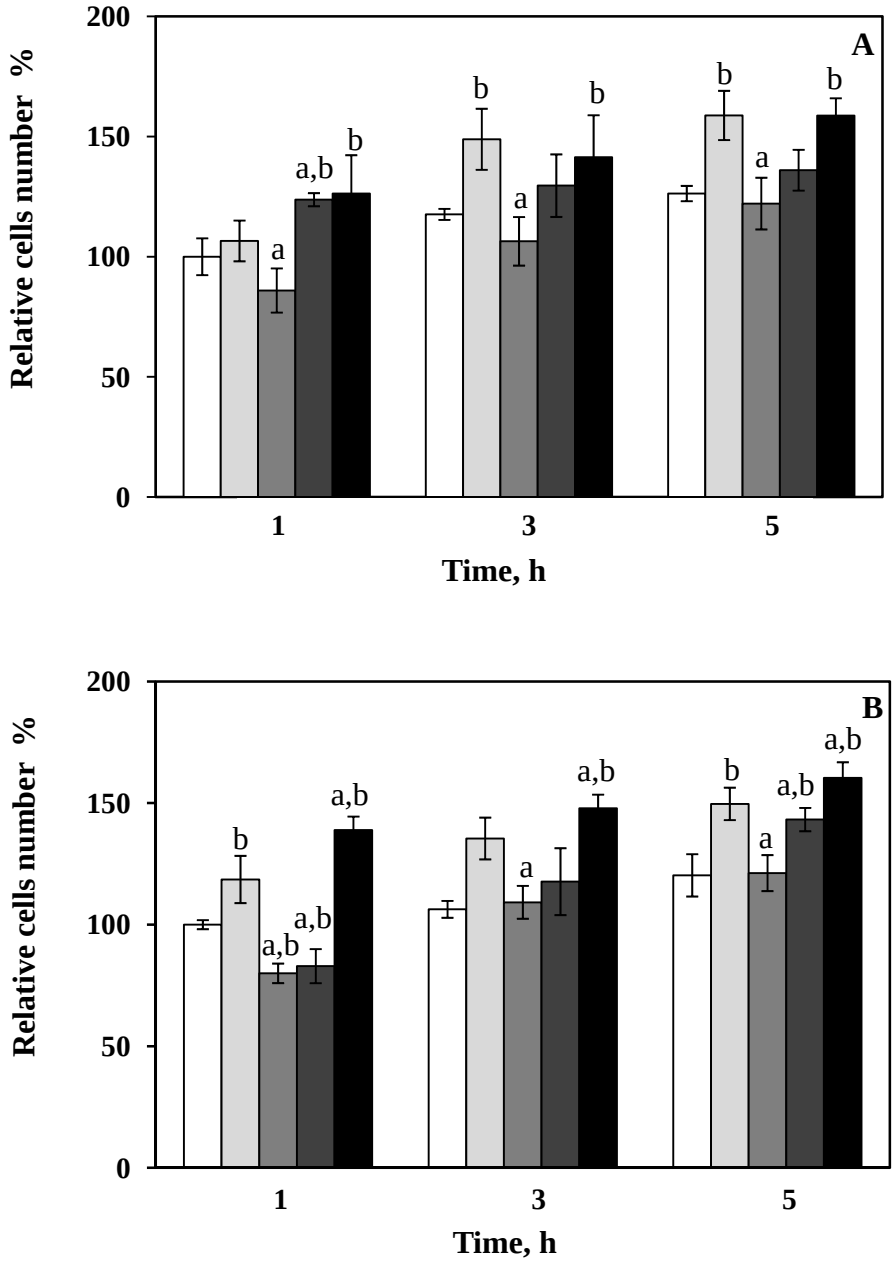

Figure 4.22 Attachment of human fibroblast cell (A) and human skin keratinocytes (B) on the (□) polystyrene control plate, (□) BC film, (□) BCC3 film, (□) BCC8 film, and (■) BCC20 film. The percentage of viable cells was assessed at 1, 3, and 5 h of culture by MTT assay ([a] significant difference in mean value relative to the control BC film ($P < 0.05$), [b] significant difference in mean value relative to the control polystyrene plate ($P < 0.05$)).

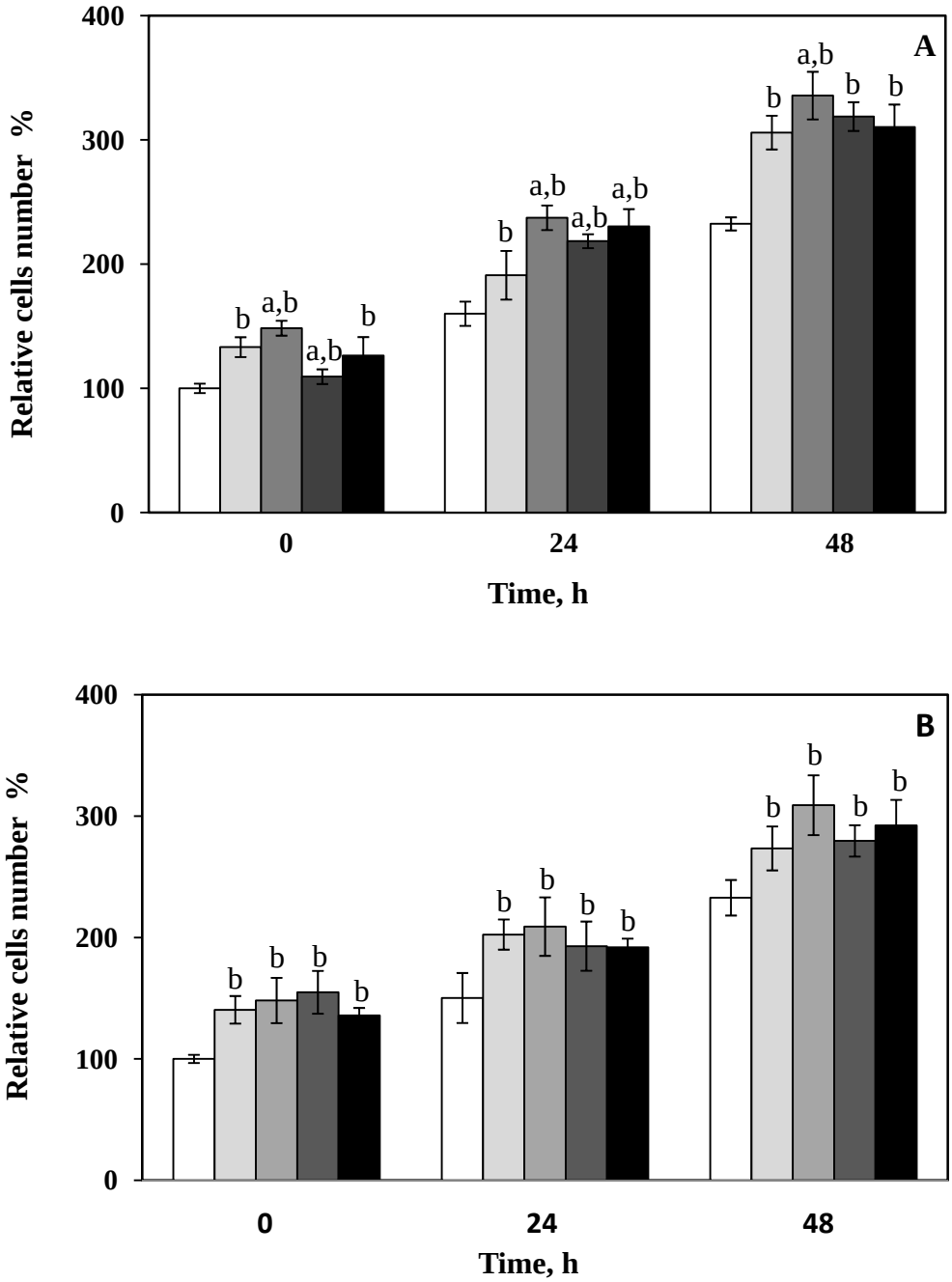

Figure 4.23 Proliferation of human fibroblasts (A) and human skin keratinocytes (B) on the (□) polystyrene control plate, (□) BC film, (□) BCC3 film, (□) BCC8 film, and (■) BCC20 film. The percentage of viable cells was assessed at 0, 24, and 48 h of culture by MTT ([a] significant difference in mean value relative to the control BC film ($P < 0.05$), [b] significant difference in mean value relative to the control polystyrene plate ($P < 0.05$)).

SEM images of GF cells on the BCC films show the flattened epithelial-like shape, whereas attachment of GF cells on the BC film showed a low degree of spreading and looser cell adhesion, indicating fewer cell material interactions. Previously, effects of chitosan on human cells have been reported. Howling et al. (2001), reported that a low molecular weight chitosan promoted proliferation rate of human fibroblasts. Moreover, chitosan with high-level deacetylation stimulated fibroblast proliferation more than the one with low-level deacetylation. They suggested that chitosan might be interacting with growth factors present in the serum, which lead to the stimulatory effect on fibroblast proliferation. The result in this study shows that the BCC films support and promote proliferations of GF and HaCat cells.

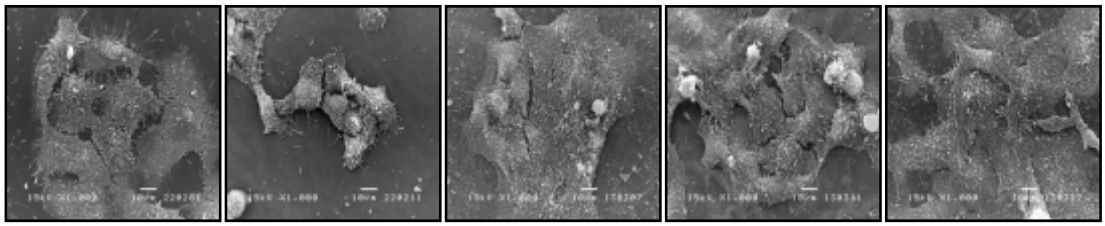

(a) (b) (c) (d) (e)

Figure 4.24 SEM images of human skin keratinocytes at magnification of 1,000 X on (a) the polystyrene control plate, (b) BC film, (c) BCC3 film, (d) BCC8 film, and (e) BCC20 film demonstrated at 24 h.

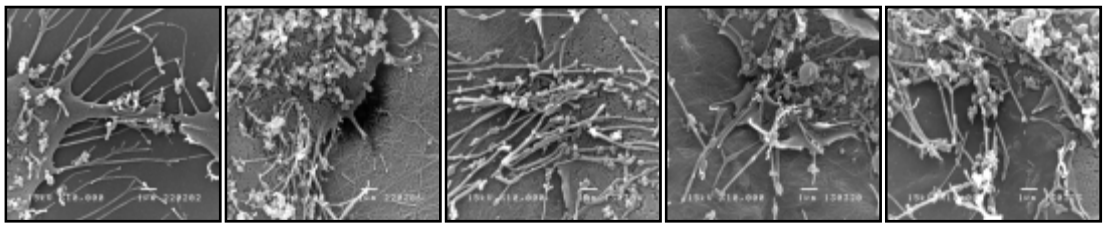

(a) (b) (c) (d) (e)

Figure 4.25 SEM images of human skin keratinocytes at magnification of 10,000X on (a) the polystyrene control plate, (b) BC film, (c) BCC3 film, (d) BCC8 film, and (e) BCC20 film demonstrated at 24 h.

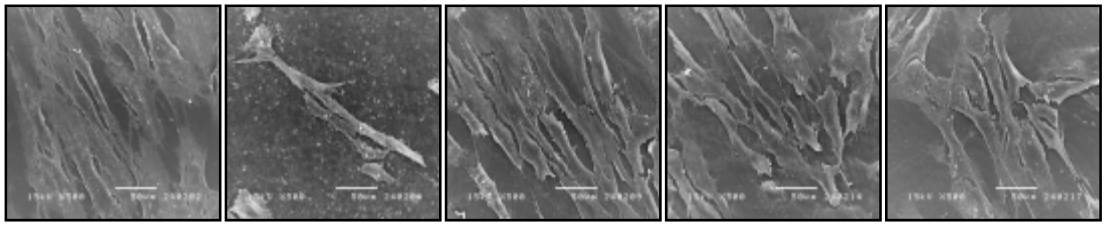

(a) (b) (c) (d) (e)

Figure 4.26 SEM images of human skin fibroblasts at 1,000X magnification on (a) the polystyrene control plate, (b) BC film, (c) BCC3 film, (d) BCC8 film, and (e) BCC20 film demonstrated at 24 h.

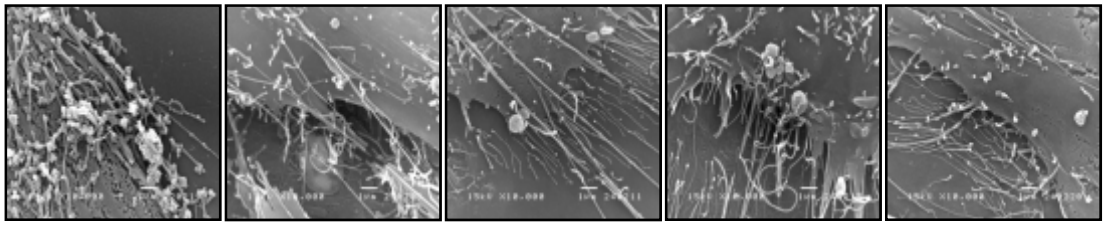

(a) (b) (c) (d) (e)

Figure 4.27 SEM images of human skin fibroblasts at 10,000 X magnification of on (a) the polystyrene control plate, (b) BC film, (c) BCC3 film, (d) BCC8 film, and (e) BCC20 film demonstrated at 24 h.

4.2.12 Antimicrobial ability

Antimicrobial ability is one of important characteristics of materials that use for wound therapy. Chitosan itself has antimicrobial activity to prevent wound infection. BC alone does not have antimicrobial activity. The incorporation of chitosan in the BCC films affected its antibacterial ability as presented in Table 4.5.

Table 4.5 Antimicrobial activities of BC and BCC films against *Escherichia coli* and *Staphylococcus aureus*.

Microorganisms	Sample	Clear zone (mm)
Escherichia coli	BC	0
	BCC3	0
	BCC8	0
	BCC20	0
Staphylococcus aureus	BC	0
	BCC3	43.00 ± 1.25^{a}
	BCC8	42.66 ± 0.90^{a}
	BCC20	46.33 ± 0.77^{a}

[a] Significant difference in mean value relative to the control BC film ($P < 0.05$).

For the antibacterial test of the BCC3, BCC8, and BCC20 film samples, the clear zones with diameters of 43.0 mm, 42.7 mm, and 46.3 mm were observed on *Staphylococcus aureus* plate, respectively but not on *Escherichia coli* plate (Table 4.5 and Figures 4.28-4.29). The BCC films showed significant impact on the growth of *Staphylococcus aureus*, whereas the BC film did not have. The results of the antibacterial testing of the BC and BCC films on *Escherichia coli* indicated that both BC and BCC films had no significant impact on the growth of *Escherichia coli*. This result is similar to the study of No et al. (2002); they reported that chitosan showed stronger bactericidal effects for gram-positive bacteria than gram-negative bacteria. Moreover, concentration, molecular weight and degree of deacetylation (DCA) are the main factors affecting the antibacterial property of chitosan. In this study, the stronger inhibitory effect on *Staphylococcus aureus* of the BCC20 film compared to that of the BCC3 and BCC8 films was observed.

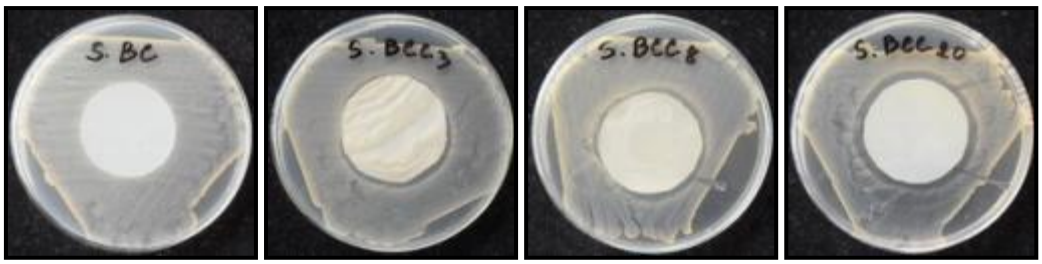

(a) (b) (c) (d)

Figure 4.28 Inhibitory effect of (a) BC film, (b) BCC3 film, (c) BCC8 film, and (d) BCC20 films on the growth of bacteria *Staphylococcus aureus* for 24 h incubated at 37^{o}C.

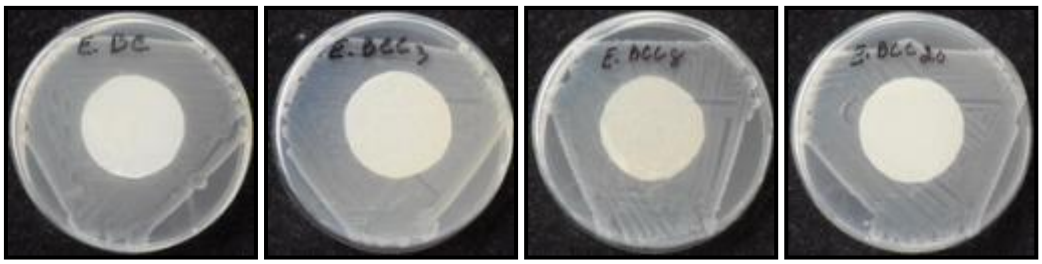

(a) (b) (c) (d)

Figure 4.29 Inhibitory effect of (a) BC film, (b) BCC3 film, (c) BCC8 film, and (d) BCC20 films on the growth of bacteria: *Escherichia coli* for 24 h incubated at 37^{o}C.

Table 4.6 showed antifungal ability of the BCC films. The result indicated that all types of BCC films exhibited the inhibitory effect on the growth of *Aspergillus niger*. In our previous work (Phisalaphong and Jatupaiboon, 2008), the BC-chitosan composite films were prepared from a biosynthesis method; it was found that those films had no significant antimicrobial ability. Therefore, the higher content of chitosan in the BCC films involved the release of chitosan during the incubation could enhance the antibacterial activities of the films.

Table 4.6 Antifungal activity of BC and BCC films against *Aspergillus niger*.

Microorganisms	Sample	Observed growth (Grade)
Aspergillus niger	BC	5
	BCC3	2
	BCC8	2
	BCC20	2

*Grade was used as a measurement of fungal growth: 0 = none, 1 = only apparent under microscope, 2 = trace (<10%), 3 = light growth (10-30%), 4 = medium growth (30-60%) and 5 = heavy growth (> 60%)

The antimicrobial abilities of chitosan have been previously reported. In 2010, Martinez-Camacho and team reported the antimicrobial abilities of chitosan with three proposed mechanisms. The first one, the positive charges present in the molecule of chitosan interact with the negative charges from the residues of macromolecules in the membranes of microbial cells, interfering with the nutrient exchange between the exterior and interior of the cells. The second one, chitosan acts as a chelating agent, creating compounds from traces of metals essential to the cells. The last one, the low molecular weight chitosan is capable of entering the cell's nucleus itself; interacting with the DNA affecting the synthesis of proteins processes of cells.

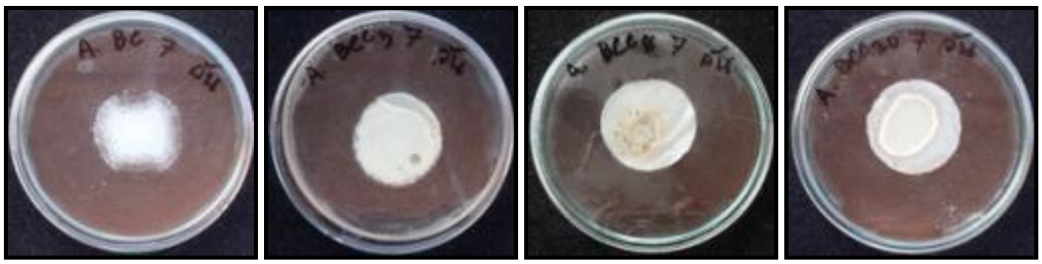

(a) (b) (c) (d)

Figure 4.30 The growth of *Aspergillus niger* on the (a) BC film, (b) BCC3 film, (c) BCC8 film, and (d) BCC20 films, at 37 ^{o}C at the end of the incubation 7 days.

CHAPTER V
BACTERIAL CELLULOSE-*ALOE VERA* FILM

The benefits of *Aloe vera* in the biomedical area have been severally reported. In this research, the biocompatible properties of BC were improved by immersing wet BC pellicle in *Aloe vera* gel. The characteristics of BC-*Aloe vera* composite (BCA) film prepared by impregnation method (as previously described in chapter III) were analyzed and discussed in this section. Herein, BC-*Aloe vera* composite film prepared by this technique was referred to a BCA film.

The optimal absorption time was evaluated by sampling residual *Aloe vera* gel at every 6 h on the 1st day and 12 h for the 2nd day to determine the concentration of active ingredient of *Aloe vera* gel as saccharide (glucose and mannose). The absorption behavior of *Aloe vera* gel as the extent of saccharide penetration into BC pellicle is showed in Figure 5.1.

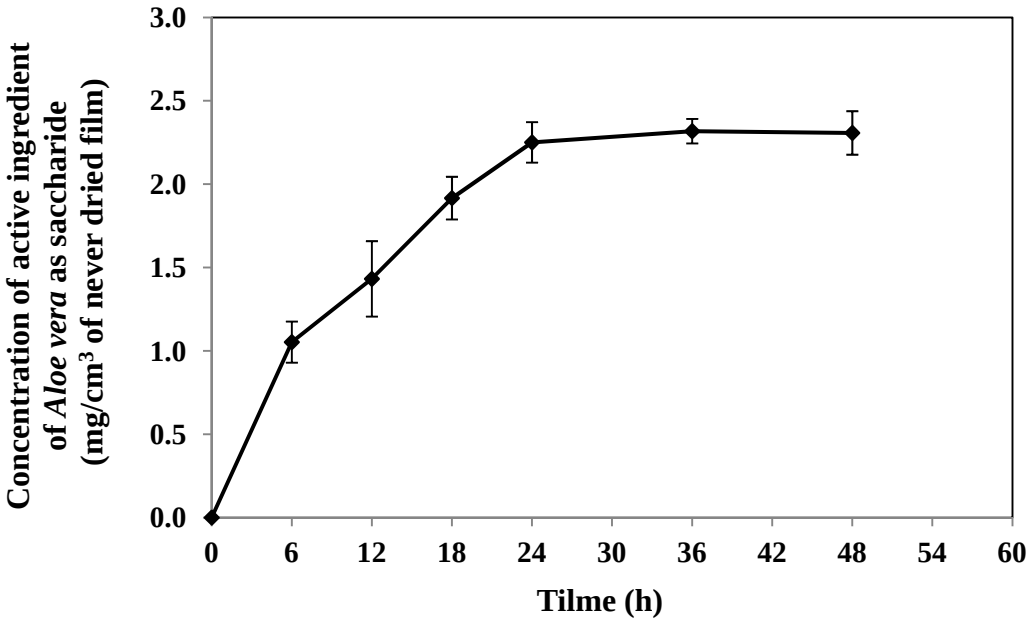

Figure 5.1 Cumulative absorption profiles of active ingredients of *Aloe vera* as saccharide penetrated into BC pellicle.

The absorption curve demonstrated that *Aloe vera* could penetrate into the BC pellicle. The absorption of saccharide rapidly increased in first period (6 h) afterward it gradually increased. After 24 h of absorption the cumulative concentration of active ingredient of *Aloe vera* as saccharide in BC pellicle was nearly constant. The optimal absorption time was around 24 h.

5.1 Morphology

After treated by *Aloe vera* gel, the morphology of the BCA film was different from the pristine BC film. The BCA film was thinner and denser than the BC film. The thickness of the BC and BCA films are 71±2 μm and 52±5 μm, respectively. SEM images in Figures 5.2 and 5.3 show the morphology of surface and cross section of the BC and BCA films, respectively. Figures 5.2(a) and (c) illustrate random well-organized fibril networks with the clear nanofibrils on the BC surface in dried and re-swollen forms. Considering Figures 5.2 (b) and (d), *Aloe vera* gel was absorbed into the film coating on BC fibrils and filling in the empty space between BC fibrils network. As a result, the hollow space of cellulose fibrils network was decreased. The average pore size diameter of the BCA film was smaller than that of the BC film. The clear cellulose nanofibrils cannot be observed on the surface of the BCA film.

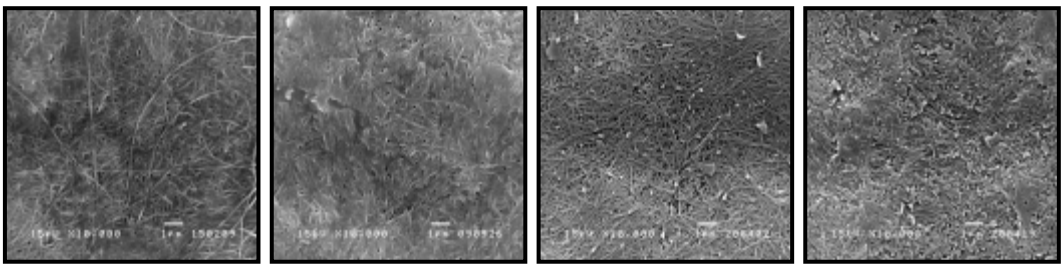

(a) (b) (c) (d)

Figure 5.2 SEM images of surface morphology of the (a) dried BC film, (c) re-swollen BC film, (b) dried BCA film, and (d) re-swollen BCA film, at magnification 10,000X.

Figures 5.3 (a) and (b) reveal the cross sectional morphologies of the re-swollen BC and BCA films at 1,500 magnifications, respectively. The images showed that the thin sheets in the BCA film were tightly packed to form denser structure than that of the BC film. However, the interlayer space between sheets was still observed. The result indicated that *Aloe vera* gel could penetrate into the empty spaces of the BC fibril network and form interaction with the BC molecules.

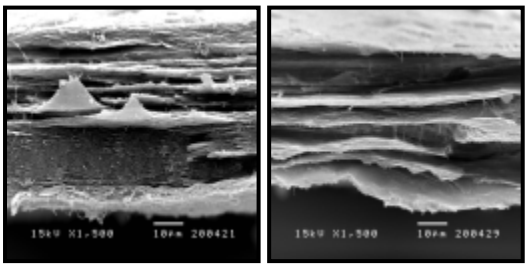

(a) (b)

Figure 5.3 SEM images of cross section morphology of the re-swollen (a) BC film and (b) BCA film, at magnification 1,500X.

5.2 Fourier transform infrared spectroscopy

The FTIR spectra of BC and BCA films were measured from 4000–400 cm^{-1} as shown in Figures 5.4. The BC spectra showed a broad band at wave number about 3,418 cm^{-1} attributed to O-H stretching vibration, a band at wave number about 2,895 cm^{-1} attributed to the aliphatic C-H stretching vibration (Kim et al., 2010), a band at around 1641 cm^{-1} attributed to the glucose carbonyl of cellulose (Phisalaphong and Jatupaiboon, 2008; Klemm et al., 2001) and a band between 1,155-1032 cm^{-1} attributed to the polysaccharide structure (Balau et al., 2004). The characteristic absorption of the *Aloe vera* is a bands at 1594 cm^{-1}, which is attributed to amide groups (Saibuatong and Phisalaphong, 2009). The spectra of the BCA film exhibited all of the characteristic bands of BC with the appearance of a new band about wave number 1,575 cm^{-1}. The shift of the characteristic band of *Aloe vera* from 1594 cm^{-1}

to 1,575 cm^{-1} implied the occurrence of the intermolecular interaction between the hydroxyl groups of cellulose and the amino groups of *Aloe vera*.

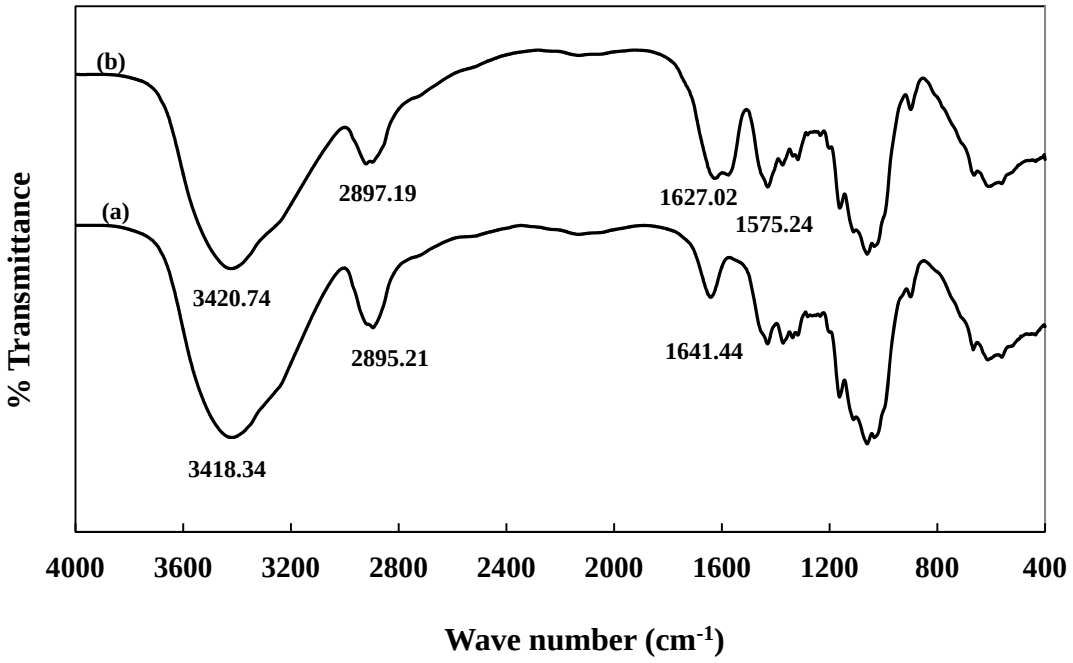

Figure 5.4 The FTIR spectra in wave number ranging from 4000 to 400 $cm^{-1}$of (a) BC film and (b) BCA film.

5.3 X-ray diffraction

The average crystallinity index (C.I.) value was calculated from X-ray diffraction pattern. Figures 5.5 shows the diffraction patterns of BC and BCA films. The pattern of BC exhibits three main peaks at 2θ = 14.50°, 16.72°, and 22.74° attributed to the $(1\ \bar{1}\ 0)$, (1 1 0) and (2 0 0) reflexions planes of cellulose I structure, respectively (Cai and Kim, 2010; Retegi, 2010). The broad diffraction peaks (2θ = 16.72°) were observed for BC film because BC is not a completely crystalline material.

The average C.I. value of BC and BCA film was 86.47and 84.63, respectively. The slightly decrease in crystallinity of BCA might be due to intermolecular interaction between amino groups of *Aloe vera* and hydroxyl groups of cellulose

fibrils (Saibuatong and Phisalaphong, 2009). Modifying BC by incorporation of other biopolymers could affect the preferential orientation of the $(1\,\bar{1}\,0)$ reflexion plane during drying process. Consequently, this incomplete orientation of the $(1\,\bar{1}\,0)$ reflexion plane resulting in a decreased in crystallinity of BC and which in turn leaded to a decrease in strength (Cai and Kim, 2010).

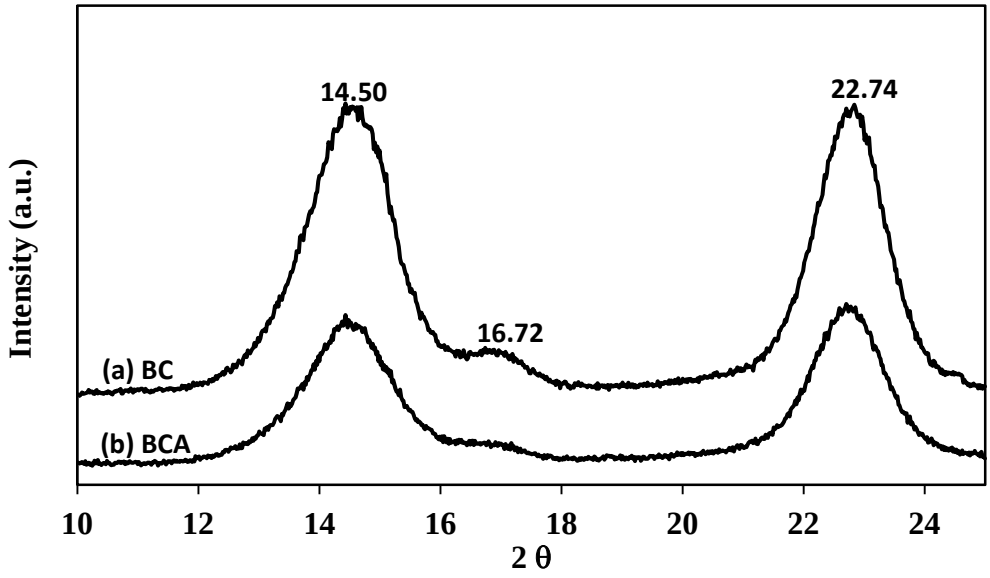

Figure 5.5 The XRD pattern of BC film and BCA film.

5.4 Brunauer-Emmett-Teller

The porosities of the BC and BCA films from BET analysis are shown in Table 5.1 and Figure 5.6.

Table 5.1 Average pore size and surface area of BC and BCA films analyzed with BET analysis.

Sample	**Surface area (m^2/g)**	**Average pore diameter (Å)**
BC	4.20±0.09	100±10.9
BCA	3.05±0.09[a]	81±6.9

[a] Significant difference in mean value relative to the control BC film ($P < 0.05$).

Corresponding to results from the SEM images, the average pore diameter of the BCA film was smaller than that of the BC film with no statistically significant difference ($P>0.05$), whereas the surface area of BCA film was significantly ($P<0.05$) decreased. Pore size distributions of the dried BC and BCA films are shown in Figure 5.6. The result confirmed that aloe vera gel could penetrate into the BC fibril network and filled the pores.

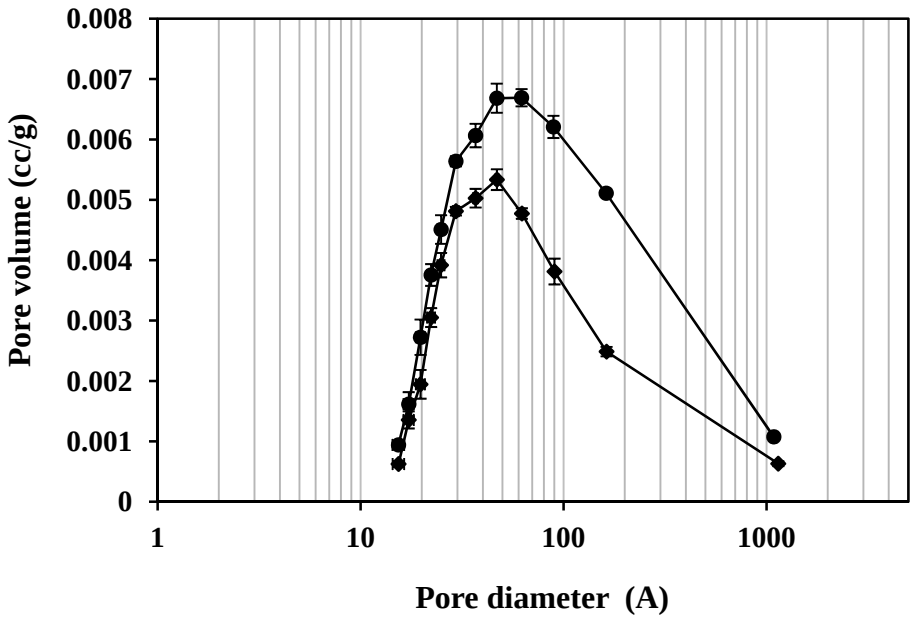

Figure 5.6 Pore size distributions of the dries (●) BC film and (◆) BCA films.

5.5 Mechanical property

In this present research, the mechanical properties of the BCA film as tensile strength, Young's modulus and elongation at break were analyzed in order to investigate the effects of *Aloe vera* content on mechanical properties of the film. The tensile strength, Young's modulus and elongation at break of BC and BCA film are shown in Figure 5.7, Figure 5.8 and Figure 5.9, respectively.

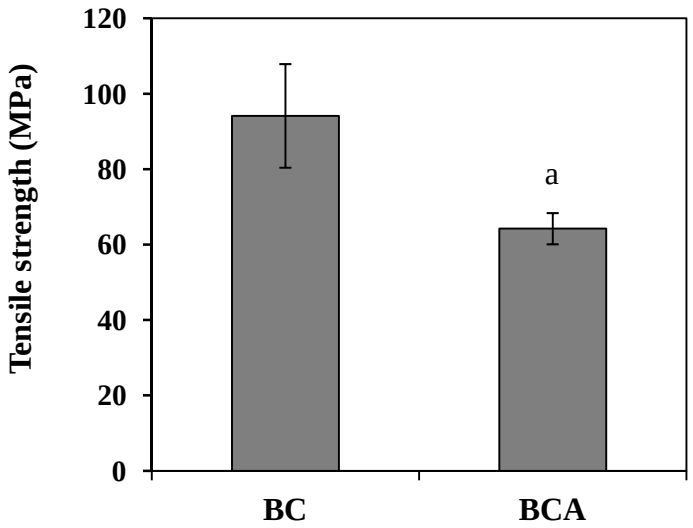

Figure 5.7 Tensile strength of BC and BCA films, [a] significant difference in mean value relative to the control BC film ($P < 0.05$).

The tensile strength of the dries films of BC and BCA were 94±13.74 MPa and 64.23±4.14 MPa, respectively. Tensile strength of the film was significantly ($P<0.05$) decreased after treated with *Aloe vera* gel. According to the SEM images of BCA film, *Aloe vera* gel could penetrate into BC fibrils network and fill in the empty space between BC fibrils network. The incorporation of aloe vera gel into the film might increase the amorphous phase fraction. The interaction between *Aloe vera* gel and BC molecules could also weaken affinity of binding of the films. These effects resulted in a decreased of tensile strength of the film.

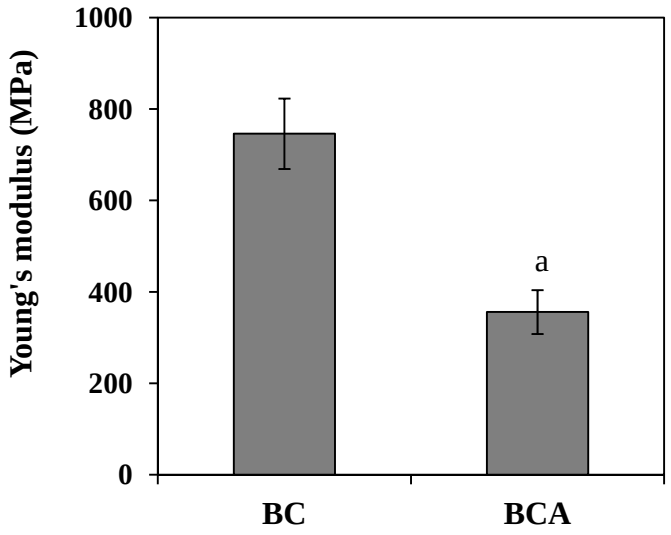

Figure 5.8 Young's modulus of BC and BCA films, [a] significant difference in mean value relative to the control BC film ($P < 0.05$).

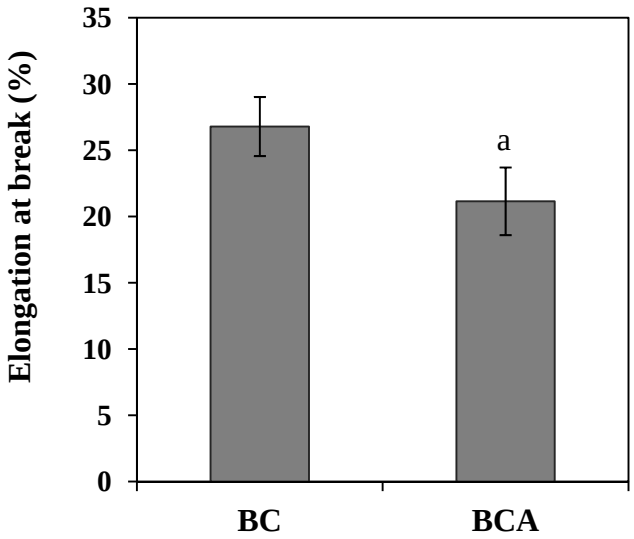

Figure 5.9 Elongation at break of BC and BCA films, [a] Significant difference in mean value relative to the control BC film ($P < 0.05$).

For the same reason as the tensile strength, Young's modulus and elongation at break of the BCA film were lower than those of the BC film with statistically significant difference ($P<0.05$). Young's modulus of the dried films of BC and BCA were 746±77 MPa and 356±48 MPa, respectively, whereas the elongations at break of were 26.79±2.23 % and 21.15±2.55 %, respectively. However, the mechanical

properties of the BCA film were still higher than those of some commercial wound dressing (Cardona et al., 1996; Lowe, 2008).

5.6 Water absorption capacity

The water absorption capacity (WAC) is an importance characteristic of materials to be used as wound dressing. This property represents as abilities to absorb exudate and control moist wound healing environment. The WACs of BC and BCA films are shown in Figure 5.10. The WAC of BCA composite film was slightly higher than that of pristine BC film with no statistically significant difference (P>0.05). It could be explained that *Aloe vera* gel is very hydrophilic and therefore, the incorporation of Aloe vera gel into the film enhanced the WAC of the film.

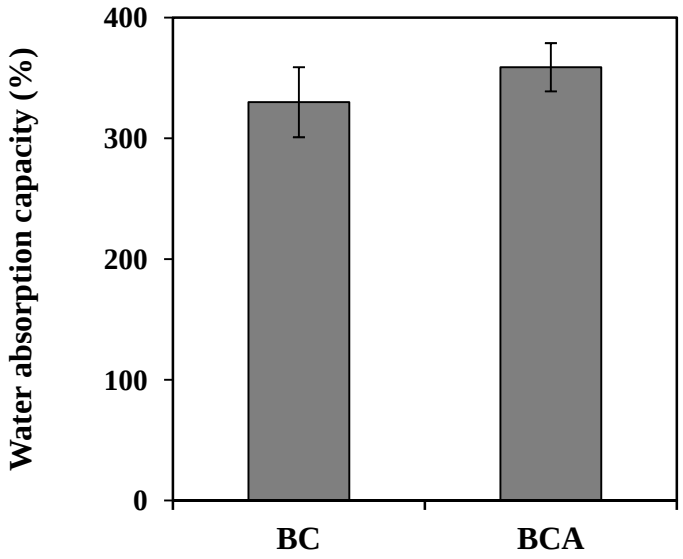

Figure 5.10 The water absorption capacity of BC and BCA films.

5.7 Water vapor transmission rate

The water vapor transmission rate (WVTR) of BC and BCA films was analyzed following the ASTM E 96-00. The result is shown in Table 5.2. The WVTR of BC and BCA film were 1049±46 g/m^2/day and 1030±41 g/m^2/day, respectively. Therefore, the incorporation of *Aloe vera* gel into the film did not significantly affect

the WVTR of the films. According to Chapter IV, the water loss for normal skin is around 204.0±115.2 g/m^2/day, while that for the injured skin can range from 207±26 g/m^2/day for the first degree of burn to 5138±202 g/m^2/day for a granulating wound (Cardona et al., 1996). When compared with the commercial wound dressing such as Bioprocess®, Biobrane II®, Op-site® and Gauze (Cardona et al, 1996, and Lowe, 2008), the WVTRs of BC and BCA films were in the range of various commercial wound dressings. This result indicated that the BCA film has good potential to be used as wound dressings.

Table 5.2 Water vapor transmission rate of BC film, BCA film, and commercial wound dressings (*Cardona et al., 1996; ** Lowe, 2008).

Sample	**WVTR (g/m^2/day)**
BC	1049 ± 16
BCA	1030 ± 41
Bioprocess®,*	2046 ± 249
Biobrane II®,*	1565 ± 281
Op-Site®,*	426 ± 9
Gauze**	800

[a] Significant difference in mean value relative to the control BC film ($P < 0.05$).

5.8 Oxygen transmission rate

Oxygen plays an important role in wound healing processes. In this study, BC and BCA films were analyzed for oxygen transmission rate by following the ASTM D3985. As seen in Table 5.3, the presence of *Aloe vera* gel in BCA film had significantly affected the oxygen transmission rate (OTR) of the film. The OTR of the BCAS film was 9.94±0.28 cm^3/m^2/day, which was about 3.75 times of that of the unmodified BC film. However, when compared with the commercial wound dressing such as Bioprocess® and Gauze (Cardona et al, 1996; Lowe, 2008), the OTR of the

BC and BCA films exhibited significant lower oxygen transmission. Due to the small nanoscale pores of the BC and BCA films in dry form, the corresponding values of the OTR were considerably low. Nonetheless, the OTR of the BC and BCA films in re-swollen form should be much higher.

Table 5.3 Oxygen transmission rate of BC film, BCA film and commercial wound dressings (*Cardona et al., 1996; ** Lowe, 2008).

Sample	**Oxygen transmission rate ($cm^3/m^2/day$)**
BC	2.65 ± 0.03
BCA	9.94 ± 0.28[a]
Bioprocess®,*	247 ± 54
Gauze**	14275

[a] Significant difference in mean value relative to the control BC film ($P < 0.05$).

5.9 Release of active ingredients of *Aloe vera* gel as saccharide from BCA film

The actual amount of saccharide in the BCA film was 44.3±0.5 mg/cm^3 of dried film. The BC and BCA films were investigated for the total amount of released chitosan in buffer pH 1.2, pH 5.5, and pH 7.4. The cumulative releases of active ingredients of *Aloe vera* gel as saccharide from the BCA film are shown in Figure 5.11. In case of the BCA film, the release rate showed similar trends for all of the releasing mediums. Rapid increases in releasing of saccharide from the BCA film were observed during the initial 12 h of the total immersion. Afterwards, the release rate of saccharide from the BCA film became slower than the former and total amount of the accumulative release of saccharide into the releasing medium gradually increased from 12 to 144 h of total immersion. Afterward, the accumulative release of saccharide was constant with the maximum amount of saccharide released in

releasing medium pH 1.2, pH 5.5, and pH 7.4 at 38.2±2.6 mg/cm^3, 36.9±2.4 mg/cm^3, and 43.5±2.1 mg/cm^3 of dried film, respectively. The release of saccharide in buffer pH 7.4 was about 98.2 % of the actual amount in the film, which was relatively higher than those in the other buffers. Slight release of saccharide was also found from the BC film in all of releasing medium, which might be due to some release of cellulose fibre from the BC film.

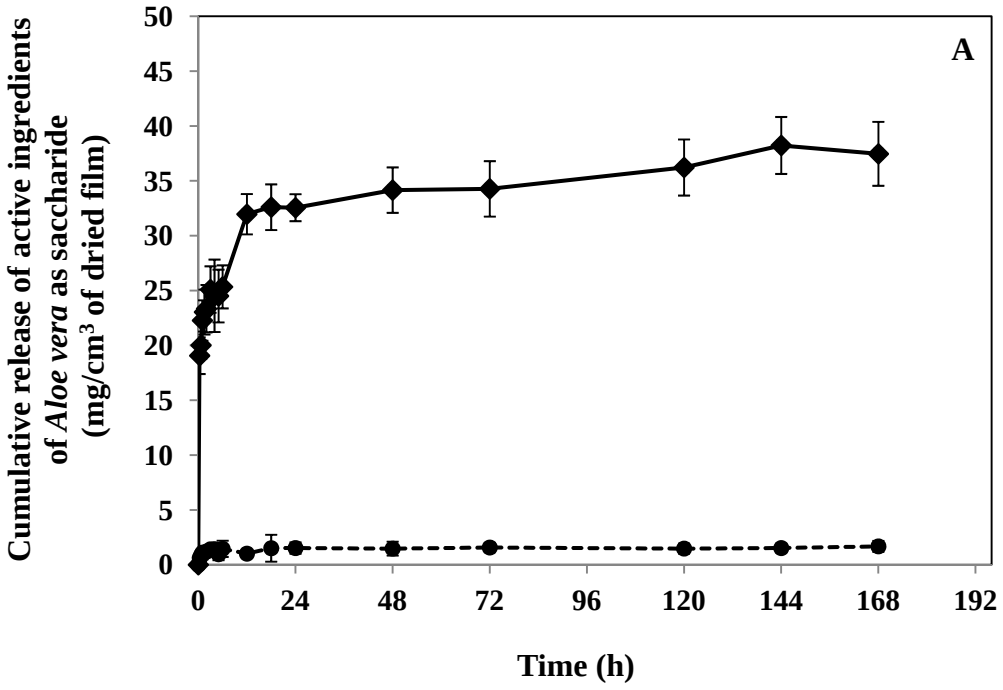

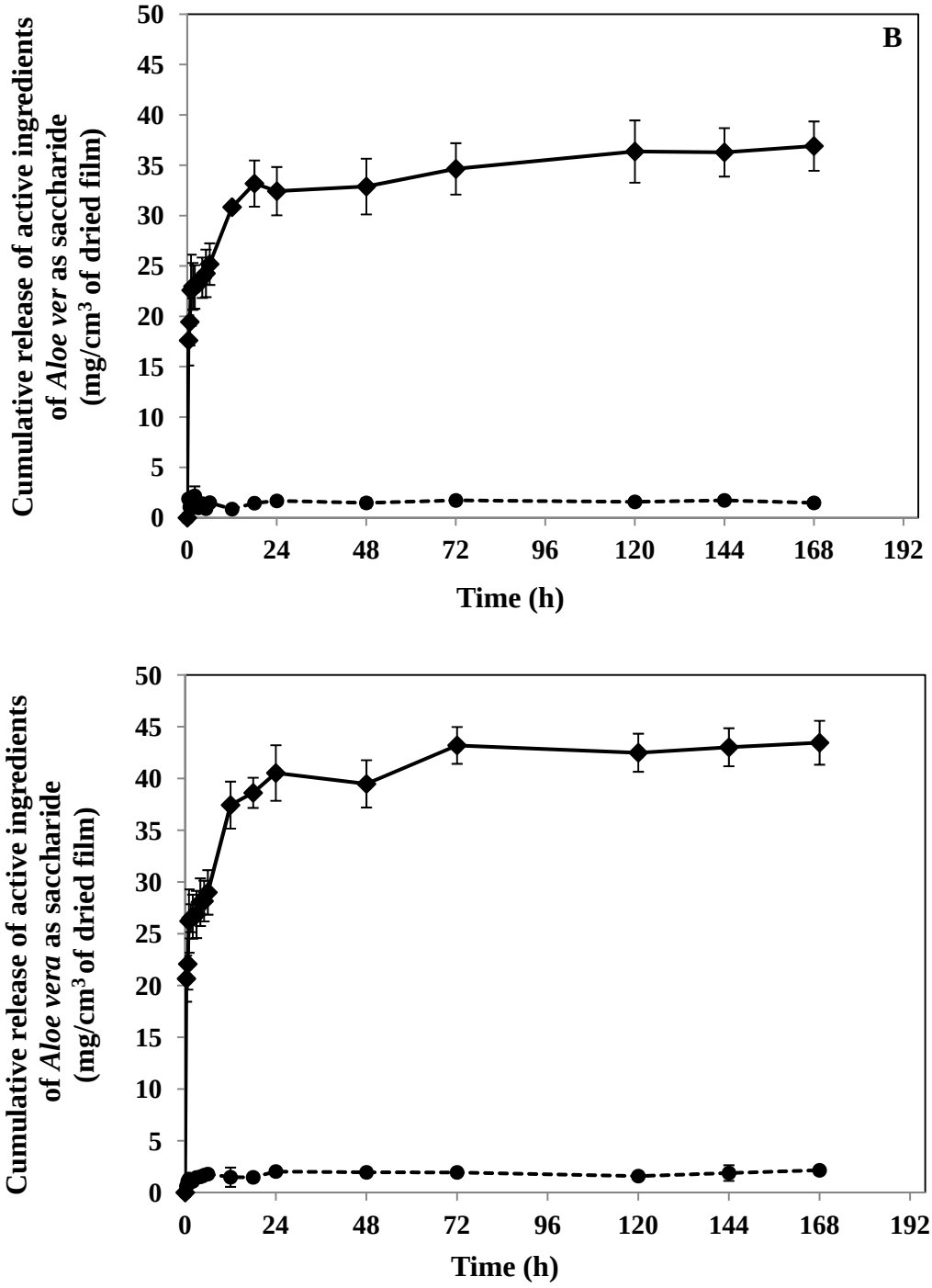

Figure 5.11 Cumulative release profile of the active ingredients of *Aloe vera* gel as saccharide from BCA film in (A) buffer pH1.2, (B) buffer pH5.5, and (C) buffer pH7.4 (●) BC and (◆) BCA films.

5.10 Cytotoxicity

The Cytotoxicity of the BCA film against L929 mouse fibroblast cells was evaluated. As seen in Figure 5.12, the percentages of viable cells with the extraction medium of the BC and BCA films for 24 h, in comparison with those cultured with fresh medium were found to be 95.5± 3.03% and 107.2±2.43% with the extraction medium concentration of 5 mg/ml and 95.2±8.74% and 120.7±3.17%, with the extraction medium concentration of 10 mg/ml, respectively. The relative cell number on the BCA film had higher value than those on both of polystyrene culture plate and the BC film with statistically significant difference (P<0.05). The results showed that not only the BCA film had no toxicity against L929 mouse fibroblast cells but also promoted the growth of these cells.

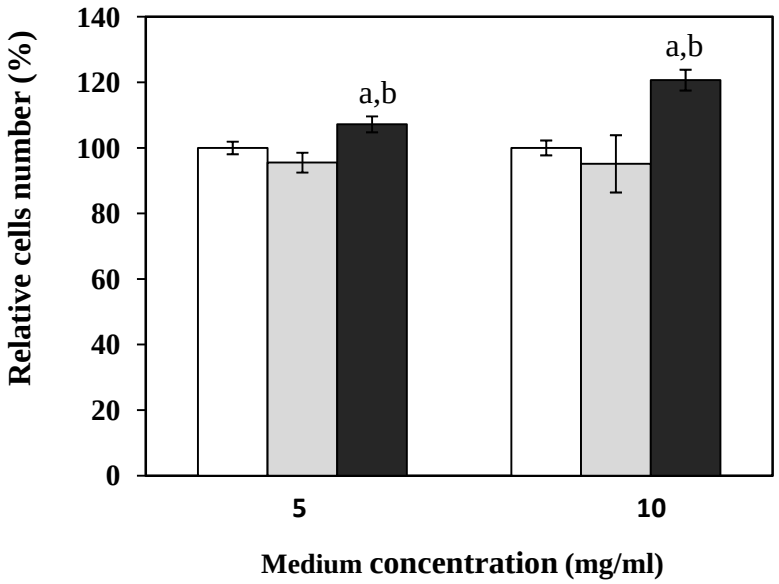

Figure 5.12 Toxicity test against L929 mouse fibroblast cells at the extraction medium concentrations of 5 mg /ml and 10 mg /ml on (□) the culture-treated polystyrene plate, (▫) BC film, and (■)BCA film. The percentage of living cells was assessed at 24 h of culture by MTT assay ([a] significant difference in mean value relative to the control BC film (P<0.05), [b] significant difference in mean value relative to the control polystyrene plate (P<0.05)).

5.11 *In vitro* cell study

To evaluate the potential use of the BCA film as material for the application in the therapy of wound healing, their biocompatibility in term of attachment and proliferation of human-transformed skin keratinocytes (HaCat) and Gingival fibroblasts (GF) was evaluated in comparison with that of the BC film and polystyrene culture plate which was a control. The results are shown in Figure 5.13 and 5.14.

Figure 5.13 shows the attachment of human fibroblasts and human skin keratinocytes on the BC and BCA films and polystyrene culture plate (control) after 1, 3, and 5 h of incubation. The relative percentage of viable human fibroblast on polystyrene culture plate and the BC film was slightly increased from 1 h to 5 h, whereas that on the BCA film was rather constant and relatively lower than that on polystyrene culture plate and the BC film. This result could imply that the complete attachment of human fibroblasts on surface of the BCA film occurred within the 1^{st} h after seeding. In case of human keratinocytes, the results showed similar trends of the cell attachments on polystyrene culture plate, the BC film and the BCA film. The results indicated that both of the cells could attach on the BCA film. Compared to the attachment of human fibroblasts, the higher relative cell number of human keratinocytes attachment on the BCA film was obtained.

The proliferations of human fibroblasts and human skin keratinocytes on the BC and BCA film compared to the culture-treated polystyrene plate (control) are shown in Figure5.14. Both of the tested cells could grow and proliferate very well on the control plate, the BC film and the BCA films. In case of fibroblasts, the percentage of viable cell number gradually increased from 100±4 % to 177±6 % and 224±11 % on the polystyrene plate, 100±2 % to 155±5 % and 206±5 % on the BC film and 100±3 % to 222±8 % and 259±19 % on the BCA film at 0, 24 and 48, respectively. The proliferation rate of GF cells on the BCA film was significantly (P<0.05) higher than those of polystyrene control plates and the BC film. In case of keratinocytes, the percentage of the relative viable cell number of keratinocytes increased from100±3 % to 150±21 % and 233±15 % on the polystyrene control plate, 100±8 % to 145±9 % and 195±13 % on the BC film and 100±9 % to 130±18 % and

185±10 % on the BCA film at 0, 24 and 48, respectively. The proliferation rate of HaCat cells were in the following order: on BCA film >BC film > control plate.

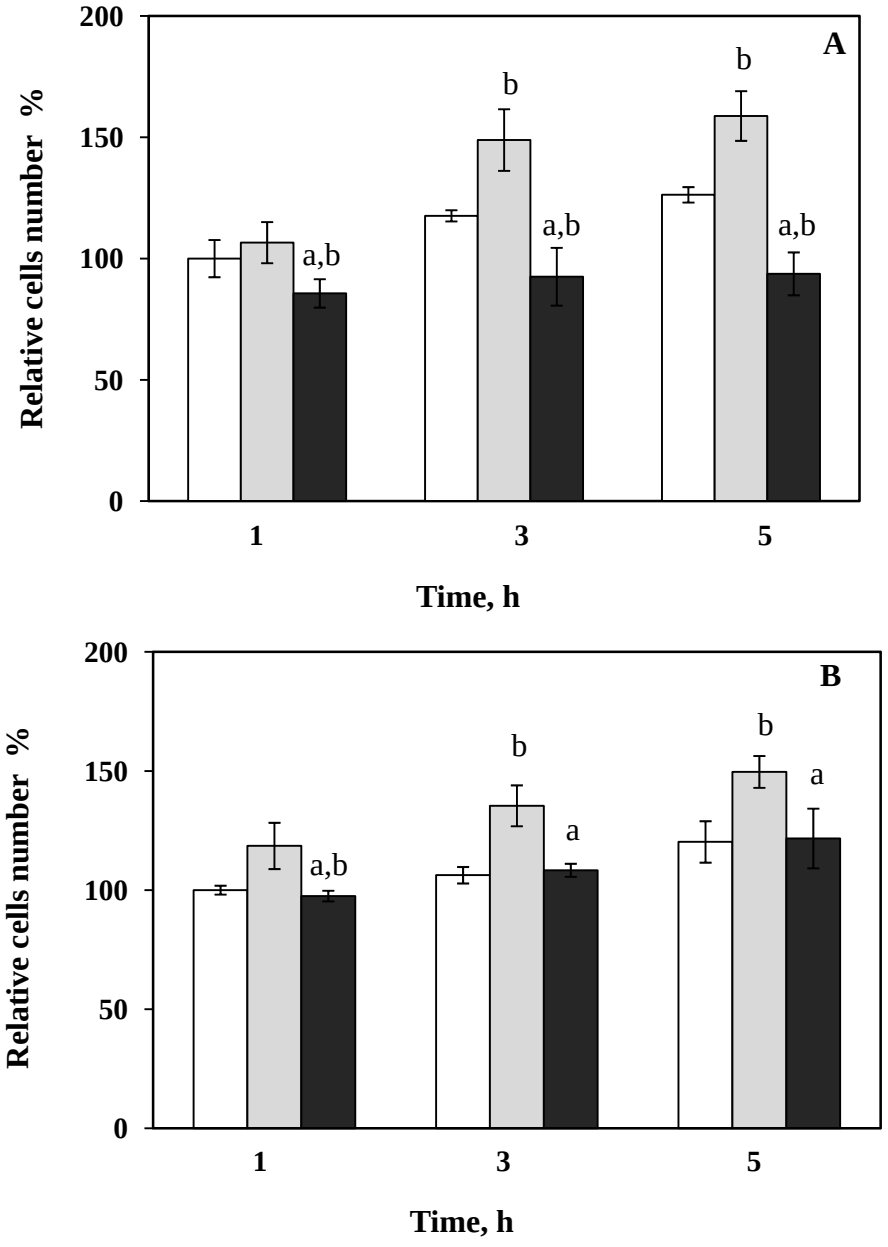

Figure 5.13 Attachment of human fibroblast cells (A) and human skin keratinocytes cells (B) on the (□) culture-treated polystyrene plate, (▭) BC film, and (■) BCA film. The percentage of viable cells was assessed at 1, 3 and 5 h of culture by MTT assay ([a] significant difference in mean value relative to the control BC film (P<0.05), [b] significant difference in mean value relative to the control polystyrene plate (P<0.05)).

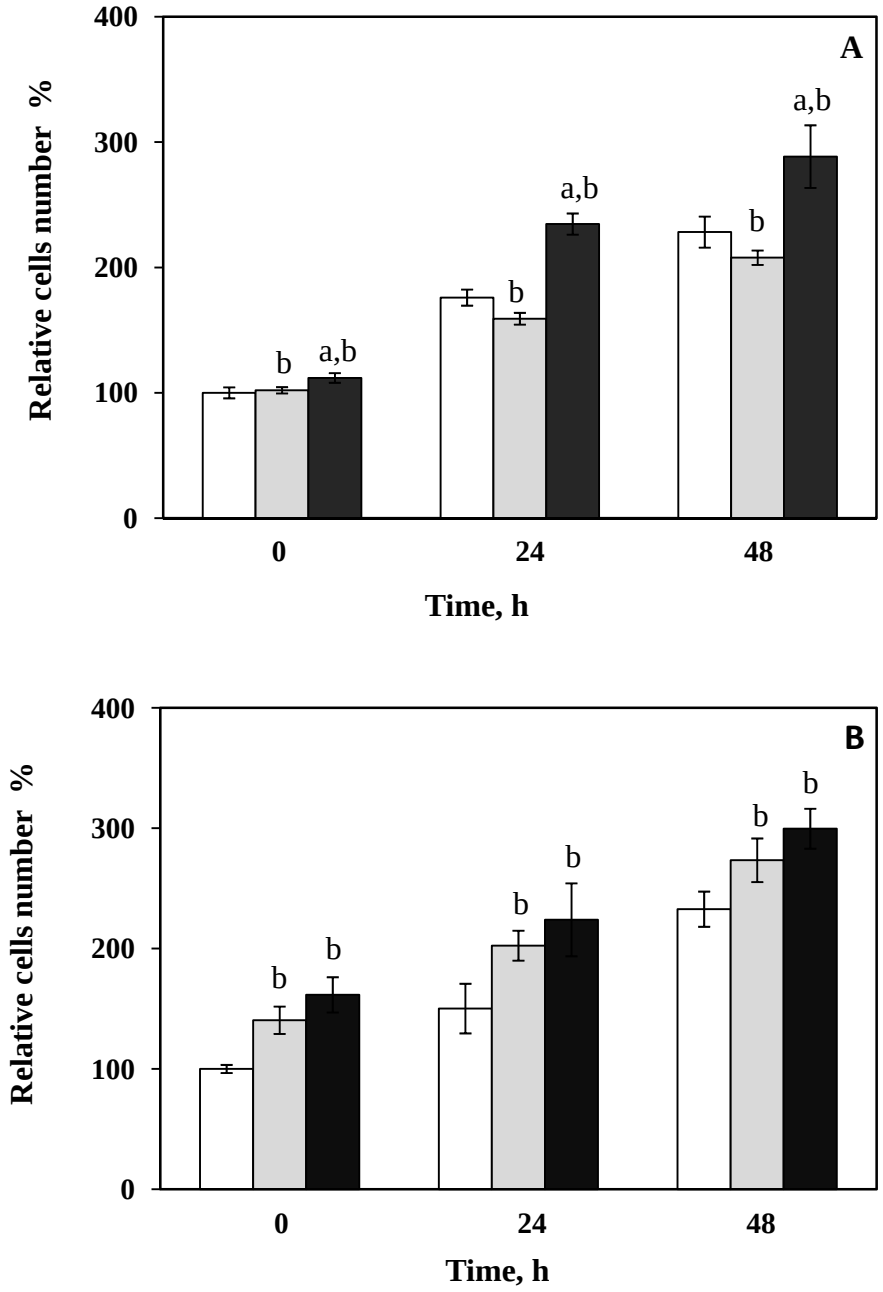

Figure 5.14 Proliferation of human fibroblast cell (A) and human skin keratinocytes cells (B) on the (□) culture-treated polystyrene plate, (□) BC film, and (■) BCA film. The percentage of viable cells was assessed at 0, 24 and 48 h of culture by MTT assay ([a] significant difference in mean value relative to the control BC film (P<0.05), [b] significant difference in mean value relative to the control polystyrene plate (P<0.05)).

A comparison of cell number showed that the numbers of both cell types on the BCA films was relatively higher than those on the polystyrene plate and the BC film. The result revealed that the BCA film promoted the growth and proliferation of human fibroblast as well as human keratinocytes cells.

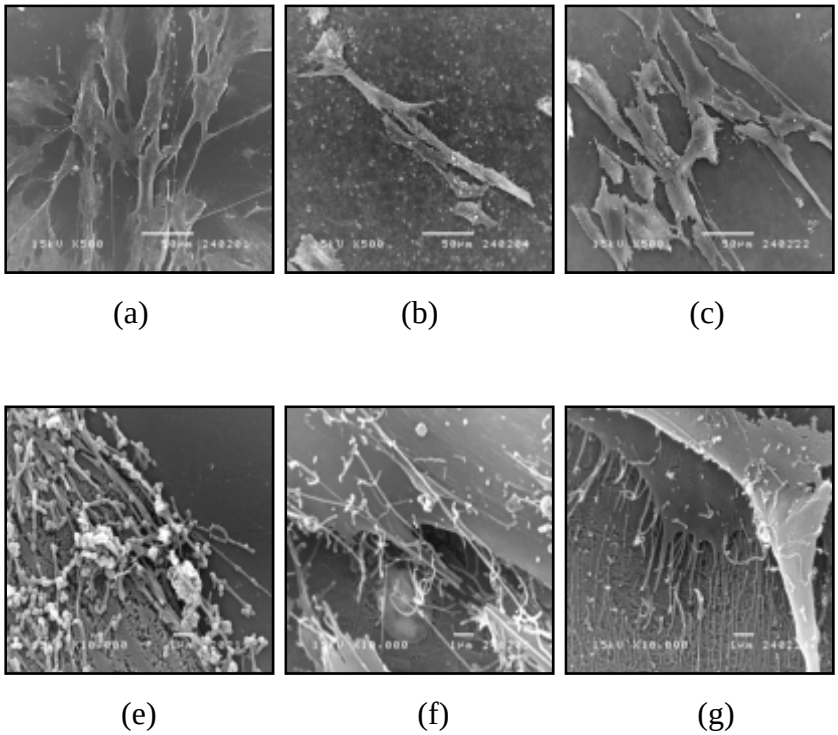

(a) (b) (c)

(e) (f) (g)

Figure 5.15 SEM images of human skin fibroblasts on (a) the polystyrene culture plate, (b) the BC film and (c) the BCA film at magnification of 1,000 X and on (e) the polystyrene culture plate, (f) the BC film, and (g) the BCA film at 10,000X magnification demonstrated at 24 h.

Since the BC and BCA films had small pore diameters in nano-scale, both of human fibroblasts and keratinocytes could grow only on the surfaces of these films. The SEM images of human fibroblasts on the control plate, the BC film, and the BCA film at 24 h are shown in Figure 5.15. It illustrated the typical elongated fibroblast pattern with the good spreading on the control plate. The extent of cell spreading on the BCA film was slightly less than that on the control plate. When compared with the

BC film, the extent of cell spreading and adhesion on surface of the BCA film was considerably higher.

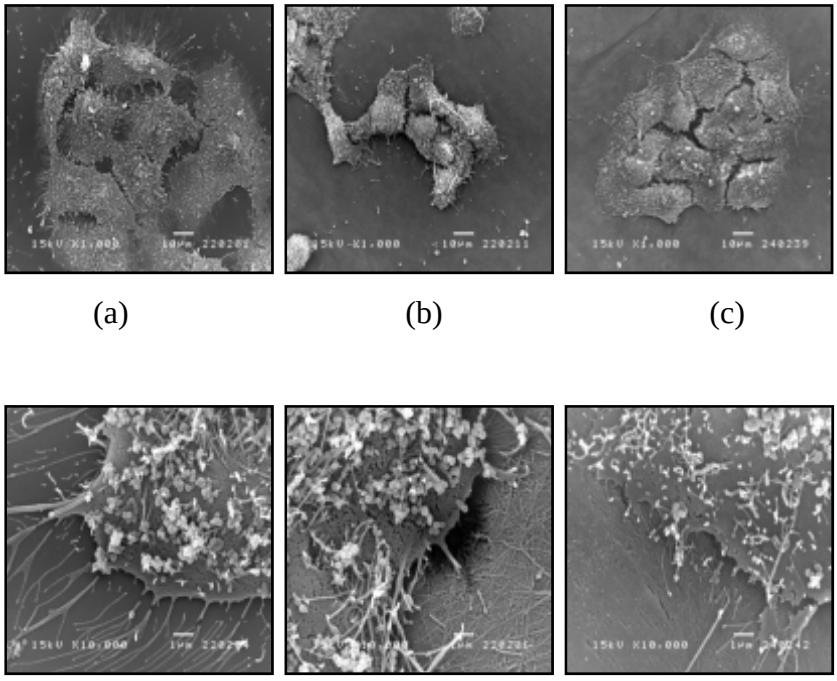

(a) (b) (c)

(e) (f) (g)

Figure 5.16 SEM images of human skin keratinocytes (a) the polystyrene control plate, (b) the BC film and (c) the BCA film at magnification of 1,000X; and on (e) the polystyrene control plate, (f) the BC film, and (g) the BCA film at 10,000X magnification of demonstrated at 24 h.

Figure 5.16 shows SEM images of human keratinocytes on the tested materials at 24 h after seeding. HaCat cells showed well-spread keratinocytes on the surface of the control plate, which was seen as a flattened epithelial-like shape with slight trace of filopodia (Figures 5.16 (a) and (e)). The pattern of spreading and attachment of HaCat cells on the BCA was similar to that on the control plate (Figure 5.16). However, compared to the BC film, HaCat cells could more spread and adhere better on the BCA film. As seen in Figure 5.16 (e-g), the angles between the cells and the tested material surface were in the following order: on culture plate < the BCA film < the BC film. The present study showed the addition of *Aloe vera* gel into to BC film

by immersion method creating beneficial bio-properties. The BCA film not only supported the attachment and proliferation of keratinocytes, but also improved cell adhesion and spreading on the film surface.

5.12 Antimicrobial ability

The antimicrobial ability of Aloe vera has been previously reported. Aloe contains many antiseptic agents such as lupeol, urea nitrogent, cinnamonic acid, salicylic acid, sulfur, phenolic compounds, anthraquinones, aloin and emodin. They all have inhibitory effects on the activity of bacteria, fungi and virus (Surjushe, et al., 2008). In this study, both *Staphylococcus aureus* and *Escherichia coli*, which are representatives the gram positive and gram negative bacteria, respectively were used as the test bacteria to examine the antibacterial properties of the BC and BCA films. As seen in Table 5.4 and Figure 5.17, the results show that the BC and BCA films had no significant impact on the growth of both of *Escherichia coli* and *Staphylococcus aureus* cells.

Table 5.4 Antimicrobial activities of BC and BCA films against *Escherichia coli* and *Staphylococcus aureus.*

Microorganisms	**Sample**	**Clear zone (mm)**
Escherichia coli	BC	0.00
	BCA	0.00
Staphylococcus aureus	BC	0.00
	BCA	0.00

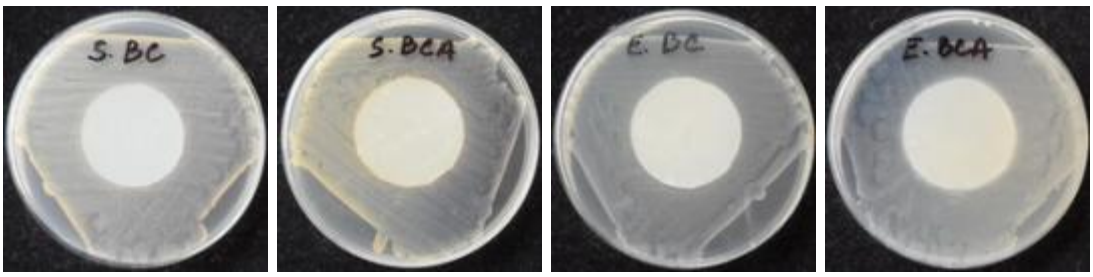

(a) (b) (c) (d)

Figure 5.17 Inhibitory effect of the BC and BCA samples on the growth of bacteria : (a,b) *Staphylococcus aureus* and (c,d) *Escherichia coli* for 24 h incubated at 37^{o}C, respectively.

For the antifungal ability, *Aspergillus niger* was used as the test fungi to examine the antifungal activity of the BC and BCA films. The antimicrobial effects of the BC and BCA films are shown in Table 5.5 and Figure 5.18, *Aspergillus niger* could grow on the BC film for more than 60% of area of the film. Whereas, *Aspergillus niger* could grow on BCA film for less than 10% of area of BCA film. The result indicated that the BCA film exhibited the inhibitory effects on the growths of *Aspergillus niger*.

Table 5.5 Antifungal activity of BC and BCA films against *Aspergillus niger*.

Microorganisms	**Sample**	**Observed growth (Grade)**	**Refference**
Aspergillus niger	BC	5	Heavy growth (> 60%)
	BCA	2	Trace growth (< 10%)

*Grade was used as a measurement of fungal growth: 0 = none, 1 = only apparent under microscope, 2 = trace (<10%), 3 = light growth (10-30%), 4 = medium growth (30-60%) and 5 = heavy growth (> 60%).

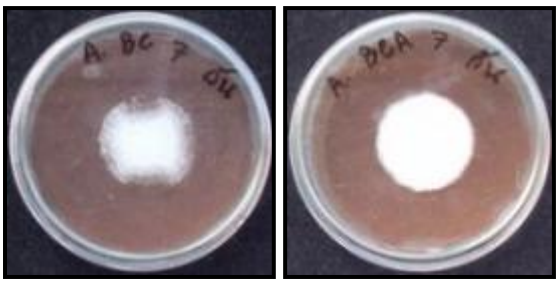

(a) (b)

Figure 5.18 The growth of *Aspergillus niger* on the BC and BCA films, at 37 ^{o}C at the end of the incubation 7 days.

CHAPTER VI
CONCLUSIONS AND RECOMMENDATIONS

6.1 Conclusions

In this study, the bacterial cellulose-chitosan (BCC) and the bacterial cellulose-*Aloe vera* (BCA) composite films were developed by the immersion method. Both of the developed composite films were characterized for physical and biological properties. The release patterns of chitosan from the BCC film and saccharide from the BCA film in buffer pH 1.2, pH 5.5, and pH 7.4 were investigated. Moreover, the cytotoxicity and biocompatibility of the BCC and BCA films on human keratinocytes and fibroblasts was evaluated.

In case of the BCC films, chitosan could penetrate into BC fibril network and fill the pores. The FTIR result indicated the intermolecular interaction between amino groups of chitosan and hydroxyl groups of cellulose. According to the SEM images and the result from the BET analysis, the average pore diameter and the surface area were decreased. Tensile strength, Young's modulus and Elongation at break were slightly declined. In the similar way, the WAC, WVTR, and OTR were decreased, whereas the antimicrobial abilities against gram positive bacteria, *Staphylococcus aureus* and fungi, *Aspergillus niger* of BCC films were improved. The BCC film had no toxicity against L929 mouse fibroblast cells. Moreover, the BCC film supported adhesion, growth and proliferation of both of human keratinocytes and fibroblasts.

In case of the BCA film, the FTIR result indicated the intermolecular interaction between BC and *Aloe vera*. When compared with the pristine BC, the mechanical properties, the crystallinity and the average pore diameter were decreased, whereas the OTR, the antifungal ability against *Aspergillus niger* were enhanced. The WVTR and the antibacterial ability of the BCA film had no significant difference from those of the BC film. The BCA film had no toxicity against L929 mouse fibroblast cells. The results of biocompatibility of human keratinocytes and fibroblasts

on the BCA film revealed that the BCA film not only supported adhesion but also promoted growth and proliferation of both of the tested cells.

6.2 Recommendations for future studies

Based on this study, further works for the improvement of the bacterial cellulose composite films are recommended as following.

1. Investigating the method to adjust the film structure in order to control the release rate of the applied active component at optimal level.
2. Seeking the methodology to improve pore structure of BC-chitosan films for achieving the optimal oxygen transmission rate, water vapor transmission rate, and the water absorption capacity.
3. Modifying the bacterial cellulose film by incorporating other bioactive substances which derived from natural products such as Lutein and Capsaicin.

REFERENCES

Alvarez, O.M., Patel, M., Booker, J., and Markowitz, L. Effectiveness of a biocellulose wound dressing for the treatment of chronic venous leg ulcers results of a single center randomized study involving 24 patients. Wounds 16 (7) (2004): 224–233.

Backdahl, H., et al. Mechanical properties of bacterial cellulose and interactions with smooth muscle cells. Biomaterials. 27 (2006): 2141-2149.

Balau, L., Lisa, G., Popa, M.I., Tura, V., and Melnig, V. Physico-chemical properties of chitosan films. Central European Journal of Chemistry 2 (4) (2004): 638-647.

Boudreau, M.D., and Beland, F.A. An evaluation of the biological and toxicological properties of *Aloe Barbadensis* (Miller) *Aloe vera*. Journal of Enviromental Science and Health Part C 24 (2006): 103-154.

Brown, E.E. Bacterial cellulose/thermoplastic polymer nanocomposites. Master's thesis, Department of chemical engineering, Faculty of Engineering, Washington state university, 2007.

Brown, R.M. Jr. The biosynthesis of cellulose. Journal of Macromolecular Science, Pure and Applied Chemistry 10 (1996): 1345-1373.

Cai, Z., and Kim, J. Bacterial cellulose/poly (ethylene glycol) composite. Cellulose. 17 (2010): 83-91.

Cardona, L., Sanzgiri, Y., Benedetti, L, Stella, V., and Topp, E. Application of benzyl hyaluronate membranes as potential wound dressings: evaluation of water vapour and gas permeabilities. Biomaterial 17 (1996): 1639-1643.

Ciechańska, D. Multifunctional Bacterial Cellulose/Chitosan Composite Materials for Medical Applications. FIBRES & TEXTILES in Eastern Europe 4(48) (2004): 12.

Czaja, W., Krystynowicz, A., and Bielecki, S. Microbial cellulose-the natural power to heal wounds. Biomaterials 27 (2006): 145–151.

Czaja, W., Young, D.J., Kawechi, M., and Brown, R.M. Jr. The future prospects of Microbial cellulose in biomedical applications, Biomacromolecules 8 (2007): 1-12.

Davis, R., DiDonato J., and Hartman G. Anti-inflammatory and wound healing activity of a growth substance in Aloe vera. J Am Pediatric Med Asso. 84 (1994): 77–81.

Dunphy, J.E. Modern biochemical concepts on the healing of wounds: Wound healing, 22-31. Baltimore, Williams and Wilkins, 1974.

Femenia, A., Sanchez, E.S., Simal, S., and Rossello, C. Compositional features of polysaccharides from Aloe vera (Aloe barbadensis Miller) plant tissues. Carbohydrate Polymers 39 (1999): 109-117.

Fontana, J.D., et al. Acetobacter cellulose pellicle as a temporary skin substitute**.** Applied Biochemistry and Biotechnology 24/25 (1990): 253-263.

Ganji, F., Abdekhodaie, M.J., and Ramazani, A. Gelation time and degradation rate of chitosan-based injectable hydrogel. J Sol-Gel Sci Techn. 42 (2007): 47-31.

Gardner, K.H., and Blackwell, J. The structure of native cellulose. Biopolymer 13 (1974): 1975-2001.

Hamman, J.H. Composition and applications of *Aloe vera* leaf gel. Molecules 13 (2008): 1599-1616.

He, Q., Ao, Q., Xiu, B., Gong, Y.D., Zhao, N. M., and Zhang, X.F. Mechanisms for biocompatibility of chitosan: A new view point. Journal of Clinical Rehabilitative Tissue Engineering Research 11 (2007): 7110-7112.

Heggers, J. P., Kucukcelebi, A., Listengarten, D., Stabenau, J., Ko, F., and Broemeling, L. D. Beneficial effect of Aloe on wound healing in an excisional wound model. Journal of Alternative and Complementary Medicine 2 (1991): 271–277.

Howling, G.I., Dettmar, P.W., Goddard, P.A., Hampson, F.C., Dornish, M., and Wood, E.J. The effect of chitin and chitosan on the proliferation of human skin fibroblasts and keratinocytes *in vitro*. Biomaterials 22(2001): 2959-2966.

Hunna, J.R., and Giacopelli, J.A. A review of wound healing and wound dressing products. The Journal of Foot and Ankle Surgery 36(1) (1997): 2-14.

Jettanacheawchankit, S., Sasithanasate, S., Sangvanich, P., Banlunara, W., and Thunyakitpisal, P. Acemannan stimulates gingival fibroblasts proliferation; Expressions of keratinocytes growth factor-1, vascular endothelial growth factor, and type I collagen; and wound healing. J. Pharmacol Sci. 109 (2009): 525-531.

Jonas, R., and Farah, L.F. Production and application of microbial cellulose. Polymer degradation and Srabiliry 59 (1998): 101-106.

Kanjanamosit, N., Muangnapoh, C., and Phisalaphong, M. Biosynthesis and Characterization of Bacteria Cellulose-Alginate Film. Applied Polymer Science 115 (2009): 1581-1588.

Kim, J., Cai, Z., Lee, H.S., Choi, G.S., Lee, D.H., and Jo, C. Preparation and characterization of a Bacterial cellulose/Chitosan composite for potential biomedical application. J Polym Res. (2010): DOI 10.1007/s10965-010-9470-9.

Kingkaeew, J., Jatupaiboon, N., Sanchavanakit, N., Pavasant, P., and Phisalaphong, M. Biocompatibility and Growth of Human Keratinocytes and Fibroblasts on Biosynthesized Cellulose-Chitosan Film. Journal of Biomaterials Science 21 (2010): 1009-1021.

Klemm, D., Schumann D., Udhardt, U., and Marsch, S. Bacterial synthesized cellulose artificial blood vessels for microsurgery. Prog. Polym. Sci. 26 (2001): 1561-1603.

Krajewska, B. Application of chitin-and chitosan-based material for enzyme immobilizations: a review. Enzyme and Microbial Technology 35 (2004): 126–139.

Kucharzewski, M., Slezak, A., and Franek, A. Topical treatment of nonhealing venous ulcers by cellulose membrane. Phlebologie. 32(2003): 147–151.

Kweon, D.K., and Kang, D.W. Drug-release behavior of chitosan-g-poly (viny lalcohol) copolymer matrix. Journal of Applied Polymer Science 74 (1999): 458–464.

Leane, M.M., Nankervis, R., Smith, A., and Illum, L. Use of the ninhydrin assay to measure the release of chitosan from oral solid dosage forms. International Journal of Pharmaceutics 271 (2004): 241-249.

Lowe, R.D. Two part wound dressing U.S. Patent 0051688, Feb. 28, 2008.

Liu, N., Chen, X.G., Park, H.J., Liu, C.G., Liu, C.S., and Meng, X.H. Effect of MW and concentration of chitosan on antibacterial activity of *Escherichia coli*. Carbohydrate Polymers 64 (2006): 60–65.

Luo, H., Xiong, G., Huang, Y., He, F., Wang, Y., and Wan, Y. Preparation and characterization of a novel COL/BC composite for potential tissue engineering scaffolds. Materials Chemistry and Physics 110 (2008): 193–196.

Majeti, N.V., and Kumar, R. A review of chitin and chitosan applications. Polymer 40(2000):1–27.

Martinez-Camacho, A.P., et al. Chitosan composite films: Thermal, structural, mechanical and antifungal properties. Carbohydrate Polymers 82 (2010): 305-315.

Mayall R.C., Mayall A.C., Mayall L.C., Rocha H.C., and Marques L.C. Tratamento das ulceras troficas dos membros com um novo substitute da pele. Rev Bras Cir. 80 (4) (1990): 257–283.

McAnally, B.H., Carpenter, R. H., and McDaniel, H.R. Use of acemannan. European Patent EP 0 965 345 A2.

Muzzarelli, R.A.A. Chitin and chitosan for the repair of wounded skin, never, cartilage and bone. Carbohydrate Polymers 76 (2009): 167 -182.

Muzzarelli, R.A.A., Mattioli-Belmonte, M., Pugnaloni, A. and Biagini, G. Biochemistry, histology and clinical uses of chitins and chitosans in wound healing. Switzerland :Basel, 1999.

Muzzarelli, R.A.A., Ramos, V., Stanic, V., Dubini, B., Mattioli-Belmonte, M., and Tosi,G. Osteogenesis promoted by calcium phosphate dicarboxyboxymethyl chitosan. Carbohydrate Polymers 36 (1998): 267–276.

National Organic Standards Board Technical Advisory Panel Review Compiled by Organic Materials Review Institute for the USDA National Organic Program. (2001).

No, H.K., Park, N.Y., Lee, S.H., and Meyers, S.P. Antibacterial activity of Chitosans and chitosan oligomers with different molecular weights. International Journal of Food Microbiology 74 (2002): 65-72.

Nogi, M., Handa, K., Nakagaito, A.N., and Yano, H. Optically transparent bionanofiber composites with low sensitivity to refractive index of the polymer matrix. Applied Physics Letters 87 (2005): 1-3.

Phisalaphong, M., and Jatupaiboon, N. Biosynthesis and characterization of bacteria cellulose-chitosan film. Carbohydrate Polymers 74 (2008): 482-488.

Phisalaphong, M., Suwanmajo, T., and Sangtherapitikul, P. Novel nonaporous membranes from regenerated bacterial cellulose. Journal of Applied Polymer Science 107 (2008): 292-299.

Retigi, A., et al. Bacterial cellulose films with controlled microstructure-mechanical property relationships. Cellulose 17 (2010): 661-669.

Saibuatong, O., and Phisalaphong, M. Novo Aloe vera-bacterial cellulose composite film from biosynthesis. Carbohydrate Polymers 79 (2) (2010): 455-460.

Sanchavanakit, N., Sangrungraugroj, W., Kaommongkolgit, R., Banaprasert, T., Pavasant, P., and Phisalaphong, P. Growth of Human Keratinocytes and Fibroblasts on Bacterial Cellulose Film. Biotechnol. Prog., 22 (2006): 1194-1199.

Seifert, M., Hesse S., Kabrelian V., and Klemm, D. Controlling the water content of never dried and reswollen bacterial cellulose by the addition of water soluble polymers to the culture medium. Journal of Polymer Science: Part A: Polymer Chemistry 42 (2004): 463-470.

Shah, J., and Brown, R.M. Jr. Towards electronic paper displays made from microbial cellulose. Applied Microbiology and Biotechnology 66 (2005): 352-355.

Shoda, M., and Sugano, Y. Recent advances in bacterial cellulose production. Biotechnology and Bioprocess Engineering 10 (2005): 1-8.

Stashak, T.S., Farstvedt, E., and Othic, A. Update on wound dressing: Indication and best use. Clinical Techniques in Equine Practice 04 (2004): 148-163.

Suwantong, O., Opanasopit, P., RuktanonChai, U., and Supaphol, P. Electrospun Cellulose Acetate Fiber Mats containing Curcumin and release characteristic of The Herbal Substance. Polymer 42 (2008): 7546-7557.

Surjushe, A., Vasani, R., and Saple, D.G. Aloe vera: A short review. Indian J Dermatol. 53 (4) (2008): 163-6.

Svensson, A., et al. Bacterial cellulose as a potential scaffold for tissue engineering of cartilage. Biomaterials 26 (2005): 419 - 431.

UI-Islam, M., Shah, N., Ha, J. H., and Park, J. K. Effect of chitosan penetration on physic-chemical and mechanical properties of bacterial cellulose. Korean J. Chem. Eng. 28(8) (2011): 1736-1743.

Wan, W.K., Hutter, J.L., Millon, L., and Guhados, G. Bacterial cellulose and its nanocomposites for biomedical applications. ACS Symposium Series 938 (2006): 221-241.

Wan, W.K., and Millon, L.E. Poly(vinyl alcohol)-bacterial cellulose nanocomposite. U.S. Pat.Appl. Publ. US 2005037082 A1 (2005): 16.

Wu, P., Nelson, A., Reid, H., Ruckley, V., and Gaylor, S. Water vapour transmission rates in burns and chronic leg ulcers: influence of wound dressings and comparison with *in vitro* evaluation. Biomaterials. 17 (1996): 1373-1377.

Yagi, A., et al. Isolation and characterization of the glycoprotein fraction with a proliferation promoting activity on human and hamster cells in vitro from *Aloe vera* gel. Planta Med. 63(1997):18-21

Yang, L., Hsiao,W.W., and Chen, P. Chitosan – cellulose composite membrane for affinity purification of biopolymers and immunoadsorption. Journal of Membrane Science 197 (2002): 185-197.

Yao, H., Chen, Y., Li, S., Huang, L., Chen, W., and Lin, X. Promotion proliferation effect of a polysaccharide from Aloe barbadensis Miller on human fibroblasts in vitro. International Journal of Biological Macromolecules 45 (2009): 152-156.

Zhang, M., Li, X.H., Gong, Y.D., Zhao, N.M., and Zhang, X.F. Properties and Biocompatibility of chitosan films modified by blending with PEG. Biomaterial 23(2002): 2641–2648.

Zimmermann, K. A., LeBlanc, J. L., Sheets, K. T., Fox, R. W., and Gatenholm, P. Biomimetic Design of A Bacterial Cellulose/Hydroxyapatite Nanocomposite for Bone Healing Applications. Materials Science & Engineering: C, 31 (2011): 43-49.

APPENDICES

Appendix A

A.1 Ninhydrin method

Chemicals

1. Chitosan MW 30,000, 80,000 and 20,000 with DAC. > 85%
2. Lithium acetate dihydrate
3. Glacial acetic aicd
4. Ninhydrin
5. Hydrindantin
6. Ethanol

Ninhydin reagent preparation

Preparation the 10 ml of lithium acetate buffer by dissolving 4.08 grams of lithium acetate dehydrate in 6 ml of DI water. The pH of resulting solution was adjusted to 5.2 using glacial acetic acid and the volume adjusted to 10 ml with DI water. The ninhydrin reagent was prepared by adding 10 ml of lithium acetate buffer to 0.8 g ninhydrin and 0.12 g hydrindantin in 30 ml DMSO.

Ninhydrin assay

0.5 ml of ninhydrin reagent was added to 0.5 ml of the sample in a glass scintillation vial. The vials were immediately capped, briefly shaken and heated in boiling water for 30 min to allow the reaction to proceed. After cooling, 15 ml of a 50:50 ethanol:water mixture was added to each vial. The vials were then vortexed for 15 s in order to oxidise the excess of hydrindantin. The absorbance of each solution was measured on a UV spectrophotometer at 570 nm and the concentration of chitosan in the sample calculated from a standard calibration curve

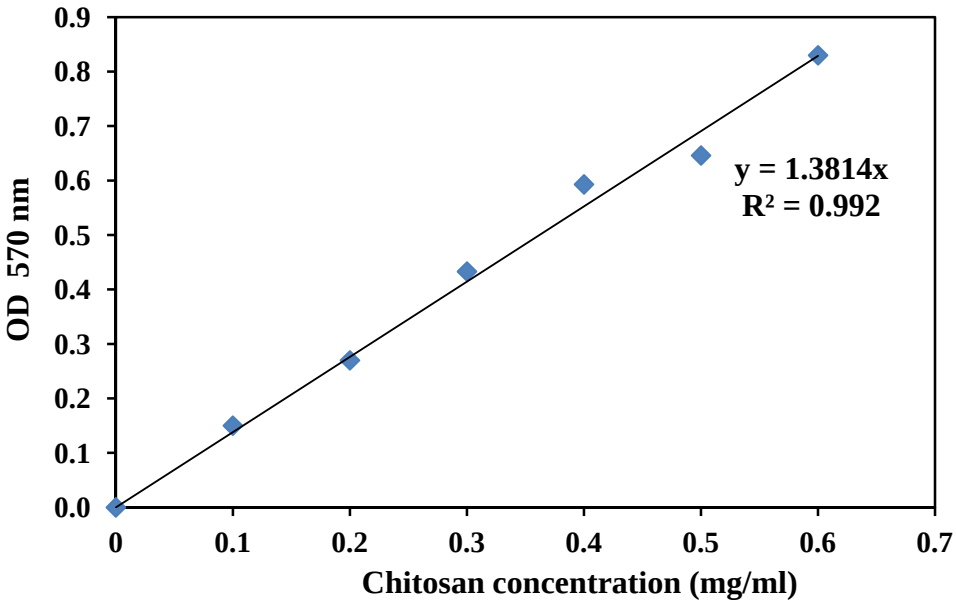

Figure A1 Chitosan standard curve for release analysis (MW 30,000)

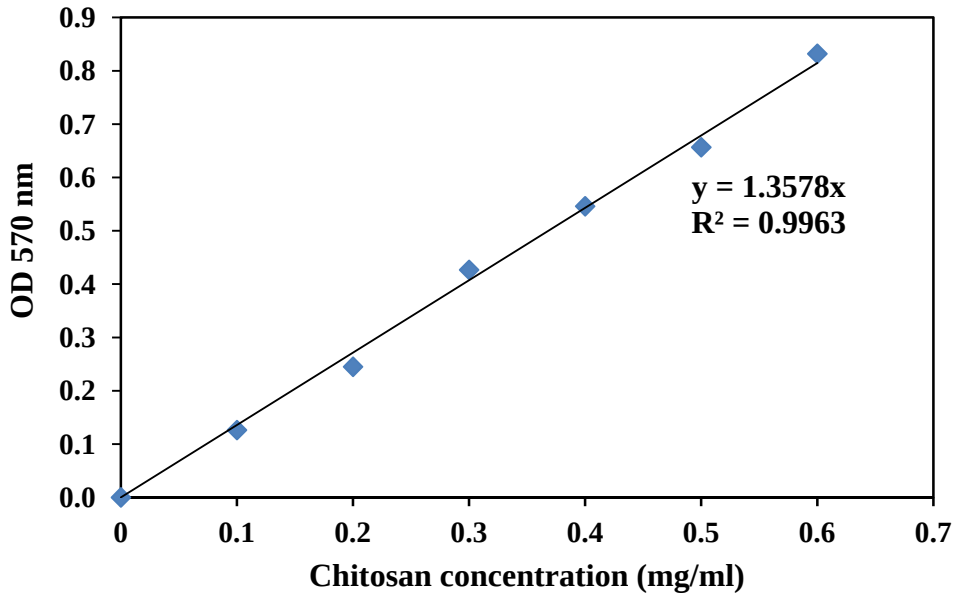

Figure A2 Chitosan standard curve for release analysis (MW 80,000)

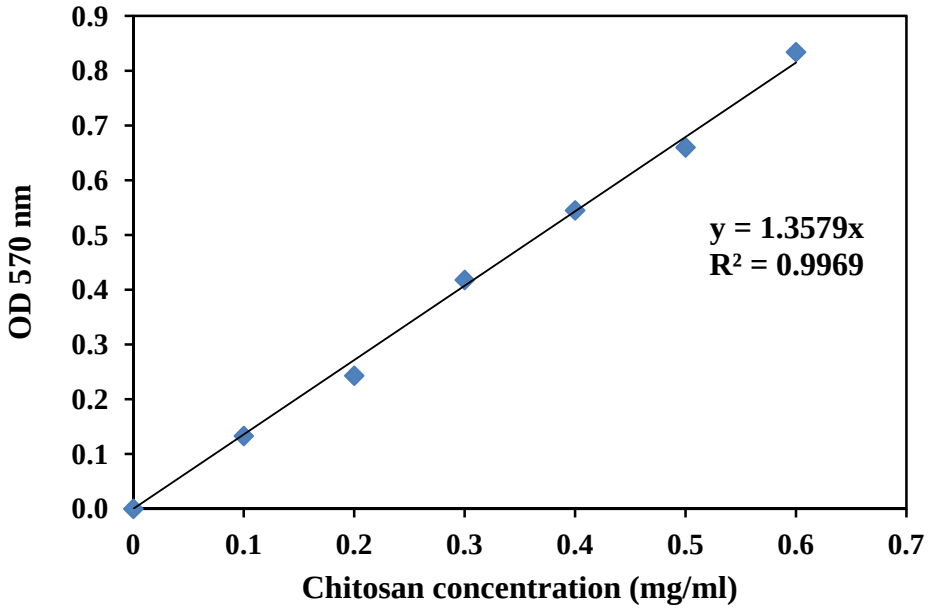

Figure A3 Chitosan standard curve for release analysis (MW 200,000)

A.2 DNS method

Chemicals

1. Glucose
2. Mannose
3. Hydrochloric acid
4. Sodium hydroxide
5. DNS
6. Sodium potassium tartrate tetrahydrate

DNS reagent preparation

Dissolve 10 grams DNS (3,5 dinitrosalicylic acid) in 200 ml 2M sodium hydroxide with worming and vigorous stirring. Dissolve 300 grams of sodium potassium tartrate tetrahydrate in 500 ml distilled water. Mix these two solutions and make up to 1 litre with distilled water.

Saccharides analysis

1. 1.0 ml of sample was added into test tube.
2. Add 0.5 ml conc. hydrochloric acid and heat in boiling water for 20 minutes. Then, cool in an ice bath.
3. Centrifuge at 3,000 rpm for 20 minutes in order to get a supernatant.
4. Pipette 1.0 ml supernatant into test tube and add 1.0 ml DNS reagent.
5. Heat all tube in boiling water for 5 minutes to allow the reaction occurred. Then, cool in an ice bath for stop reaction.
6. Add 10.0 ml Distilled water and mix well.
7. Read an absorbance at 540 nm.

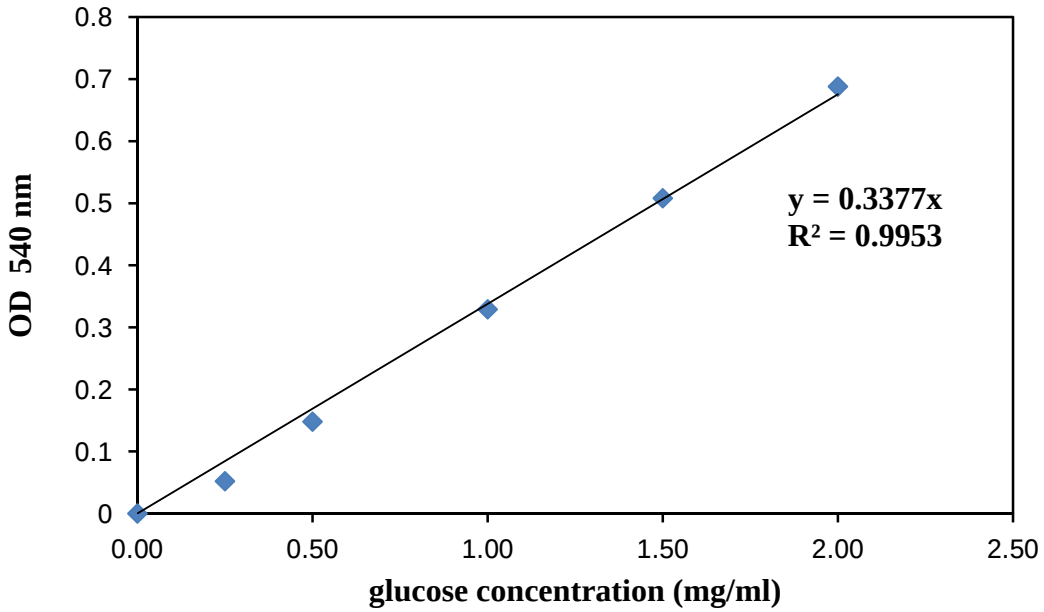

Figure A4 Glucose standard curve for hydrolyzed polysaccharide analysis

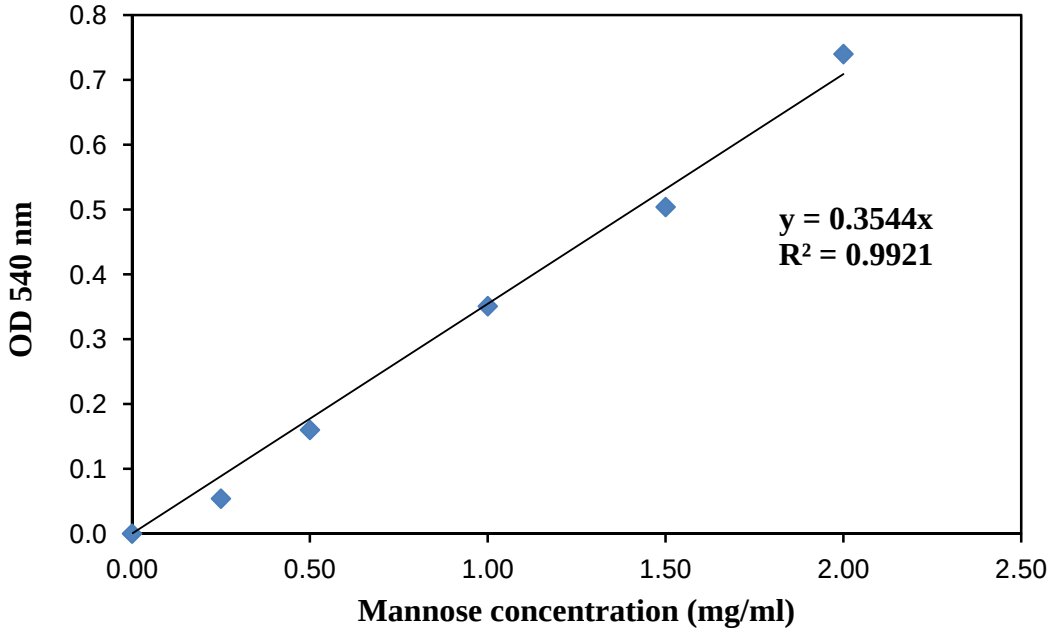

Figure A5 Mannose standard curve for hydrolyzed polysaccharide analysis

Table A1 Percentage Points of the *t* -Distribution[a]

ν\α	.04	.25	.10	.05	.025	.01	.005	.0025	.001	.0005
1	.325	1.000	3.078	6.314	12.706	31.821	63.657	127.32	318.31	636.62
2	.289	.816	1.886	2.920	4.303	6.965	9.925	14.089	23.326	31.598
3	.277	.765	1.638	2.353	3.182	4.541	5.841	7.453	10.213	12.924
4	.271	.741	1.533	2.132	2.776	3.747	4.604	5.598	7.173	8.610
5	.267	.727	1.476	2.015	2.571	3.365	4.032	4.773	5.893	6.869
6	.265	.727	1.440	1.943	2.447	3.143	3.707	4.317	5.208	5.959
7	.263	.711	1.415	1.895	2.365	2.998	3.499	4.019	4.785	5.408
8	.262	.706	1.397	1.860	2.306	2.896	3.355	3.833	4.501	5.041
9	.261	.703	1.383	1.833	2.262	2.281	3.250	3.690	4.297	4.781
10	.260	.700	1.372	1.812	2.228	2.764	3.169	3.581	4.144	4.587
11	.260	.697	1.363	1.796	2.201	2.718	3.106	3.497	4.025	4.437
12	.259	.695	1.356	1.782	2.179	2.681	3.055	3.428	3.930	4.318
13	.259	.694	1.350	1.771	2.160	2.650	3.012	3.372	3.852	4.221
14	.258	.692	1.345	1.761	2.145	2.624	2.997	3.326	3.787	4.140
15	.258	.691	1.341	1.753	2.131	2.602	2.947	3.286	3.733	4.073
16	.258	.690	1.337	1.746	2.120	2.583	2.921	3.252	3.686	4.015
17	.257	.689	1.333	1.740	2.110	2.567	2.898	3.222	3.646	3.965
18	.257	.688	1.330	1.734	2.101	2.552	2.878	3.197	3.610	3.922
19	.257	.688	1.328	1.729	2.093	2.539	2.861	3.174	3.579	3.883
20	.257	.687	1.325	1.725	2.086	2.528	2.845	3.153	3.552	3.850
∞	.253	.674	1.282	1.645	1.960	2.326	2.576	2.807	3.090	3.291

ν = degrees of freedom.

[a]Adapted with percussion from Biometrika Tables for statisticians. Vol.1 3rd edition by E.S. Pearson and H.O. Hartley, Cambridge University Press, Cambridge, 1996.

Appendix B

Table B1 Data of Figure 4.9

Time (h)	Chitosan Concentration (mg/cm^3 of never-dried BC)				
	BCC3				
	1	2	3	Average	SD.
0	0.00	0.00	0.00	0.00	0.00
6	4.06	4.34	4.34	4.83	4.83
12	5.02	4.28	4.28	4.83	4.83
18	4.58	4.28	4.28	4.75	4.75
24	4.69	4.58	4.58	5.27	5.27
36	4.94	4.12	4.12	5.16	5.16
48	4.83	4.42	4.42	5.21	5.21
60	4.88	4.31	4.31	5.13	5.13
BCC8					
0	0.00	0.00	0.00	0.00	0.00
6	3.14	3.61	3.61	4.16	4.16
12	3.53	3.58	3.58	4.49	4.49
18	3.61	3.58	3.58	4.80	4.80
24	3.50	3.75	3.75	4.66	4.66
36	3.28	4.05	4.05	4.44	4.44
48	3.42	3.75	3.75	4.49	4.49
60	3.19	3.89	3.89	4.41	4.41
BCC20					
0	0.00	0.00	0.00	0.00	0.00
6	1.58	2.00	2.00	2.38	2.38
12	1.94	2.00	2.00	2.27	2.27
18	1.86	2.53	2.53	2.47	2.47
24	2.30	2.36	2.36	2.38	2.38
36	2.36	2.14	2.14	2.49	2.49
48	2.11	2.28	2.28	2.63	2.63
60	1.94	2.36	2.36	2.80	2.80

Table B2 Data of Figure 4.13

Sample	Tensile strength (MPa)						
	1	2	3	4	5	Average	SD.
BC	89.40	83.50	97.02	95.80	105.00	94.14	8.13
BCC3	78.62	69.72	65.20	73.20	68.28	71.00	5.14
BCC8	92.18	80.32	84.43	77.31	73.10	81.47	7.28
BCC20	89.48	93.50	85.32	77.80	92.84	87.79	6.46

Table B3 Data of Figure 4.14

Sample	Young's modulus (MPa)						
	1	2	3	4	5	Average	SD.
BC	768	776	821	668	699	746	62
BCC3	594	582	685	706	632	640	55
BCC8	617	672	620	642	591	628	30
BCC20	702	636	687	674	751	690	42

Table B4 Data of Figure 4.15

Sample	Elongation at break (%)						
	1	2	3	4	5	Average	SD.
BC	24.70	26.25	30.16	25.07	27.75	26.79	2.23
BCC3	28.04	20.82	21.48	26.37	20.14	23.37	3.58
BCC8	23.79	20.86	21.57	28.91	28.01	24.63	3.68
BCC20	22.69	20.25	22.88	20.12	22.07	21.60	1.33

Table B5 Crystallinity Index of BC and BCC films

Sample	$2\theta = I_{max}$	$2\theta = I_{am}$	C.I. (%)
BC	5300	717	86.47
BCC3	8743	1917	78.07
BCC8	5499	1143	79.21
BCC20	4983	1120	77.52

Table B6 Data of Figure Table 4.2

Sample	Pore size (Å)			
	1	2	Average	SD.
BC	92.28	107.72	100.00	10.9
BCC3	46.18	57.32	51.75	7.9
BCC8	43.23	56.45	49.84	9.3
BCC20	50.22	62.92	56.57	9.0

Table B7 Data of Table 4.2

Sample	Surface area (m^2/g)			
	1	2	Average	SD.
BC	4.26	4.14	4.2	0.085
BCC3	4.28	4.51	4.40	0.163
BCC8	3.31	3.47	3.39	0.113
BCC20	2.6	2.68	2.64	0.057

Table B7 Data of Figure 4.19

Sample	Water absorption capacity (%)						
	1	**2**	**3**	**4**	**5**	**Average**	**SD.**
BC	336	306	316	314	379	330	29
BCC3	184	223	177	172	175	186	21
BCC8	164	176	197	157	178	174	15
BCC20	201	188	253	233	203	216	27

Table B8 Data of Table 4.3

Sample	WVTR ($g/m^2/day$)			
	1	**2**	**Average**	**SD.**
BC	1038	1060	1049	16
BCC3	505	553	529	34
BCC8	789	767	778	16
BCC20	855	804	830	36

Table B9 Data of Table 4.4

Sample	OTR($cm^3/m^2/day$)			
	1	**2**	**Average**	**SD.**
BC	2.63	2.67	2.63	2.67
BCC3	1.74	1.61	1.74	1.61
BCC8	1.55	1.59	1.55	1.59
BCC20	1.42	1.47	1.42	1.47

Table B10 Data of Figure 4.20 **(A)**

Time (h)	**Chitosan concentration (mg/cm^3 of dried film) (Buffer pH 1.2)**							
	BC	**SD.**	**BCC3**	**SD.**	**BCC8**	**SD.**	**BCC20**	**SD.**
0	0.00	0.00	0.00	0.00	0.00	0.00	0.00	0.00
0.33	0.30	0.08	3.03	0.45	2.11	0.88	1.37	0.42
0.67	0.32	0.18	6.05	0.91	4.23	1.76	2.73	0.84
1	0.33	0.18	7.99	0.79	10.27	2.13	5.31	1.24
1.5	0.36	0.08	9.78	0.52	11.30	1.05	5.81	1.25
2	0.24	0.06	11.57	1.29	12.33	0.86	6.31	1.35
3	0.36	0.10	12.27	1.31	14.04	1.34	7.32	0.90
4	0.18	0.16	14.56	0.51	15.27	1.49	10.71	2.19
5	0.28	0.15	15.87	2.58	16.50	2.05	10.83	1.88
6	0.32	0.16	16.21	3.04	16.21	1.51	10.85	1.29
12	0.37	0.06	19.00	1.86	18.64	2.21	13.11	0.42
18	0.28	0.16	24.87	2.85	20.61	1.68	15.16	1.08
24	0.41	0.37	23.88	2.32	21.68	0.50	15.75	2.03
48	0.23	0.14	24.87	1.80	22.07	0.45	16.75	2.19
72	0.14	0.10	27.17	1.85	21.83	0.75	17.98	1.32
96	0.23	0.20	27.01	1.74	21.65	0.56	17.16	1.17
120	0.05	0.06	26.52	1.65	21.63	1.18	17.14	2.03
144	0.09	0.08	26.39	1.94	21.61	0.72	17.12	1.55
168	0.06	0.08	26.04	1.89	21.47	0.87	17.06	1.60
216	0.05	0.04	26.16	1.78	21.34	0.64	16.77	1.70
264	0.15	0.07	26.16	1.81	21.51	0.94	17.00	1.09

Table B11 Data of Figure 4.20 **(B)**

Time (h)	**Chitosan concentration (mg/cm^3 of dried film) (Buffer pH 5.5)**							
	BC	**SD.**	**BCC3**	**SD.**	**BCC8**	**SD.**	**BCC20**	**SD.**
0	0.00	0.00	0.00	0.00	0.00	0.00	0.00	0.00
0.33	0.45	0.18	1.24	0.06	0.53	0.06	0.43	0.03
0.67	0.04	0.41	2.48	0.12	1.06	0.12	0.86	0.06
1	0.27	0.37	3.65	0.44	1.86	0.36	1.52	0.61
1.5	0.19	0.04	5.01	0.24	2.47	0.12	2.20	0.84
2	0.46	0.30	6.37	0.27	3.07	0.57	2.89	1.09
3	0.10	0.08	9.14	0.62	5.20	0.47	3.09	0.48
4	0.10	0.24	9.52	0.33	6.40	0.59	3.86	0.78
5	0.23	0.13	10.91	0.95	6.56	0.42	4.44	0.59
6	0.17	0.14	12.17	1.03	7.54	0.54	4.41	0.66
12	0.03	0.23	16.22	2.31	9.71	1.01	6.14	0.76
18	0.17	0.23	18.50	2.16	12.96	0.62	7.40	0.94
24	0.12	0.08	20.24	1.77	13.21	0.71	7.76	1.11
48	0.06	0.02	25.17	2.91	15.78	0.13	9.44	0.97
72	0.13	0.06	25.67	2.52	18.30	0.90	10.21	1.19
96	0.09	0.08	26.43	1.57	18.63	0.82	10.71	1.29
120	0.09	0.02	26.21	1.96	20.61	1.33	11.30	1.51
144	0.14	0.12	27.03	2.27	20.40	0.82	11.09	1.53
168	0.04	0.04	26.39	1.00	20.27	1.00	11.34	1.31
216	0.09	0.10	26.01	1.30	20.11	0.73	10.93	1.53
264	0.12	0.04	26.12	1.48	20.25	0.96	10.99	1.27

Table B12 Data of Figure 4.20 (C)

Time (h)	Chitosan concentration (mg/cm^3 of dried film) (Buffer pH 7.4)							
	BC	**SD.**	**BCC3**	**SD.**	**BCC8**	**SD.**	**BCC20**	**SD.**
0	0.00	0.00	0.00	0.00	0.00	0.00	0.00	0.00
0.33	0.14	0.15	0.11	0.10	0.21	0.12	0.02	0.20
0.67	0.30	0.23	0.09	0.05	0.06	0.07	0.10	0.23
1	0.27	0.15	0.19	0.08	0.12	0.03	0.07	0.06
1.5	0.31	0.15	0.13	0.09	0.10	0.06	0.22	0.20
2	0.30	0.02	0.12	0.08	0.17	0.03	0.51	0.68
3	0.28	0.16	0.19	0.17	0.12	0.06	0.18	0.13
4	0.42	0.21	0.21	0.05	0.19	0.07	0.21	0.03
5	0.23	0.13	0.19	0.08	0.29	0.05	0.36	0.22
6	0.44	0.26	0.56	0.24	0.13	0.13	0.17	0.24
12	0.22	0.08	0.32	0.16	0.29	0.17	0.27	0.14
18	0.39	0.31	0.37	0.03	0.33	0.09	0.14	0.29
24	0.41	0.17	0.26	0.14	0.46	0.12	0.16	0.06
48	0.32	0.26	0.60	0.07	0.14	0.03	0.13	0.06
72	0.32	0.27	0.27	0.10	0.13	0.13	0.11	0.02
96	0.37	0.28	0.40	0.52	0.14	0.09	0.10	0.04
120	0.19	0.10	0.19	0.05	0.28	0.13	0.19	0.12
144	0.15	0.04	0.10	0.06	0.13	0.17	0.15	0.08
168	0.18	0.10	0.11	0.11	0.09	0.04	0.14	0.07
216	0.22	0.06	0.15	0.08	0.13	0.05	0.15	0.09
264	0.26	0.09	0.18	0.12	0.14	0.03	0.17	0.16

Table B13 Data of Table 4.5

Microorganisms	**Sample**	**Clear zone (mm)**				
		1	**2**	**3**	**Average**	**SD.**
Staphylococcus aureus	BC	0.00	0.00	0.00	0.00	0.00
	BCC3	44.33	42.80	41.85	43.00	1.25
	BCC8	41.66	43.40	42.93	42.66	0.90
	BCC20	47.16	46.18	45.65	46.33	0.77
Escherichia coli	BC	0.00	0.00	0.00	0.00	0.00
	BCC3	0.00	0.00	0.00	0.00	0.00
	BCC8	0.00	0.00	0.00	0.00	0.00
	BCC20	0.00	0.00	0.00	0.00	0.00

Table B16 Data of Figure 5.1

Time (h)	**Saccharide concentration (mg/cm^3 of never-dried BC)**						
	1	2	3	4	5	Average	SD.
0	0.00	0.00	0.00	0.00	0.00	0	0
6	1.22	0.99	0.99	0.89	0.89	1.05	0.12
12	1.79	1.16	1.16	1.36	1.36	1.43	0.23
18	2.14	1.83	1.83	1.83	1.83	1.92	0.13
24	2.45	2.12	2.12	2.26	2.26	2.25	0.12
36	2.40	2.20	2.20	2.35	2.35	2.32	0.07
48	2.53	2.20	2.20	2.29	2.29	2.31	0.13

Table B17 Data of Figure 5.4

Sample	Tensile strength (MPa)						
	1	2	3	4	5	Average	SD.
BC	89.40	83.50	97.02	95.80	105.00	94.14	8.13
BCA	66.69	61.88	69.53	64.23	58.84	64.23	4.14

Table B18 Data of Figure 5.5

Sample	Young's modulus (MPa)						
	1	2	3	4	5	Average	SD.
BC	768	776	821	668	699	746	62
BCA	329	318	397	327	409	356	43

Table B19 Data of Figure 5.6

Sample	Elongation at break (%)						
	1	2	3	4	5	Average	SD.
BC	24.70	26.25	30.16	25.07	27.75	26.79	2.23
BCA	18.42	19.33	25	21.18	21.81	21.15	2.55

Table B5 Crystallinity Index of BC and BA films

Sample	$2\theta = I_{max}$	$2\theta = I_{am}$	C.I. (%)
BC	5300	717	86.47
BCA	2967	456	84.63

Table B20 Data of Figure 5.7

Sample	Water absorption capacity (%)						
	1	**2**	**3**	**4**	**5**	**Average**	**SD.**
BC	336	306	316	314	379	330	29
BCA	379	369	341	335	373	359	20

Table B21 Data of Table 5.1

Sample	Pore size (Å)			
	1	**2**	**Average**	**SD.**
BC	92.28	107.72	100	10.9
BCA	76.34	86.08	81.21	6.9

Table B22 Data of Table 5.1

Sample	Surface area (m^2/g)			
	1	**2**	**Average**	**SD.**
BC	4.26	4.14	4.2	0.085
BCA	2.98	3.11	3.05	0.092

Table B23 Data of Table 5.2

Sample	WVTR ($g/m^2/day$)			
	1	**2**	**Average**	**SD.**
BC	1038	1060	1049	16
BCA	1001	1059	1030	41

Table B24 Data of Table 5.3

Sample	OTR($cm^3/m^2/day$)			
	1	**2**	**Average**	**SD.**
BC	2.63	2.67	2.63	2.67
BCA	9.74	10.14	9.74	10.14

Table B25 Data of Table 5.4

Microorganisms	Sample	Clear zone (mm)				
		1	**2**	**3**	**Average**	**SD.**
Staphylococcus aureus	BC	0.00	0.00	0.00	0.00	0.00
	BCA	0.00	0.00	0.00	0.00	0.00
Escherichia coli	BC	0.00	0.00	0.00	0.00	0.00
	BCA	0.00	0.00	0.00	0.00	0.00

Table B26 Data of Figure 5.11

Time (h)	Saccharide concentration (mg/cm^3)											
	Buffer pH 1.2				Buffer pH 5.5				Buffer pH 7.4			
	BC	SD.	BCA	SD.	BC	SD.	BCA	SD.	BC	SD.	BCA	SD.
0	0.00	0.00	0.00	0.00	0.00	0.00	0.00	0.00	0.00	0.00	0.00	0.00
0.33	0.61	0.40	19.07	1.68	1.88	0.62	17.61	2.49	0.61	0.53	20.66	2.23
0.67	0.89	0.50	20.01	1.25	1.08	0.67	19.44	2.34	1.09	0.47	22.08	2.47
1	1.10	0.62	22.27	1.84	1.82	0.85	22.60	3.53	1.31	0.35	26.23	3.06
1.5	1.10	0.42	23.04	2.05	1.08	0.16	22.98	2.33	1.01	0.45	26.50	1.35
2	1.21	0.10	23.34	2.16	2.17	0.95	22.92	2.16	1.10	0.28	26.65	2.13
3	1.41	0.27	25.09	2.12	0.99	0.40	23.27	0.25	1.46	0.24	26.86	2.28
4	1.42	0.56	24.52	3.30	1.41	0.16	23.83	2.01	1.52	0.49	28.05	2.30
5	0.96	0.55	24.50	2.40	0.91	0.32	24.27	2.36	1.68	0.37	28.16	1.96
6	1.46	0.74	25.33	1.96	1.51	0.24	25.19	2.07	1.79	0.31	29.00	2.15
12	1.02	0.31	31.96	1.84	0.86	0.38	30.84	0.14	1.48	0.93	37.43	2.27
18	1.51	1.23	32.60	2.08	1.45	0.08	33.19	2.29	1.47	0.18	38.61	1.46
24	1.53	0.52	32.55	1.23	1.68	0.23	32.43	2.40	2.03	0.31	40.53	2.68
48	1.48	0.63	34.15	2.07	1.48	0.45	32.89	2.77	1.95	0.24	39.48	2.28
72	1.58	0.42	34.27	2.53	1.73	0.26	34.64	2.55	1.95	0.17	43.20	1.78
120	1.48	0.45	36.22	2.56	1.58	0.26	36.37	3.09	1.59	0.30	42.49	1.84
144	1.52	0.40	38.23	2.60	1.73	0.15	36.29	2.41	1.88	0.76	43.02	1.83
168	1.68	0.50	37.46	2.92	1.48	0.09	36.91	2.45	2.15	0.34	43.45	2.12

VITA

Mr. Jeerun Kingkaew was born in Bangkok, on June 2, 1974. He finished high school from Suwannaranwittayakom School, Bangkok in 1991. He received his Bacheler's Degree in Science (Biotechnology) from Mahidol University in 1997 and Master's Degree in Chemical Engineering from Chulalongkorn University in 2004. He subsequently continued studying Doctoral degree of Chemical Engineering, Chulalongkorn University since October 2007 and received grant fund under the program Strategic Scholarships for Frontier Research Network for the Join Ph.D. Program Thai Doctoral degree from the Office of the Higher Education Commission,
His academic publications are as follows:

1. BIOCOMPATIBILITY AND GROWTH OF HUMAN KERATINOCYTES AND FIBROBLASTS ON BIOSYNTHESIZED CELLULOSE-CHITOSAN FILM: Journal of Biomaterials Science 21 (2010) 1009 - 1021
2. DEVELOPMENT OF BACTERIAL CELLULOSE COMPOSITE FILM FOR MEDICAL APPLICATION in the Commission on Higher Eduction Congress III University Staff Development Consortium (CHE-USDC Congress III) on September 9-11, 2010 at The Royal Cliff Grand Hotel and spa, Pattaya, Chonburi , Thailand, pp.236. (The Excellent Poster Presentation Award).
3. DEVELOPMENT OF BACTERIAL - CELLULOSE COMPOSITE FILM FOR POTENTIAL WOUND DRESSING in the 4^{th} AUN/SEED-Net Regional Conference on Biotechnology: EMERGING BIOTECHOLOGY FOR GREEN ENGINEERING on January 26-27, 2012 at The Montien Hotel Bangkok, Thailand, pp.16.
4. BIOSYNTHESIS OF CELLULOSE-CHITOSAN COMPOSITE: Chitin, Chitosan, Oligosaccharides and Their Derivatives, pp 53-63. USA : CRC Press, 2011.